

ON-LINE WEB-BASED STRUCTURAL EVALUATION PROGRAM
DEVELOPMENT FOR EXISTING REINFORCED CONCRETE BUILDINGS
AGAINST EARTHQUAKES

A THESIS SUBMITTED TO
THE GRADUATE SCHOOL OF NATURAL AND APPLIED SCIENCES
OF
MIDDLE EAST TECHNICAL UNIVERSITY

BY

MUSTAFA CAN YÜCEL

IN PARTIAL FULFILLMENT OF THE REQUIREMENTS
FOR
THE DEGREE OF DOCTOR OF PHILOSOPHY
IN
CIVIL ENGINEERING

JANUARY 2017

Approval of the thesis:

**ON-LINE WEB-BASED STRUCTURAL EVALUATION PROGRAM
DEVELOPMENT FOR EXISTING REINFORCED CONCRETE BUILDINGS
AGAINST EARTHQUAKES**

submitted by **MUSTAFA CAN YÜCEL** in partial fulfillment of the requirements for the degree of **Doctor of Philosophy in Civil Engineering Department, Middle East Technical University** by,

Prof. Dr. Gülbin Dural Ünver
Dean, Graduate School of **Natural and Applied Sciences**

Prof. Dr. İsmail Özgür Yaman
Head of Department, **Civil Engineering**

Prof. Dr. Ahmet Türer
Supervisor, **Civil Engineering Department, METU**

Examining Committee Members:

Prof. Dr. Ahmet Yakut
Civil Engineering Dept., METU

Prof. Dr. Ahmet Türer
Civil Engineering Dept., METU

Prof. Dr. Tamer Topal
Geology Dept., METU

Assoc. Prof. Dr. Baki Öztürk
Civil Engineering Dept., Hacettepe University

Assist. Prof. Dr. Saeid Kazemzadeh Azad
Civil Engineering Dept., Atılım University

Date:

20/01/2017

I hereby declare that all information in this document has been obtained and presented in accordance with academic rules and ethical conduct. I also declare that, as required by these rules and conduct, I have fully cited and referenced all material and results that are not original to this work.

Name, Last Name: MUSTAFA CAN YÜCEL

Signature :

ABSTRACT

ON-LINE WEB-BASED STRUCTURAL EVALUATION PROGRAM DEVELOPMENT FOR EXISTING REINFORCED CONCRETE BUILDINGS AGAINST EARTHQUAKES

Yücel, Mustafa Can

Ph.D., Department of Civil Engineering

Supervisor : Prof. Dr. Ahmet Türer

January 2017, 172 pages

Structural assessment is a very hot topic in earthquake-prone countries since the evaluation of building stock is necessary for existing aged or shady buildings, after a major earthquake, or after major seismic code changes. Many different techniques are proposed in this context, but there are very limited studies on applying assessment methods using internet-based technologies even though web-based approaches will have many advantages such as formation of a building condition database, integration with other cloud services (like GIS), implementing hardware capabilities (taking photos, voice recording, vibration measurements by accelerometers, geolocation by GPS... etc.), automated simple analysis and reporting, access and applicability to many users and large geographic areas, and mobilization of the process using mobile platforms (smartphones and tablets). The structure of the developed on-line system has three root modules; client, analysis server, and database servers. The system performs two levels of assessment. In this study, existing assessment methods have been implemented to the web-based analysis tool as well as new improved assessment techniques are proposed. The first method evaluates a building based on simple observable parameters (such as number of floors, window sizes... etc.) that can be entered by residents and non-technical people as well, while the second level requires a more comprehensive data entry including column locations and column geometric dimensions. The first level method has been improved by adding addi-

tional evaluation parameters and increased interaction between these parameters such as soil condition and building height (or period). The second developed technique is more advanced and has minimal structural analysis while approximately mimicking a full three-dimensional finite element analysis. The developed simplistic method and the advanced method are both experimentally implemented to the internet and results are correlated with other first level and SAP2000 analyses for randomly generated buildings and successful correlations were obtained.

Keywords: Earthquake, evaluation, on-line, seismic assessment, structural condition identification

ÖZ

MEVCUT BETONARME BİNALARIN DEPREM YÜKÜ ALTINDA YAPISAL PERFORMANS DEĞERLENDİRMESİ YAPAN İNTERNET TABANLI YAZILIM GELİŞTİRİLMESİ

Yücel, Mustafa Can

Doktora, İnşaat Mühendisliği Bölümü

Tez Yöneticisi : Prof. Dr. Ahmet Türer

Ocak 2017 , 172 sayfa

Yapısal durum tespiti, deprem riski altındaki ülkelerde, bina stokunun yaşlı ya da şüpheli binalar için, büyük bir deprem sonrasında ya da büyük deprem şartnamesi değişiklikleri sonrasında incelenmesi gerektiği için popüler bir alandır. Bu konuda birçok teknik önerilmiştir, ancak bu yöntemlerin, birçok avantajına rağmen internet tabanlı teknolojilerle birleştirilmesi nadirdir. Bu avantajlardan bazıları bina durum veri tabanlarının oluşturulması, diğer bulut bilişim sistemleri ile entegrasyon (örneğin GIS), donanım yeteneklerinin kullanılabilmesi (fotoğraf çekme, ses kayıtları, ivme ölçerler ile titreşim ölçülmesi, GPS ile yer bulma... vb.), otomatik yapılacak basit analizler ve raporlama, çok sayıda kişiye ve geniş coğrafi alanlara ulaşabilme, mobil platformlarla (akıllı telefon, tablet) işlemlerin hareket halinde de uygulanabilir olması şeklindedir. Geliştirilen internet tabanlı sistemin yapısı üç ana modülden oluşmaktadır; kullanıcı tarafı, analiz sunucusu ve veri tabanı sunucuları. Sistem iki seviye analiz yapmaktadır. Bu çalışmada, mevcut değerlendirme metotları internet tabanlı analiz yazılımına eklenmiş, ayrıca yeni geliştirilmiş değerlendirme metotları önerilmiş ve geliştirilmiştir. İlk yöntem bina sakinleri ve teknik olmayan kişiler tarafından girilebilen basit gözlemlerle elde edilebilen parametreler (kat sayısı, pencere boyutu... vb.) üzerinden bina değerlendirmesi yapmaktadır. İkinci yöntem ise kolon boyutları ve yerleri gibi daha detaylı veri girişine ihtiyaç duymaktadır. İlk seviye yöntem, yeni değerlendirme pa-

parametrelerinin eklenmesi ve bu parametrelerin birbiriyle etkileşimlerinin artırılması (örneğin zemin tipi ve kat sayısı/periyot gibi) şeklinde geliştirilmiştir. İkinci geliştirilen yöntem ise minimum yapısal analiz ile daha detaylıdır ve tam üç boyutlu sonlu elemanlar analizini yaklaşık olarak taklit etmektedir. Geliştirilen basit ve daha detaylı yöntemler deneysel olarak internet ortamına uyarlanmış, rastgele oluşturulmuş binalar için diğer birinci seviye yöntemler ve SAP2000 analizleri ile kontrol edilmiş ve başarılı korelasyonlar elde edilmiştir.

Anahtar Kelimeler: Deprem, değerlendirme, internet, sismik durum tespiti, yapısal durum tespiti

To my family

ACKNOWLEDGMENTS

Firstly, I would like to express my sincere gratitude to my advisor Prof. Dr. Ahmet Türer for the continuous support of my Ph.D study and related research, for his patience, motivation, and immense knowledge. His guidance helped me in all the time of research and writing of this thesis.

Besides my advisor, I would like to thank the rest of my thesis committee: Prof. Dr. Ahmet Yakut, Prof. Dr. Tamer Topal, Assoc. Prof. Dr. Baki Öztürk, and Assist. Prof. Dr. Saeid Kazemzadeh Azad, not only for their insightful comments and encouragement, but also for their questions which incited me to widen my research from various perspectives.

Last but not the least, I would like to thank my family: my parents for supporting me spiritually throughout writing this thesis and my life in general.

TABLE OF CONTENTS

ABSTRACT	v
ÖZ	vii
ACKNOWLEDGMENTS	x
TABLE OF CONTENTS	xi
LIST OF TABLES	xx
LIST OF FIGURES	xxii
LIST OF CODES	xxvi
LIST OF ABBREVIATIONS	xxvii
CHAPTERS	
1 INTRODUCTION	1
2 PREVIOUS STUDIES	3
2.1 Previous Studies and Methods On Rapid Seismic Vulnerability Assessment	3
2.1.1 First Level (Walk-Down) Methods	3
2.1.1.1 ATC21/FEMA154 Procedure	3
2.1.1.2 Sucuoğlu et al's Procedure	4

	2.1.1.3	RBTY Method	6
	2.1.1.4	FEMA 310 Tier 1 Method	8
2.1.2		Second Level (Preliminary) Methods	9
	2.1.2.1	Hassan and Sozen Method	9
	2.1.2.2	Rodriguez and Aristizabal Method	11
	2.1.2.3	Wasti, Sucuoğlu, and Utku Method for Damaged Buildings	11
	2.1.2.4	Using Artificial Neural Networks in Seismic Assessment	12
	2.1.2.5	Özcebe et al's Procedure	12
	2.1.2.6	P25 Method	13
	2.1.2.7	Yakut's Procedure	15
2.2		Previous Studies and Methods On Detailed Seismic Vulnerability Assessment	16
	2.2.1	Determination of Seismic Effect	17
	2.2.2	Determination of Structural Capacity	17
	2.2.2.1	Push-over Analysis	17
	2.2.2.2	N2 Method	20
	2.2.2.3	Time Domain Analysis	21
	2.2.3	Determination of Performance Point	22
	2.2.3.1	Capacity Spectrum Method	22
	2.2.3.2	Displacement Coefficients Method	23
	2.2.4	Determination of Seismic Performance of Structure	24

2.3	Previous Studies and Applications on On-line Assessment Solutions	24
2.3.1	Development of a Web-Based Information System for Urban Seismic Risk Management	24
2.3.2	Development of Internet Based Seismic Vulnerability Assessment Tools	26
2.3.3	Use of On-line Assessment Systems in Real Estate Business	27
3	AN IMPROVED WALK-DOWN METHOD	29
3.1	Proposed Algorithm	30
3.1.1	Evaluation Parameters	32
3.1.1.1	Number of Stories (N)	32
3.1.1.2	Seismicity (A)	32
3.1.1.3	Irregularities (I)	33
3.1.1.4	Heavy Overhangs (O)	34
3.1.1.5	Apparent Quality (AQ)	34
3.1.1.6	Building Order (BO) and Pounding (Hammering) Effect (H)	35
3.1.1.7	Short Column (SC)	35
3.1.1.8	Soft Story (SS)	36
3.1.1.9	Ground Slope (GS)	36
3.1.1.10	Local Soil Conditions (Z)	37
3.1.1.11	Construction Year (Y)	39
3.1.1.12	Window Size (W)	40

3.1.1.13	Basement (B)	40
3.1.1.14	Mezzanine (M)	41
3.1.1.15	Existing Minor Damage and Past Repairs (D)	41
3.1.1.16	Optional Parameters	42
3.1.1.16.1	Structural System and Shear Wall Spatial Distribution (SW ^o)	42
3.1.1.16.2	Presence of Strong Beam and Weak Column (SBWC ^o)	43
3.1.1.16.3	Fundamental Period (T ^o)	43
3.1.1.16.4	Stirrup Presence and Bending Angle (ST ^o)	44
3.1.1.16.5	Liquefaction (LI ^o)	45
3.1.2	Interaction of Evaluation Parameters	46
3.1.3	Calculating Overall Building Score	46
3.2	Comparison of Proposed Method and Discussion of Results	47
3.3	Limitations of the Proposed Method	50
3.4	PeriodFinder Android Application	51
4	A SIMPLIFIED CAPACITY DETERMINATION METHOD	59
4.1	Algorithm for Finding Structure Capacity Curve	60
4.1.1	Calculating Element Lateral Effective Stiffnesses	61
4.1.1.1	Columns	61
4.1.1.2	Verification of Column Results	64

	4.1.1.2.1	Height of the First Story	65
	4.1.1.2.2	Total Number of Stories	67
	4.1.1.2.3	Column Size	67
	4.1.1.2.4	Beam Size	69
	4.1.1.2.5	Compressional Strength of Concrete	70
	4.1.1.2.6	Column Size Changes In Upper Stories	73
	4.1.1.2.7	Discussion of Verification Results	74
	4.1.1.3	Shear Walls	74
	4.1.1.4	Verification of Shear Wall Approach	76
4.1.2		Creating Story Stiffness Matrix	77
4.1.3		Calculating Member Force-Deformation Relations	78
	4.1.3.1	Custom Force-Deformation Equation Set	80
	4.1.3.2	Using FEMA356 Modeling Parameters	82
	4.1.3.3	Member Section Analysis	82
	4.1.3.3.1	Calculating Section Yield Capacity	85
	4.1.3.3.2	Calculating Section Ulti- mate Capacity	86
	4.1.3.3.3	Converting Moment-Curvature to Moment-Rotation	87
4.1.4		Applying Unit Load to Story	89

4.1.5	Calculating Member End Deflections and Forces . . .	89
4.1.6	Finding First Yield Point of Structure (End of Linear Range)	91
4.1.7	Constructing Inelastic Region of Structure Capacity Curve	92
4.1.7.1	Optimizing For Force Equilibrium . . .	92
4.1.7.1.1	Numerical Unconstrained Optimization Methods . . .	93
4.1.7.1.2	Metaheuristic Algorithms	95
4.1.7.2	Implementing Custom Incremental Search Method	98
4.1.7.3	Implementing Custom Steepest Descent Algorithm	100
4.1.8	Converting Critical Story Displacements to Roof Displacements	102
4.2	Deciding Overall Seismic Condition	103
4.2.1	Finding Performance Point	103
4.2.1.1	Displacement Coefficients Method . . .	104
4.2.2	Calculating Seismic Performance Level	106
4.2.2.1	Turkish Earthquake Code Approach . .	106
4.2.2.2	A Simpler Approach	108
4.3	Verification and Comparison Analyses for Proposed Capacity Determination Method	109
4.3.1	Finite Element Modeling Notes	109
4.3.2	Symmetrical Structures With No Shear Walls . . .	110

4.3.2.1	Symmetrical Structure 1	110
4.3.2.2	Symmetrical Structure 2	110
4.3.2.3	Symmetrical Structure 3	112
4.3.2.4	Symmetrical Structure 4	112
4.3.2.5	Symmetrical Structure 5	115
4.3.2.6	Symmetrical Structure 6	116
4.3.3	Unsymmetrical Structures With No Shear Walls . .	117
4.3.3.1	Unsymmetrical Structure 1	117
4.3.3.2	Unsymmetrical Structure 2	117
4.3.4	Structures with Shear Walls	118
4.3.4.1	Shear Wall Structure 1	118
4.3.4.2	Shear Wall Structure 2	120
4.3.5	Comparison of Verification Analyses Results and Discussions	120
4.4	Limitations of the Proposed Method	125
5	DEVELOPMENT OF AN ON-LINE CONDITION ASSESSMENT SYSTEM	127
5.1	Overview of the System	128
5.2	Graphical User Interface	128
5.2.1	Standalone Software vs. Web Application	129
5.2.2	Web Application Properties	131
5.2.3	Technologies and Services Used	132

5.2.3.1	Programming Language	133
5.2.3.2	Web Application Framework	133
5.2.3.3	Web Application Architecture	133
5.2.3.4	Page Style and Design	134
5.2.3.5	Authentication and Authorization	135
5.2.3.6	Data Access Layer	136
5.2.3.7	Other Components	139
5.2.4	Visual Aid and Help System	139
5.2.5	Localization of User Interface	142
5.3	Database Layer	143
5.4	Analysis and Reporting Engine	143
5.4.1	Calculation Methods	146
5.4.1.1	Sample Method 1: Slab Area and Centroid Calculations	147
5.4.1.2	Sample Method 2: Walk-Down Method Calculations	149
5.4.2	File (IO) Methods	152
5.4.3	Reporting Methods	152
5.4.4	Shared Components	153
5.5	Combining Components and Deployment	154
6	CONCLUSIONS	157
6.1	First Level Building Evaluation Against Earthquakes	157

6.2	A New Capacity Calculation Method: Two and a Half Level Evaluation Against Earthquakes	159
6.3	A Web Application for Basic Seismic Assessment of Structures	160
6.4	Future Projections	162
REFERENCES		163
APPENDICES		
CURRICULUM VITAE		171

LIST OF TABLES

TABLES

Table 2.1	Ozcebe et al.'s Classification Criteria	13
Table 3.1	Parameters Included in Walk-Down Methods	31
Table 3.2	Scores for Apparent Quality (S_{AQ})	34
Table 3.3	Penalty Scores for Building Order and Pounding Effect (S_{BO})	35
Table 3.4	Penalty Scores for Ground Slope (S_{GS})	37
Table 3.5	Base Scores for Soil Types and Number of Stories (S_{soil})	38
Table 3.6	Bonus and Penalty Scores for Window Size (S_W)	40
Table 3.7	Bonus and Penalty Scores for Basement (S_B)	41
Table 3.8	Scores for Shear Wall Spatial Distribution (S_{SW})	42
Table 3.9	Penalty Scores for Presence of Strong Beam-Weak Column (S_{SBWC})	43
Table 3.10	Bonus and Penalty Scores for Stirrup Presence and Detailing (S_{ST})	44
Table 3.11	Minimum and Maximum Bounds for Evaluation Parameters	48
Table 3.12	Comparison of New Method with Existing Procedures	50
Table 4.1	Parameters Used and Their Default Values	65
Table 4.2	Parameter Sets and Their Values	80
Table 4.3	Modeling Parameters for Reinforced Concrete Columns by FEMA356	83
Table 4.4	Empirical Expressions for Plastic Hinge Length	88
Table 4.5	Member End Displacement Equation Signs	90
Table 4.6	System State at $\Delta_{yield} + n \cdot \varepsilon$	92

Table 4.7	Values for Modification Factor C_0 [1]	106
Table 4.8	Values for Modification Factor C_2 [1]	106
Table 4.9	Strain Limits for Columns in Turkish Earthquake Code	107
Table 4.10	Comparison of Verification Analyses Results	124

LIST OF FIGURES

FIGURES

Figure 2.1	FEMA-154 Data Collection Form for High Seismicity Regions . . .	5
Figure 2.2	Hassan Sozen Method Resultant Chart	10
Figure 2.3	Capacity Spectrum Method Procedure A	23
Figure 2.4	Risk Based Approach for Seismic Risk Analysis and Management .	25
Figure 2.5	Spectral Amplification Ratio Mapping for Quebec City	26
Figure 3.1	Penalty Scores for Soil Types and Number of Stories	38
Figure 3.2	Interaction of Walk-Down Parameters	47
Figure 3.3	Sliding-MAC Search with Perfect Reference Wave	55
Figure 3.4	Sliding-MAC Results for Complex Search, $f=1.1\text{Hz}$	56
Figure 3.5	Sliding-MAC Results for Complex Search, $f=0.1\text{Hz}$	57
Figure 3.6	Sliding-MAC Results for Complex Search, $f=0.3\text{Hz}$	57
Figure 3.7	Different Screens of the Application	58
Figure 4.1	Inner and Outer 2-D “Ladder” Structures and Respective DOFs . .	62
Figure 4.2	Sub-Matrices of Overall Stiffness Matrix	63
Figure 4.3	Effect of First Story Height on Stiffness Coefficient - 1	66
Figure 4.4	Effect of First Story Height on Stiffness Coefficient - 2	66
Figure 4.5	Ladder Approach vs SAP2000 Results for First Story Height	67
Figure 4.6	Effect of Number of Stories on Stiffness Coefficient	68
Figure 4.7	Ladder Approach vs SAP2000 Results for Total Number Of Stories	68

Figure 4.8 Effect of Column Size on Stiffness Coefficient	69
Figure 4.9 Ladder Approach vs SAP2000 Results for Column Size	69
Figure 4.10 Effect of Beam Size on Stiffness Coefficient - 1	70
Figure 4.11 Effect of Beam Size on Stiffness Coefficient - 2	71
Figure 4.12 Ladder Approach vs SAP2000 Results for Beam Size	71
Figure 4.13 Effect of Compressive Strength on Stiffness Coefficient	72
Figure 4.14 Ladder Approach vs SAP2000 Results for Compressive Strength of Concrete	72
Figure 4.15 Column Size Control Structures	73
Figure 4.16 Effect of Column Size Variation Along Height	74
Figure 4.17 Shear Wall Stiffness Components	75
Figure 4.18 Components of Shear Wall Stiffness	76
Figure 4.19 Shear Wall FEM Details	77
Figure 4.20 Shear Wall Approach Comparison Results	77
Figure 4.21 Stiffness Calculations for Most Critical Story	79
Figure 4.22 Possible Element Capacity Types	79
Figure 4.23 Proposed Equation Types for Regions	80
Figure 4.24 Overall Force-Deformation Relation	81
Figure 4.25 Results of Four Parameter Sets	81
Figure 4.26 Generalized Force-Deformation Relations for Concrete Elements	82
Figure 4.27 Sample Longitudinal Reinforcement Distributions	84
Figure 4.28 A General Interaction Diagram	85
Figure 4.29 Column Sectional Response at Yield Point for Two Axes	86
Figure 4.30 Deformations at Yielding Instant	87
Figure 4.31 Signs of Column End Displacements	90
Figure 4.32 Relation of Unit Force With Yield Base Shear for Structure	91
Figure 4.33 Resultant Capacity Curve	93

Figure 4.34 Level Sets for a Steepest Descent Solution	101
Figure 4.35 Finding Next Guess	102
Figure 4.36 Displacement Patterns for Different Structure Types	103
Figure 4.37 Bilinear Capacity Curve for Displacement Coefficients Method	104
Figure 4.38 Symmetrical Verification Structure 1	111
Figure 4.39 Analyses Results for S1	111
Figure 4.40 Symmetrical Verification Structure 2	112
Figure 4.41 Analyses Results for S2	113
Figure 4.42 Symmetrical Verification Structure 3	113
Figure 4.43 Analyses Results for S3	114
Figure 4.44 Symmetrical Verification Structure 4	114
Figure 4.45 Analyses Results for S4	115
Figure 4.46 Symmetrical Verification Structure 5	115
Figure 4.47 Analyses Results for S5	116
Figure 4.48 Symmetrical Verification Structure 6	116
Figure 4.49 Analyses Results for S6	117
Figure 4.50 Unsymmetrical Verification Structure 1	118
Figure 4.51 Analyses Results for Unsymmetrical Structure 1	119
Figure 4.52 Unsymmetrical Verification Structure 2	120
Figure 4.53 Analyses Results for Unsymmetrical Structure 2	121
Figure 4.54 Shear Wall Structure 1	122
Figure 4.55 Analyses Results for Shear Wall Structure 1	122
Figure 4.56 Shear Wall Structure 2	123
Figure 4.57 Analyses Results for Shear Wall Structure 2	123
Figure 5.1 Generic and ASP.NET MVC Implementations	134
Figure 5.2 Help Hyperlink for ‘Soft Story’ Question	140

Figure 5.3	Modal Help Page for ‘Soft Story’ Question	140
Figure 5.4	Localization Syntax in Page	143
Figure 5.5	Database ER Diagram for Application Data	144
Figure 5.6	Database ER Diagram for Users	145
Figure 5.7	An Overview of Several Calculation Methods	147
Figure 5.8	Codemap	155

LIST OF CODES

CODES

Code 5.1	data-checkId Attribute for Modal Help Windows	141
Code 5.2	Sample Slab Calculations in C#	148
Code 5.3	Sample Sucuoglu Calculations in C#	150

LIST OF ABBREVIATIONS

API	Application programming interface
CM	Center of mass
CR	Center of rigidity
CQC	Complete quadratic combination
DOF	Degree of freedom
f_c	Compressive strength of concrete
GUI	Graphical user interface
ISD	Inter-story drift ratio
MCI	Modal criticality index
MPA	Modal pushover analysis
OS	Operating System
SRSS	Square root of sum of squares
WPF	Windows Presentation Foundation
ρ_s	Volumetric ratio of existing lateral reinforcement in the element
ρ_{sm}	Volumetric ratio of required lateral reinforcement in the element

CHAPTER 1

INTRODUCTION

Structural evaluation (or assessment) against seismic hazard is commonly defined as the process of determining the damage level a structure will sustain when it is subjected to an earthquake. There are different levels of seismic assessment, each yielding more accurate and detailed results yet requiring more information and computation time than the previous level. The lowest tier is called walk-down surveys. As the name implies, the objective is to rank the structures by seismic risk based on the information that could be collected by walking in and around the structure. The second tier of assessment is called preliminary; though more calculation involved than walk down surveys, these assessments only need basic numerical data such as total height, column and shear wall areas... etc. This level of assessment has the ability to rank structures based on numerical calculations, yet it does not return a definitive and final evaluation result; the only analyses outputs are risk status with respect to other structures in the stock. To obtain a definite answer for earthquake risk, detailed level (third tier) analyses should be utilized. These computations require extensive amount of work for both data acquisition (such as determination of reinforcement sizes and locations, material properties, soil conditions, nearest faults... etc.) and analysis (creation and calibration of finite element models, defining analysis properties, post-processing results into meaningful parameters and predicting structural condition based on these result... etc.). Therefore, if the target building stock is too large (for example; the scale of a medium or large city), the most common practice is first to determine the most critical structures with walk down methods, then ranking by preliminary approaches, and finally applying detailed analysis based on the ranking determined in a previous step.

There are different methods defined in the literature for these assessment layers, but the number of studies that combine these techniques with the power of Internet-based technologies for a centralized assessment network is inadequate. Network-based approaches will have many advantages and superiorities to traditional methods in terms of solution speed, process and result standardization, widespread use, and mobility. In this study, development of an on-line structural seismic hazard evaluation software will also be researched. In addition, during the course of the study, the existing walk-down and preliminary methods will be analyzed for incorporating additional parameters that are found to play a critical role in the dynamic response of the structure. By this way, new and more effective methods are to be devised for further academic research.

Advanced non-destructive techniques (NDT) are not commonly used in standard assessment applications. The most conventional NDT used is Schmidt hammer, and most of the time destructive methods such as core drilling are utilized that damage the structure and are not easy to apply (considering the messy application and number of samples required). There are several high-technology NDT methods (such as dynamic tests under ambient vibration, Windsor probe, reinforcement radars) that will provide useful information about the structure if applied during the assessment process. This study also aims to incorporate these contemporary solutions with the web-powered assessment techniques.

The first objective of this study is creating a new walk-down screening procedure and a simplified method for obtaining capacity curve of a structure, which is essential for seismic performance assessment of structures.

As a second objective, an on-line system will be created for a centralized seismic assessment service, which can be used both by professionals and public. Non-technical people will be able to perform first two levels of analyses and obtain an automatically-generated report which includes both assessment results and informative sections to increase public awareness towards seismic events and basic principles of earthquake-resistant design.

CHAPTER 2

PREVIOUS STUDIES

In this section, the previous studies done on seismic vulnerability assessment and its on-line application implementations will be presented.

2.1 Previous Studies and Methods On Rapid Seismic Vulnerability Assessment

2.1.1 First Level (Walk-Down) Methods

2.1.1.1 ATC21/FEMA154 Procedure

Many institutions and agencies published guidelines for outlining the basic concepts of walk-down assessment procedures due to the fact that visual screening is a highly subjective approach which almost completely depends on the experience and individual judgment of the inspector. Two of these publications are *FEMA 154 Rapid Visual Screening for Potential Seismic Hazards: A Handbook* and *FEMA 155 Rapid Visual Screening for Potential Seismic Hazards: Supporting Documentation* [2]. These documents were developed by the Applied Technology Council (ATC) and were referred to as ATC 21. In 1996, ATC, under the contract with Federal Emergency Management Agency (FEMA), published a training manual and a slide set to accompany FEMA 154 that was referred to as ATC 21-T. In 2002, FEMA published the second version of FEMA 154. This second edition was also prepared by ATC. These projects were funded by FEMA under the National Earthquake Technical Assistance Program.

The evaluation parameters used in this procedure are [2]:

1. Earthquake intensity, with the parameter peak ground acceleration obtained from available national hazard maps.
2. Building type such as timber, masonry, reinforced concrete, steel . . . etc.
3. Age
4. Material condition
5. Configuration

Vulnerability assessment is done by a score-based procedure where first a basic structural score (BSS) is assigned to the structure according to construction type. Then BSS is modified by bonuses and penalties according to structural and seismic properties of the structure and the location. The final score (S) is calculated by summing the bonuses and subtracting the penalties from BSS as in Equation (2.1), and if the final score of the target structure is less than three, it is concluded that detailed evaluation is required for the building.

$$S = BSS + \sum \text{bonuses} - \sum \text{penalties} \quad (2.1)$$

There are three predefined forms to be used during screening procedure in different seismic zones; low, medium and high. A form for a “high seismicity” region can be seen in Figure 2.1.

2.1.1.2 Sucuoğlu et al’s Procedure

This procedure is one of the widely recognized walk-down methods (which are few in number). It is proposed based on statistical correlations between damage and several structural parameters, and the calibration studies are done on 1999 Düzce earthquake database [3]. Similar to other rapid screening methods, the aim is to assess the severity of the current condition of the structure based on different visible parameters.

The evaluation parameters are:

- Earthquake intensity, based on peak ground velocity (PGV) of three zones,
- Total number of stories,

Rapid Visual Screening of Buildings for Potential Seismic Hazards
 FEMA-154 Data Collection Form

HIGH Seismicity

<p>Scale: _____</p>	Address: _____ _____ Zip _____ Other Identifiers _____ No. Stories _____ Year Built _____ Screener _____ Date _____ Total Floor Area (sq. ft.) _____ Building Name _____ Use _____														
PHOTOGRAPH															
OCCUPANCY SOIL TYPE FALLING HAZARDS															
Assembly Commercial Emer. Services	Govt Historic Industrial	Office Residential School	Number of Persons 0 – 10 11 – 100 101-1000 1000+	A Hard Rock	B Avg. Rock	C Dense Soil	D Stiff Soil	E Soft Soil	F Poor Soil	<input type="checkbox"/> Unreinforced Chimneys	<input type="checkbox"/> Parapets	<input type="checkbox"/> Cladding	<input type="checkbox"/> Other:		
BASIC SCORE, MODIFIERS, AND FINAL SCORE, S															
BUILDING TYPE	W1	W2	S1 (MRF)	S2 (BR)	S3 (LM)	S4 (RC SW)	S5 (URM INF)	C1 (MRF)	C2 (SW)	C3 (URM INF)	PC1 (TU)	PC2	RM1 (FD)	RM2 (RD)	URM
Basic Score	4.4	3.8	2.8	3.0	3.2	2.8	2.0	2.5	2.8	1.6	2.6	2.4	2.8	2.8	1.8
Mid Rise (4 to 7 stories)	N/A	N/A	+0.2	+0.4	N/A	+0.4	+0.4	+0.4	+0.4	+0.2	N/A	+0.2	+0.4	+0.4	0.0
High Rise (> 7 stories)	N/A	N/A	+0.6	+0.8	N/A	+0.8	+0.8	+0.6	+0.8	+0.3	N/A	+0.4	N/A	+0.6	N/A
Vertical Irregularity	-2.5	-2.0	-1.0	-1.5	N/A	-1.0	-1.0	-1.5	-1.0	-1.0	N/A	-1.0	-1.0	-1.0	-1.0
Plan Irregularity	-0.5	-0.5	-0.5	-0.5	-0.5	-0.5	-0.5	-0.5	-0.5	-0.5	-0.5	-0.5	-0.5	-0.5	-0.5
Pre-Code	0.0	-1.0	-1.0	-0.8	-0.6	-0.8	-0.2	-1.2	-1.0	-0.2	-0.8	-0.8	-1.0	-0.8	-0.2
Post-Benchmark	+2.4	+2.4	+1.4	+1.4	N/A	+1.6	N/A	+1.4	+2.4	N/A	+2.4	N/A	+2.8	+2.6	N/A
Soil Type C	0.0	-0.4	-0.4	-0.4	-0.4	-0.4	-0.4	-0.4	-0.4	-0.4	-0.4	-0.4	-0.4	-0.4	-0.4
Soil Type D	0.0	-0.8	-0.6	-0.6	-0.6	-0.6	-0.4	-0.6	-0.6	-0.4	-0.6	-0.6	-0.6	-0.6	-0.6
Soil Type E	0.0	-0.8	-1.2	-1.2	-1.0	-1.2	-0.8	-1.2	-0.8	-0.8	-0.4	-1.2	-0.4	-0.6	-0.8
FINAL SCORE, S															
COMMENTS _____ _____ _____													Detailed Evaluation Required YES NO		

* = Estimated, subjective, or unreliable data BR = Braced frame MRF = Moment-resisting frame SW = Shear wall
 DNK = Do Not Know FD = Flexible diaphragm RC = Reinforced concrete TU = Tilt up
 LM = Light metal RD = Rigid diaphragm URM INF = Unreinforced masonry infill

Figure 2.1: FEMA-154 Data Collection Form for High Seismicity Regions

- Presence of soft story,
- Presence of short column,
- Apparent quality,
- Overhang,
- Topographic effect,
- Pounding.

Similar to ATC 21 method, Sucuoğlu's procedure is also a score-based technique. The overall vulnerability score (PS) is calculated as in Equation (2.2).

$$PS = \text{Initial Score} + \sum (\text{parameter} \cdot \text{score}) \quad (2.2)$$

The vulnerability score is compared with the statistical processing results of the Düzce earthquake database, and the need for additional assessment is decided accordingly.

2.1.1.3 RBTY Method

This method is proposed in the latest (2013) Turkish Seismic Assessment Code version [4] for ranking structures in a large building stock in order to determine their priority level of detailed analysis need. It has two distinct versions; one for reinforced concrete and another for masonry buildings. The survey is quite detailed and includes several parameters like building order and adjacent slab levels, which are not considered in any other existing screening procedure. It is applicable to buildings with up to 7 stories, and has the following evaluation parameters for reinforced concrete structures:

- Structural system type, as 'reinforced concrete frame' or 'reinforced concrete frame with shear walls'.
- Number of free stories, which is determined from the total number of stories and the condition of the low-level floors. If these stories are under the ground

level, free story count is determined according to the figures given in the specification (Figure A.1)

- Apparent quality, as good, mediocre, or bad
- Soft/Weak story
- Vertical irregularity
- Horizontal irregularity
- Heavy overhangs
- Plan irregularity/torsional effects
- Short column effect
- Building order/pounding, where the location of a structure in a group of adjacent structures is evaluated
- Slope effect, as low or high slope
- Earthquake zone and soil types

For masonry structures, the list changes almost completely and includes the following evaluation parameters:

- Masonry structure type, as ‘combined masonry and reinforced concrete’, ‘reinforced masonry’ . . . etc.
- Free story count, defined as in reinforced concrete structures
- Building order/pounding, defined as in reinforced concrete structures
- Apparent quality, defined as in reinforced concrete structures
- Plan irregularity, defined by the presence of lentos and the ratio of voids to the overall wall length. It is classified as low, medium, and high.
- Vertical irregularity, defined by the presence of soft story and order of voids such as windows and doors. It is classified as low, medium, and high.

- Wall discontinuities
- Out-of-plane behaviors such as lack of rigid slab, out of plane movements, and the presence of shield walls.
- Presence of soil on roof (roof type)
- Earthquake zone and soil type

The overall score of the structure is determined by Equation (2.3) where PP is performance point, TB is base score determined according to the earthquake zone and soil type, O_i is evaluation parameter, OP_i is the corresponding penalty score, and YSP is structural system score.

$$PP = TP + \sum_{i=1}^n O_i \cdot OP_i + YSP \quad (2.3)$$

2.1.1.4 FEMA 310 Tier 1 Method

The American Society of Civil Engineers (ASCE) contracted with FEMA to convert *FEMA 178, NERHP Handbook for the Seismic Evaluation of Existing Buildings* into a pre-standard. The development of the pre-standard was the first step in turning FEMA 178 into an American National Standards Institute (ANSI) approved national consensus standard. The document was completed in 1998 and is published as *FEMA 310, the handbook for the Seismic Evaluation of Buildings – A Pre-standard* [5]. After these works are completed, FEMA 310 has turned into a national consensus-based standard as ASCE 31-02 which supersedes FEMA 310.

The evaluation process consists of three tiers, screening phase (Tier 1), evaluation phase (Tier 2), and detailed evaluation phase (Tier 3). The purpose of a Tier 1 evaluation is to screen out buildings that comply with the provisions of FEMA 310 or quickly identify potential deficiencies. In some cases “Quick Checks” may be required during a Tier 1 evaluation, however, the level of analysis necessary is minimal. If deficiencies are identified for a building using the checklists, the design professional may proceed to Tier 2 and conduct a more detailed evaluation of the building or conclude the evaluation and state that potential deficiencies were identified. In some cases, a Tier 2 or Tier 3 evaluation may be required.

Screening phase (Tier 1) includes checklists and quick calculations for computing the stiffness and strength of certain building components to see whether these parameters comply with the certain evaluation criterion. Some of these quick calculations include the base and story shear forces, story drifts for moment frames, and element forces.

Evaluation phase (Tier 2) includes an analysis using one of the following linear methods: linear static, linear dynamic, special. If further deficiencies are found in a Tier 2 analysis, the designer may want to proceed with a Tier 3 analysis or he may report these deficiencies directly.

2.1.2 Second Level (Preliminary) Methods

2.1.2.1 Hassan and Sozen Method

Hassan and Sozen [6] proposed a method for assessing the seismic vulnerability of a structure based on column and wall dimensions (both shear and infill walls are considered), and it is seen as one of the very first and fundamental studies on the preliminary assessment. The method is a graphical technique; the scatter plotted “wall index (WI)” and “column index (CI)” values are said to yield a rank for the expected damage. These parameters are calculated as in Equations (2.4) and (2.5).

$$\text{Wall Index (WI)} = \frac{A_{cw} + A_{mw}/10}{A_{ft}} \cdot 100 \quad (2.4)$$

$$\text{Column Index (CI)} = \frac{A_{ce}}{A_{ft}} \cdot 100 \quad (2.5)$$

It should be noted that as a preliminary method, this technique results in ordering the level of seismic risk for a group of buildings; it does not give a conclusive answer for damage prediction. The parameter “priority index” (PI) is simply the sum of the wall index and column index, and for a building stock, a lower PI value is predicted as an earlier need for action than a structure with higher PI [7]. Still, authors of this study used their method on a stock of structures, which consists of Erzincan earthquake database and several other buildings, and determined two boundaries for light, moderate, and severe damage levels (Figure 2.2).

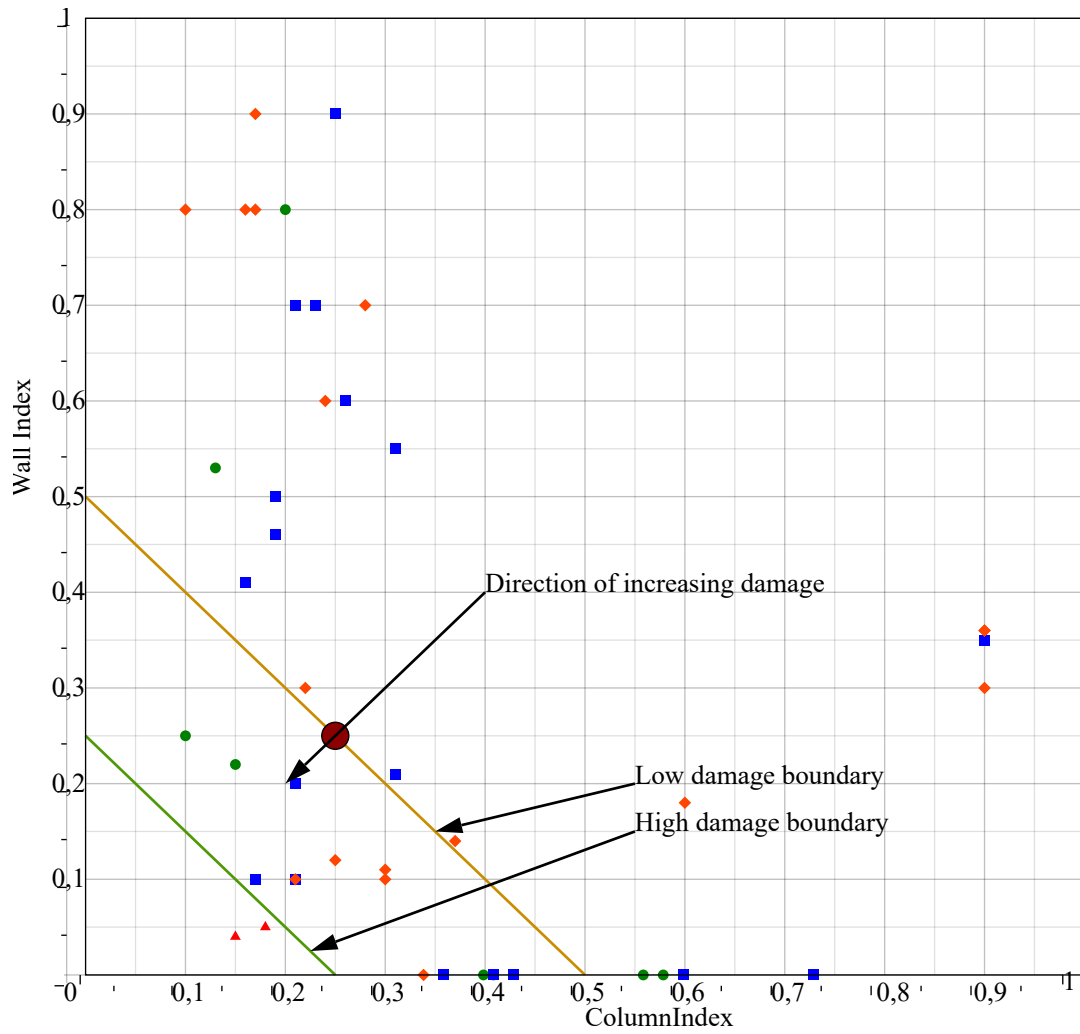


Figure 2.2: Hassan Sozen Method Resultant Chart

2.1.2.2 Rodriguez and Aristizabal Method

Rodriguez and Aristizabal proposed a parameter [8] that can be used in assessment considering the concept of energy dissipated by a single degree of freedom system and several other parameters related to the target structure (Equation (2.6)).

$$I_d = \frac{\gamma^2 E_h}{(2\pi\lambda h D_{rd})^2} \quad (2.6)$$

The numerator of Equation (2.6) is a measure of the hysteretic energy dissipated by a multi-story structure responding to an earthquake, and the denominator is the energy absorbed in a full cycle by an elastic model of the multi-story structure (assuming maximum overall drift values are $+D_{rd}$ and $-D_{rd}$). This parameter is tested using 11 different ground motions, and the authors conclude that I_d parameter could be used as a measure of structural response, therefore could be used for rapid assessment of reinforced concrete buildings.

It should be noted that the proposed parameter does not include structural information except number of stories and fundamental period of the structure (which is a function of mass and stiffness of the structural system). The presence and effect of columns and shear walls are embedded in the dynamic properties.

2.1.2.3 Wasti, Sucuoğlu, and Utku Method for Damaged Buildings

Unlike the other methods, this method is developed for quickly assessing the damage in a building after an earthquake [9]. Individual member type damage grades (D_m) are calculated for all members of the structure, and then they are summed to obtain total member damage grade (TMDG) of the target building, which is in turn used for computing structural damage grade (SDG) (Equations (2.7) and (2.8)).

$$D_m = \alpha_m \frac{(1 \cdot L + 2 \cdot M + 4 \cdot S)}{N_m} \quad (2.7)$$

$$\text{SDG} = \text{TMDG} \cdot 100(4\delta_b + 8\delta_c + 24\delta_{sw} + 4\delta_j + 2\delta_i) \quad (2.8)$$

In this set of equations, parameter δ is the presence factor and it is either 0 or 1, depending on the existence of the member type it belongs (b: beam, c: column, sw: shear wall, j: connection, i: infill wall). The damage grade calculated is used to classify the status of the building as “no/light/moderate/heavy structural damage”.

This method is intended for rapid screening of buildings of an area after an earthquake happens, which is different from other application methods listed in this section.

2.1.2.4 Using Artificial Neural Networks in Seismic Assessment

The use of the artificial neural networks (ANN) in all fields of engineering increased significantly in the recent decade due to the rapid increase in computation power and memory capabilities of modern computers. Training an ANN on an earthquake damage database and using this trained network for determining expected damage levels is an alternative approach to empirical or analytical solutions. In 2005, Guler proposed an approach using neural networks to assess seismic performance based on several input variables [10]. These parameters considered in training ANN are number of stories, normalized redundancy score, soft story index, overhang ratio, and total column and wall area. The databases used for training are Düzce, Afyon, Erzincan, Ceyhan, and Zeytinburnu. In the study, different levels and configurations of ANN are created and processed, and as a conclusion, almost 85% successful prediction rate is achieved.

2.1.2.5 Özcebe et al's Procedure

In this procedure, the effect of several structural parameters on the response of building to a specific ground motion is studied by statistical tools, similar to other preliminary methods [11]. The evaluation parameters are:

- Number of stories (n),
- Minimum normalized lateral stiffness index ($mnlstfi$), an indication of the lateral rigidity of ground story, which is most of the times most critical floor,
- Minimum normalized lateral strength index ($mnlssi$), a clue on the base shear capacity of the critical floor,
- Normalized redundancy score (nrs),
- Soft story index (ssi),

- Overhang ratio (*oh*).

In the technique, two different damage indices (for life safety and immediate occupancy) are calculated as in Equations (2.9) and (2.10).

$$DI_{LS} = 0.620n - 0.246mnlstfi - 0.182mnlisi - 0.699nrs + 3.269ssi + 2.728or - 4.905 \quad (2.9)$$

$$DI_{IO} = 0.808n - 0.334mnlstfi - 0.107mnlisi - 0.689nrs + 0.508ssi + 3.884or - 2.868 \quad (2.10)$$

Limits for these indices are expressed in terms of cutoff functions that are based on number of stories only:

$$CF(lspc) = -0.090 \cdot n^3 + 1.498 \cdot n^2 - 7.518 \cdot n + 11.885 \quad (2.11)$$

$$CF(iopc) = -0.085 \cdot n^3 + 1.416 \cdot n^2 - 6.951 \cdot n + 9.979 \quad (2.12)$$

The overall judgment on the seismic performance of analyzed structure is given based on both of Equations (2.11) and (2.12); decision table is given in Table 2.1.

Table 2.1: Ozcebe et al.'s Classification Criteria

Classification	Indicator Variable		Result	Result Definition
	LSPC	IOPC		
Safe	0	0	0	None or light damage
Unsafe	1	1	1	Severe damage or collapse
Intermediate	1	0	2	Further analysis required
Intermediate	0	1	2	Further analysis required

As seen, if life safety and immediate occupancy levels yield inconsistent results, method does not reach a definitive conclusion, and suggests further investigation. The accuracy of the proposed methodology is validated for 1992 Erzincan and 2002 Afyon earthquake databases, and it is claimed that reasonably high correct estimations are obtained.

2.1.2.6 P25 Method

This method is a highly detailed preliminary technique which originated from the method first published by Tezcan and Bal in 2002 [12]. After conducting studies and

research, this method was improved and renamed as P24, and then within a TUBITAK funded research, it took its final form as P25.

It is a combination of walk-down and preliminary assessment approaches; several evaluation parameters are determined as per a screening procedure, and the others are calculated as in preliminary approaches. The parameters involved are as follows [13]:

P1 is the basic structural score and it is determined according to the following structural properties:

- Torsional irregularity
- Slab discontinuity
- Vertical discontinuity
- Mass irregularity
- Corrosion presence
- Heavy facade elements
- Mezzanine presence
- Partial basement or uneven floor heights
- Concrete quality
- Strong beam-weak column
- Stirrup spacing
- Soil class
- Foundation type
- Foundation depth

P2 represents short column presence and determined from the ratio of short column length to the story height.

P3 represents soft story presence and determined using story heights and effective stiffness values of columns, shear walls and infill walls.

P4 represents overhangs and frame discontinuities.

P5 represents pounding effect and determined in a similar approach with RBTY method.

P6 represents liquefaction potential and calculated according to the ground water table level.

P7 represents soil movements such as large settlements, landslides, retaining wall collapses...etc. The possibility of these events should be determined separately.

α represents the correction factor to be applied to the minimum of the P_i scores defined above. It is a function of building importance factor, earthquake zone, live load coefficient, and topographical conditions.

β represents the correction factor for the interaction of the P_i scores defined above and has predefined values which are calculated empirically.

2.1.2.7 Yakut's Procedure

This method determines the condition of the target structure as either safe or unsafe based on a capacity index that is calculated and modified according to the following structural properties [14]:

- Member sizes and orientations
- Material properties
- Architectural features
- Quality of workmanship

In order to calculate the basic capacity index (BCPI), the parameter yield base shear capacity with infill walls is required (V_{yw}), which in turn is a function of yield base shear capacity (V_y) (Equation (2.13)).

$$\text{BCPI} = \frac{V_{yw}}{V_{code}} \quad (2.13)$$

For taking the effects of architectural and other factors, the basic capacity index is modified by coefficients, and the result is called the capacity index (CPI) (Equation (2.14)).

$$\text{CPI} = C_A C_M \text{BCPI} \quad (2.14)$$

In Equation (2.14), the coefficient C_A represents the effects of soft story, short column, plan irregularities, overhang, and vertical discontinuities whereas the coefficient C_M represents the quality of construction and workmanship.

One of the powerful aspects of this approach is said to be combining the effect of soil properties and seismicity of target location via the V_{code} parameter.

The method is tested and verified on different databases of earthquakes happened in Turkey in recent decades such as Erzincan (1992), Afyon (2002), Bingöl (2003).

2.2 Previous Studies and Methods On Detailed Seismic Vulnerability Assessment

Beyond preliminary assessment methods, the detailed approaches exist where mathematical finite element models of the structures are constructed and then analyzed using expected ground motions. These analyses are much more complex than walk-down and preliminary methods, therefore they require more time and computing power. Because of these reasons, only a small portion of the overall structure stock could be assessed in detail within a limited time and budget.

There are different methods for determining the seismic performance of a structure from analysis results even though modeling and analysis parameters are common. The acceptance criteria are given in terms of deformations such as strains in members or rotations of joints.

The general path to be followed in detailed methods is first determination of earthquake effect (seismic load), then calculating the response of the structure to this load, and then finding the structural demand. After the displacement demands are found, the member end deformations (strains or rotations) are compared with their respective capacities, and seismic performance of the structure is calculated based on the ratio of failed members. This flow could be applied either by time-history or pushover analysis methods.

Some of the detailed methods to be followed during this study are defined in Turkish Earthquake Code 2007, FEMA 273/356 and ATC 40.

2.2.1 Determination of Seismic Effect

The seismic effect used for finding the performance point of a structure by pushover analysis is almost always response spectrum graphs for a constant damping ratio (typically 5%). The response spectrum could be obtained using a specific (synthetic or real) earthquake record. In this case, the “minimum number of earthquakes” conditions in the codes should be met. Alternatively, the design spectrum given in specifications could also be used.

In time history analysis, the applied dynamic excitation is earthquake accelerograms directly.

2.2.2 Determination of Structural Capacity

2.2.2.1 Push-over Analysis

The most common method to find the capacity of a structure is pushover analysis (sometimes referred *quasi-static* to indicate variance of loads over time), which gives envelope behavior of the structure. It could be done either as force or displacement controlled, thus requires statically applied load/displacement distribution. It uses member load-deformation envelopes and results in a response that is valid for all seismic actions (i.e. results are independent of seismic activity). The essence is to push the structure step by step where a member yields in every increment, reducing the overall stiffness. The base shear and roof displacement values are recorded for every step, and by plotting this base shear versus displacement graph gives the capacity of the structure. Although simple in theory, the nonlinear nature of materials and structural behavior makes this analysis type more difficult to apply. The overall response of the system is also highly affected by the torsional condition of the building [15]. In addition, the dominant presence of higher modes in a structure changes the approximated response, therefore if participation ratios of these modes are too significant to be neglected, they should be included in the analysis as well [16].

Using non-linear static analysis in conjunction with some simplified procedures relies on an equivalent single degree of freedom (SDOF) system. This approach is

first introduced by Saaidi and Sozen at the beginning of 1980s [17]. In this paper, the technique followed was representing the force-deformation relation of an SDOF system by top displacement and overturning moment under triangular loading, and this opened the path to contemporary pushover analyses approaches. Nevertheless, as SDOF systems can represent only single mode at a time, the accuracy of this simplification is always a debate and a field of research. The early conclusions were that structures whose behavior is heavily influenced by the first mode, nonlinear pushover is superior to standard elastic analysis as it can display manifestations of structural weaknesses invisible otherwise [18]. Nonetheless, many efforts are made to incorporate the effect of higher modes, as modern structures rarely show single mode dominant behavior. One way of admittance of higher modes is proposed to be modifying the load vector according to the mode shapes. Combining these orthogonal vectors by directional vector addition (SRSS) is said to result in more accurate values [19]. However, even with these improvements, the accuracy of nonlinear static analyses is said to be mediocre at best for long-period buildings, which has roots in the fact that constant load distribution failing to capture higher mode effects within post-elastic range [20]. The most basic precaution against deviations caused by this effect is introducing separate response parameters at different stages of analysis, in other words, “adapting” the parameters to the pushover stage. This adaptive approach is first suggested by Bracci et. al. [21], by dividing the overall response into four phases (elastic, transition, mechanism formation, and failure). Later, Gupta and Kunnath improved this method by proposing to re-calculate every modal property on each lateral load increment instead of four stages only [22]. This approach greatly improved the errors caused by the changes in the structure during the analysis process, yet deviations caused by higher mode effects were unaffected. Antoniou and Pinho first proposed that combining modal static forces before analysis rather than adding results after will yield increased accuracy [23]. Later, they improved their own approach by considering a displacement-based adapting; a deformation created by utilizing an adequate number of modes summed via a combination rule is applied to the structure [24]. However, with all these improvements, single mode pushover analysis still cannot achieve the accuracy of time-history calculations, especially for high-rise buildings where higher modes are much more dominant than the fundamental mode [25]. Moreover, increased complexity of these approaches makes time domain analyses more ap-

pealing for engineers as the amount of computation power and time are comparable in both cases but obtained results are not of equal quality.

Realizing the ineffectiveness of representing all modes with a single load effect (force or displacement), researchers turned to multiple pushover analyses, one for each mode with its own loading pattern. Instead of combining these orthogonal vectors, Paret et al. suggested to determine the most critical mode by Modal Criticality Index (MCS) [26]. This procedure is formally named as “Modal Pushover Analysis” (MPA) and extended such that each modal response is computed separately and finally combined with SRSS or CQC [27]. Verifying this approach on regular frames acquainted that it is superior to conventional pushover types and yields similar results to nonlinear time-history analysis [28]. Even so, further investigations revealed out that vertical irregularities [29] and horizontal unsymmetrical distributions [30] cause unexpected deviations which cause member forces exceeding their capacities [31]. They proposed several remedies for overcoming these effects, and newer procedures are also developed incorporating joint uses of capacity spectrum method (Section 2.2.3.1), MPA, and adaptive pushover approaches [32]. Further studies for increasing the accuracy and decreasing required computing power also continues; limiting the number of parameters updating so that performing lesser re-analyses are suggested to be effective if results are combined by modal combinations [33]. Pushover analyses techniques are also improved on different fields than how to include higher modes, such as seismic effects on two orthogonal directions simultaneously. Three-dimensional MPA is suggested by Reyes and Chopra [34] where two orthogonal horizontal directions are analyzed and results are combined by multi-component SRSS.

Alternative approaches for incorporating higher modes include using various parameters such as force vectors or energy. Capacity curves of individual modes are created using the amount of absorbed energy during pushover analysis for taking higher modes into account, and energy-based deformations are calculated [35]. Other techniques include the use of “generalized force vectors”, which is defined as the forces acting on the structure at the moment a specific response variable is at its maximum [36]. It is claimed that these vectors include the manifestation of all modes, and if applied to the system they belong, the peak value of the respective parameter will be achieved. Later, its usability is validated by proving that mean response spectrum

for force vectors lead to similar results to an average of the results of a set of strong ground motions [37].

Aside from higher modes, torsional irregularities are one of the largest sources of errors in pushover procedures. Considerable effort was made in the last decades to minimize deviations due to stiffness and/or mass distribution irregularities, starting with early research on non-symmetrical wall-frame structures [38] and torsionally-coupled tall systems [39]. More advanced techniques are devised where planar macro elements are used for modeling highly irregular systems [40] and higher modes are also included [41]. Modifications to finite element definitions and formulations are also conducted for increased accuracy; Wilkinson and Thambiratnam suggested that improved shear beam elements will lead to better results [42]. Several pieces of research for combining higher mode effects and irregularities focused on improving modal pushover algorithm; force vectors are improved to contain torques, too, and multiple curves for each mode is computed [27].

2.2.2.2 N2 Method

N2 is a nonlinear method for determining the seismic performance of structures proposed by Fajfar and Gasperic[43]. For buildings whose response is mainly composed of the first vibration mode, the method is said to yield reasonably reliable assessment of seismic demand for the whole structure. Local vulnerabilities that affect the global response, such as soft story or excessive deformation demands could also be identified. The method requires elastic acceleration spectrum and strong motion duration, a non-linear push-over analysis result of target structure and its equivalent SDOF model, seismic demands of SDOF and MDOF models. The approach is to calculate a global damage index based on damage indices of members, which in turn is a function of the local seismic demands calculated from deformations of members (rotations, story drifts . . . etc.). For the limitations of this study, first of all, it should be noted that the response of the system is assumed to be temporally independent (i.e. independent of time). Therefore, the effects of modes other than the fundamental mode are greatly underestimated. In addition, as this method is based on the pushover curve, the limitations of pushover analysis also apply.

For lifting the limitations of single mode inclusion, further suggestions are published which uses correction factors that are based on ratios of elastic modal analysis and basic N2 method results [44]. These extensions are claimed to increase the accuracy of method extensively. Nevertheless, deviations and errors were still comparable for non-symmetrical (both in lateral and longitudinal directions), though they are conservative. Hence, further augmentations are proposed for structures with plan and elevation irregularities in the form of additional set of correction factors (one set for displacements and another for story drifts) [45].

For incorporating torsional irregularities, Fajfar et al. extended their method by additional factors representing irregularity effects by linear modal analyses results [46].

2.2.2.3 Time Domain Analysis

The time-history analysis is a dynamic analysis type which gives response quantities for a specific ground motion at every time step, eliminating the need to compute overall structural capacity. Hysteretic load-deformation behavior models are used for members, and the analysis is more tedious and demanding (in terms of computing time and power) than pushover analysis. However, results are considered as “exact” and are used most of the time as a basis for computing the error in other methods. For simple SDOF systems, the maximum response to a ground motion $\ddot{u}_g(t)$ can be determined from the response spectrum for the applied force $p(t)$ with the same time variation as $\ddot{u}_g(t)$, because the ground acceleration can be replaced by the effective force $p_{\text{eff}}(t) = -m\ddot{u}_g(t)$. If whole response of system during the excitation duration is required, analytical solution if the equation of motion will be impossible since the ground acceleration varies arbitrarily with time. Such cases are solved by numerical time-stepping methods for integration of differential equations. [47]. There are many approaches in literature, such as interpolation of excitation, central difference methods, and Newmark’s method. The latter one is one of the most used techniques with many improvements over the years. MDOF systems are also solved in a similar way, but the parameters in equation of motion will be matrices instead of scalars. Several modifications should also be introduced since excitation and movement directions may or may not coincide. The effective earthquake forces are found

as $[p_{\text{eff}}](t) = -[m][l]\ddot{u}_g(t)$, and numerical methods should be implemented as in SDOF case.

2.2.3 Determination of Performance Point

Once the seismic demand and capacity are obtained, it is necessary to find the response of the structure to the demand. Two widely used methods are time history analysis and processing the results of demand and capacity curves. Two common techniques of finding performance point of a structure are capacity spectrum method and displacement coefficients method.

2.2.3.1 Capacity Spectrum Method

In general case, determination of the performance point requires a trial and error search for finding the point. There are three alternate approaches referred in ATC40 [1], all based on same concepts and mathematical relationships but varying in their dependence on analytical and graphical techniques[2].

Procedures A and B are analytical, but B is simpler due to several simplifying assumptions that may not be always valid. Procedure C is a graphical approach and most convenient method for hand analysis.

All approaches require that both the demand response spectra and structural capacity curves be plotted in the spectral acceleration vs. spectral displacement domain, namely Acceleration-Displacement Response Spectra (ADRS)[48]. Every point on a response spectrum curve is matched to the ADRS graph as in Equation (2.15).

$$S_{d_i} = \frac{T_i^2}{4\pi^2} S_{a_i} g \quad (2.15)$$

For creating the capacity spectrum from the pushover curve, point-by-point conversion to first mode spectral coordinates is necessary as in Equations (2.16) and (2.17).

$$S_{a_i} = \frac{V_i}{W \cdot \alpha_1} \quad (2.16)$$

$$S_{d_i} = \frac{\Delta_{\text{roof}}}{\text{PF}_1 \cdot \Phi_{1, \text{roof}}} \quad (2.17)$$

where PF_1 and α_1 are modal mass coefficient and participation factor for the first natural mode of the structure respectively, and $\Phi_{1,roof}$ is the roof level amplitude of first mode.

The essence of the methods is to scale the demand curve by damping until both curves intersect within a tolerance level. If the performance point is calculated in the close neighborhood of a step in the sawtooth pushover curve, the actual response could be on the either side of the step and both points should be considered in finding the building performance (Figure 2.3).

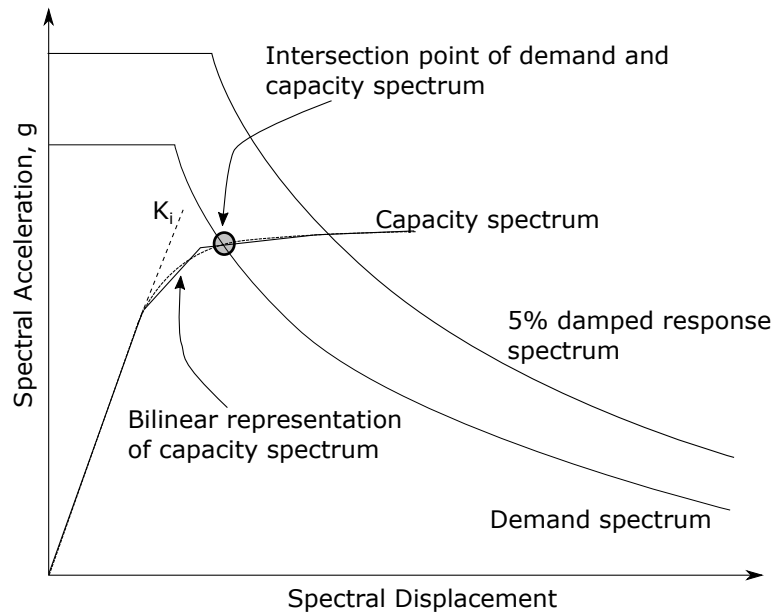


Figure 2.3: Capacity Spectrum Method Procedure A

2.2.3.2 Displacement Coefficients Method

It is a direct numerical process that computes the displacement demand. It does not require any ADRS conversion, but bilinear representation of the capacity curve is still necessary. This method approximates the deformation of MDOF system from the equivalent SDOF system by using several coefficients that represent the effect of P- Δ , hysteretic behavior and inelastic response (Equation (2.18)).

$$\delta = C_0 C_1 C_2 C_3 S_a \frac{T_e^2}{4\pi^2} g \quad (2.18)$$

In this equation, C_0 is the modification factor to relate SDOF displacement to the MDOF roof displacement, C_1 is the factor relating elastic response to inelastic response, C_2 represents the effect of hysteretic behavior, C_3 incorporates the effect of P- Δ , and the remaining terms are the elastic spectral displacement of the equivalent SDOF system.

2.2.4 Determination of Seismic Performance of Structure

After performance point of the structure is determined, the overall seismic performance is found by calculating conditions of the individual members at the performance point. First of all, failure types of the members will be resolved as either ductile or brittle. Brittle failures require the control of the forces only since this failure mechanism is very sudden and has almost zero deformation range. A member expected to fail in a brittle manner could only be in either elastic range (no damage) or failure point. Ductile failing members, however, need both force and deformation checks, and they could be in any of the following ranges; minimum damage, safety limit, collapse limit. Once force and deformation controls are done for every member, the overall performance is determined by criteria given in codes and specifications. These criteria are based on several parameters such as the ratio of failed ones to all members, ratio of seismic force carried by failed members to cumulative shear force, presence of brittle failures... etc.

2.3 Previous Studies and Applications on On-line Assessment Solutions

2.3.1 Development of a Web-Based Information System for Urban Seismic Risk Management

It is known that the sophistication of contemporary urban systems like lifeline systems or infrastructure facilities necessitates multi-disciplinary methods of risk management where different domains of engineering and science like geology, civil engineering, and seismology are involved. This diversity results in a flow of excessive data, thus information management becomes an important part of the subject. In the

study of LeBoeuf et al., an on-line information system with three-tier architecture (of client part, the server part, and the data part) is developed and it is combined with the existing GIS network[49]. The main objective is to integrate and handle all the information in geotechnical and structural fields and use this combined data to help in the process of deciding in seismic hazard identification and risk management. The two phases of the study are first determining the seismic hazard locally, and then assessing the seismic vulnerability status of buildings using the structural, geological, and geotechnical data (Figure 2.4). The first tier, the client side, consists of the

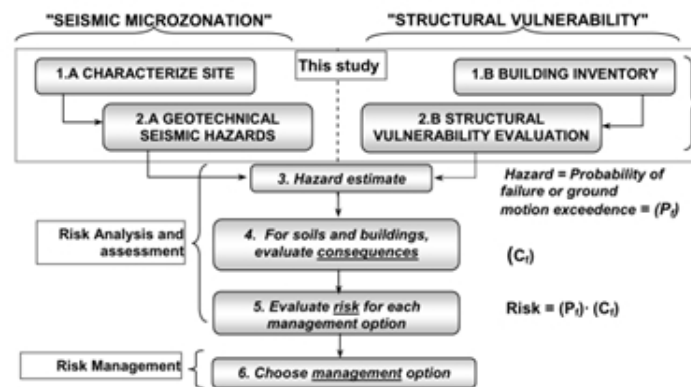


Figure 2.4: Risk Based Approach for Seismic Risk Analysis and Management

graphical user interface which is responsible for displaying and local processing of data, which is mainly verification and formatting of the input data so that it fits the database. A website is used as a client rather than a standalone software. The application execution is the second tier and it exists in a web server. The final tier is the storage of processed information, and MySQL was preferred as a relational database software. It handles the access to two distinct databases, geotechnical and structural (DbGeo and DbBAT).

One of the most prominent qualities of this study is combining geotechnical and structural data in calculating and drawing seismic hazard levels. In addition, two different types of information could be used separately for different attributes. For example, the geotechnical database could be used to fabricate different maps of parameters like superficial soil deposits or spectral amplification maps (Figure 2.5). This study shows a good implementation of on-line systems, yet it does not include any structural analysis capability.

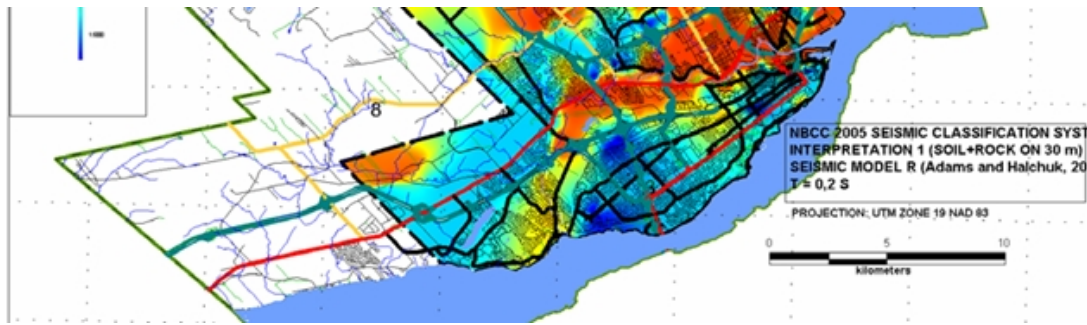


Figure 2.5: Spectral Amplification Ratio Mapping for Quebec City

2.3.2 Development of Internet Based Seismic Vulnerability Assessment Tools

In this study, a basic main analysis server accessed by multiple users via the Internet is created [50]. Structural information is sent to the server by user software, and the assessment results based on the input data are generated using the developed server software and sent back to the user.

Two different approaches used for analysis are the simplistic approach and detailed approach. In the simple analysis, a technique similar to walk-down assessment methods is used; the user is asked to answer several simple questions over a website about the target structure such as number of floors, floor height, window frame sizes, overhang ... etc. The answers users give are used to generate an overall score for the structure by applying penalty on a base score for each negative effect. The report is automatically generated that includes the final score of structure, penalties applied, earthquake zone properties of target location. The detailed approach, on the other hand, is based on structural analysis of the system. The user is required to download and install the client software. The graphical user interface is used to define column and beam properties, floor plans...etc. After defining all required information, data is sent to the server, a linear structural analysis is performed, and member forces are calculated. The analysis is done by creating a general stiffness matrix of the structure along with appropriate load vectors. After a stiffness solution is done, member forces are determined by slope deflection equations. The effects of infill and shear walls are considered as additional stiffness in appropriate coordinates of the global stiffness matrix. The study of Türer and Yalım could be considered as a pioneering research for this study.

2.3.3 Use of On-line Assessment Systems in Real Estate Business

Before investing in a residence or office building, all investors would like to know the earthquake risk of the structure that they are paying a great sum. However, most of the time the detailed techniques need academic know-how and engineering expertise to be applied without the intervention of an expert. The walk-down and some of the preliminary methods, however, are easier to apply, and with the appropriate guides to follow, people with no background in structural and geological engineering could perform data input for seismic assessment. One of the examples of this approach is the HomeRisk[®] web site[51]. However, this system is purely based on geographical information and gives estimates on the fault near target address, and intensity and magnitude of biggest likely earthquake. The input parameters are the address of the building, and the results served to the user are the nearest or most important fault zone, the design basis earthquake (named as the “Big One”), the level of shaking indicated as Modified Mercalli Intensity Scale, and some examples of the most common types of residential buildings in the target neighborhood with information on how they are affected by an earthquake. The weak points of different types are identified in a user-friendly context. There said to be an additional service, named Seismic Snapshot[®], which is claimed to generate an on-line risk profile for a property of interest that combines significant information about seismic hazard in the vicinity of the address with important structural features of the building that affect earthquake vulnerabilities. It is claimed that the resultant report is a preliminary summary of the earthquake risk of the property. Unfortunately, reporting part of the website is currently off-line, but additional contact with the site owners is sought. These initiatives clearly demonstrate the business uses of the study; there are many application possibilities on real estate and insurance domains where even basic reports are important for determination of estate value or insurance premium.

CHAPTER 3

AN IMPROVED WALK-DOWN METHOD

Walk-down (or sometimes called visual screening) methods are surveys to identify the presence of key structural strength and weaknesses that may cause the building to survive or fail during earthquakes. The inspections are done by trained field teams using pre-generated forms which include all questions and possible answers. The analysis process is basically a grading approach; the presence or lack of each evaluation parameter have either a bonus or penalty. Summing these modifiers with the base score the overall grade of the structure is calculated. This final score may be used to rank structures in a stock on the urgency of their condition. Moreover, the score can also be compared with limits to have a coarse idea on the expected seismic performance of target building.

Although it might be easy to name a set of evaluation parameters for a building, modeling their interaction with each other is not a trivial task. One of the most basic ways to proceed is neglecting any cross-connections except expected ground motion intensity. Most of the existing methods use this approach; the penalty scores are modified only according to the seismic region where the structure is located. This approach can be implemented by either assigning a factor of earthquake intensity or providing a different set of scores for every seismic zone available. For example, FEMA156 method includes different grading sheets for low, medium and high seismicity levels [52] whereas RBTY method determines a category based on earthquake zone, soil type and number of stories [4], on which the penalty scores are based.

The improved seismic evaluation method proposed in this study not only includes new parameters but also develops new intrinsic relationships between parameters that

were not available in the existing methods.

In addition to increased interaction between parameters, several optional evaluation criteria are defined. These items are not recognizable only by visual inspection, therefore they are considered as optional. However, if their condition can be determined by site measurements or known a priori, they considerably elucidate seismic performance of the structure. As they are optional indices, overall building score is not modified if these parameters cannot be determined by any means. All the screening methods are score-based analyses with bonus and penalty values assigned to the included evaluation parameters (Equation (3.1)).

$$S = \text{Base score} + \sum \text{bonuses} - \sum \text{penalties} \quad (3.1)$$

The only small variation in the general form of this equation is base score; some methods include a base score according to the structure type and structural system, whereas others include this value as a parameter, too. If the final score (S) is less than a definite limit, it is concluded that detailed evaluation is required for the building. This final score is also used for ranking a set of structures in terms of vulnerability.

The damage indicator parameters included in some of the available methods are listed in Table 3.1 with their symbols that are used throughout the context of this study. Each parameter is further explained in Section 3.1.1.

3.1 Proposed Algorithm

As a general inherent property of observation-based approaches, walk-down methods almost always include questions whose answers are based on subjective judgments such as “overall quality”. Moreover, as explained and exemplified in Section 2, walk down methods are not evolved much in the latest decade where fast measurement devices and computational power for processing these measurements increased vastly. In order to minimize the inquiries with non-objective answers and introduce measured structural responses for increasing accuracy, an improved approach (called Yucel&Turer) was developed by i) defining additional parameters, ii) fundamental period measurement by using mobile phones, iii) defining interactions and relationships between different parameters, iv) utilizing a mobile PC or tablet to enter inputs

Table 3.1: Parameters Included in Walk-Down Methods

Parameter	Sym.	FEMA	Suc. ^[1]	Y.&T. ^[2]	RBTY ^[3]	New
Number of Stories	N	✓	✓	✓	✓	✓
Seismicity	A	✓	✓	✓	✓	✓
Irregularities	I	✓	▪	✓	✓	✓
Overhang	O	▪	✓	✓	✓	✓
Apparent Quality	AQ	▪	✓	✓	✓	✓
Building Order	BO	▪	▪	▪	✓	✓
Pounding (Hammering)	H	▪	✓	✓	▪ ^[4]	▪ ^[4]
Short Column	SC	▪	✓	✓	✓	✓
Soft Story	SS	▪	✓	✓	✓	✓
Ground Slope	GS	▪	✓	✓	✓	✓
Soil Type	Z	✓	▪	✓	✓	✓
Age	Y	✓	▪	✓	▪	✓
Structural System	SYS	✓	▪	✓	✓	✓
Window Size	W	▪	▪	✓	▪	✓
Basement	B	▪	▪	✓	▪	✓
Mezzanine	M	▪	▪	✓	▪	✓
Shear Wall Distribution	SW	▪	▪	✓	▪	✓
Strong Beam-Weak Column	SBWC	▪	▪	✓	▪	✓

^[1] Sucuoglu's method

^[2] Yalim and Turer method

^[3] RBTY (Regulations for Evaluation of Risky Buildings in Turkish) method includes item lists for both reinforced concrete and masonry structures. For comparison purposes, only reinforced concrete list is considered [4].

^[4] Pounding effect is included within *BO* parameter.

while making use of visual aids and examples provided in the developed software, v) capture geographic location by GPS and recording location of structure on map, vi) web access for building a comprehensive database from multiple teams working in the field, and vii) automatically and instantly generating PDF reports for later use and/or residents of a building. One additional advantage of the new method is to be accessed by residents and a national database can be formed by millions of users around the country; in this way eliminating the use and need for inspectors roaming the streets. The method has utilized some algorithms and drawings from Yalim&Turer method[50].

3.1.1 Evaluation Parameters

Most of the available methods use similar parameters since there are a limited number of visual indicators that can be assessed by walk-down survey. In the proposed method, the bonus or penalty scores for these evaluation parameters are determined by common practices and engineering judgment combined with expertise. Some of the scores are tweaked by first applying the analysis to a structure and then identifying the weights of each parameter on the overall score.

3.1.1.1 Number of Stories (N)

The number of stories has a direct influence on the overall risk, even though it is not a direct indication of poor quality or low performance. If structures are designed in compliance with codes and regulations, number of stories would be an irrelevant factor. However, site inspections after 1999 Kocaeli and Duzce Earthquakes clearly reveal a strong correlation between building damage and the number of stories [53]. Although the lack of shear walls, low concrete strength, rebar detailing, and poor workmanship have a major role in building collapses, other parameters such as number of stories and past national code revisions are also factors in the performance. Furthermore, the larger number of people residing in taller buildings is another concern. In the proposed method, number of stories itself is not a reason of bonus or penalty; instead, it increases or decreases the effect of other detrimental evaluation parameters.

3.1.1.2 Seismicity (A)

Seismicity is one of the most important parameters considering the fact that inertial forces which a structure will encounter are based on the magnitude of the earthquake. Though this is not an easy task to determine without site-specific computations, design codes usually specify expected PGA values for locations in the form of seismic level or earthquake zone maps. In a walk-down assessment, as structure location is known, it is used to find out on which zone the building resides, and then adjust the penalty scores accordingly or introduce additional penalties.

In the developed method, earthquake zone does not result in a direct penalty (or bonus) due to the fact that if the structure is designed accordingly, seismic effects should not be penalized. Instead, punishments of other structural defects are magnified for higher seismic zones. Since earthquake zonation differs from one country to another, the following equation shall be used to determine the seismicity factor S_A :

$$S_A = 2.5 \cdot \text{PGA} \quad (3.2)$$

The minimum and maximum values for PGA in Equation (3.2) are assumed to be 0.1 and 0.4 for calculation of the overall building score, as explained in Section 3.1.3. These limits are derived from earthquake zone definitions given in Turkish Earthquake Code [54] and they should be modified for locations with different maximum and minimum expected seismicity levels.

3.1.1.3 Irregularities (I)

There may be different kinds of irregularities (vertical, horizontal, plan... etc.) in a structure, and all of them affect the overall response negatively. Unsymmetrical story plans or uneven distribution of lateral load-carrying members in one or both axes causes a considerable increase in shear and bending forces due to augmented torsional deformations. Similarly, discontinuous frames where beams are resting on other beams and do not form a two-dimensional (2D) regular frame are penalized. Sudden changes of frame continuity in either horizontal and vertical direction lead to modified load distribution and concentration in elements. In some rare cases, one or more columns at the ground level were reported to be removed in order to open space for commercial uses. Therefore, the presence of irregularities is an undesirable condition for a good seismic response.

In the proposed method, both vertical (S_{IV}) and horizontal (S_{IH}) irregularities are penalized with a score of -30 , and then modified according to the seismicity parameter, as in Equations (3.3) and (3.4).

$$S_{IV} = -30 \cdot S_A \quad (3.3)$$

$$S_{IH} = -30 \cdot S_A \quad (3.4)$$

3.1.1.4 Heavy Overhangs (O)

If the most critical story (most commonly the first floor) area is significantly lower than stories above, or if there are considerably large/heavy balconies, overhangs, extensions... etc., these occurrences induce increased forces in members and decrease seismic resistance. Overhangs are quite commonly used in Turkish structures [3] to increase the floor area of upper stories where the area of the ground level is limited by either legislative or physical conditions.

In the developed method, no penalty is applied for overhangs with a length smaller than 1 meter. Otherwise, the punishment score can be calculated as in Equation (3.5).

$$S_o = -4 \cdot (N - 1) \cdot S_A \quad (3.5)$$

3.1.1.5 Apparent Quality (AQ)

Even if a structure has all the drawings and documents of design, quality of the material used during construction or depreciation during the course of the building's service life may cause great deviations from the analysis stage. Though not an objective parameter, overall apparent quality of the structure is a coarse indication of concrete properties (mainly compressive strength) and rebars as well if spalling and rusting can be seen visually. A structure with spalled concrete and visibly corroded reinforcing bars should not be expected to perform fully close to its original design strength.

In the proposed method, bonus and penalty scores for good, moderate, and poor apparent quality are given in Table 3.2.

Table 3.2: Scores for Apparent Quality (S_{AQ})

Good	Moderate	Poor
+10	$-10 \cdot S_A$	$-20 \cdot S_A$

3.1.1.6 Building Order (BO) and Pounding (Hammering) Effect (H)

If buildings are located very close to each other, then it is highly probable that one will hit and hammer the other during an earthquake. These crashes will definitely cause additional damage; they even may result in a total column collapse. The presence of such cases will induce penalties on the overall score. In the recent codes, this item is further detailed by several additional parameters such as a) adjacent building slab levels are matching or not, and b) if the building is located between two adjacent buildings or one side is free. It is assumed that if slabs of two structures are on the same level, their collisions will result in less damage than the case where the slab of one building crashes into columns of the other. Additionally, structures on edges (i.e. at the corner of a street or if there is a gap after a series of adjacent buildings) are assumed to sustain more damage than the ones in between two other buildings.

In the developed method, the penalty scores for building order are given in Table 3.3.

Table 3.3: Penalty Scores for Building Order and Pounding Effect (S_{BO})

No Adjacent Structure	Structure In Middle		Structure On Edge	
	Same Slab Level	Different Slab Level	Same Slab Level	Different Slab Level
0	$-5 \cdot S_A$	$-10 \cdot S_A$	$-8 \cdot S_A$	$-15 \cdot S_A$

3.1.1.7 Short Column (SC)

The existence of a short column means the effective length of that vertical elements is reduced. These shorter columns will attract large shear forces under the same lateral deformation. Displacement-induced forces are related to the third power of flexural members' length; if an element is 3 times shorter than another, under same displacement (such as in the case of an earthquake), the shorter one will encounter 27 times more forces. This effect is rarely considered in the design and becomes active as a function of shallow windows at the top of continuous brick walls. Short columns usually end up having heavy damage during an earthquake and affect the

overall building seismic performance.

In the proposed method, the effect of a short column is intertwined with the seismic zone to consider the fact that short column failures occur under lateral force effects (Equation (3.6)).

$$S_{SC} = -25 \cdot S_a \quad (3.6)$$

3.1.1.8 Soft Story (SS)

The total lateral stiffness of a story diminishes when columns of that story are taller or the number of vertical elements is less than the remaining floors, which results in increased inter-story drift values. Reduction in lateral stiffness of a floor may also be caused by the existence of glass facades that replace brick partition walls as used in the side or rear of a building. The existence of soft story condition amplifies the effect of second-order moments and worsens any consequence of other defects. Furthermore, the existence of glass facade on one side generates eccentricity between the mass and stiffness centers. If elements are not designed to withstand these increased deformations, a soft story would contribute to damage and story collapses.

In the proposed new method, the effect of the soft story is determined by the ratio of the soft story height (H_y) to standard floor height (H) and modified with building age, number of stories, and earthquake zone:

$$S_{SS} = -10 \cdot \frac{H_y - H}{H} \cdot S_{age} \cdot S_{story} \cdot S_A \quad (3.7)$$

where

$$S_{age} = \frac{\text{Building age} + 50}{50} \quad (3.8)$$

$$S_{story} = \frac{N - 1}{3} \quad (3.9)$$

3.1.1.9 Ground Slope (GS)

Topographical (or sometimes referred as geographical) effect is encountered in structures constructed on high slope areas if the ground is not leveled during construction.

In these structures, single footings are commonly used as foundation, and when the ground slope exceeds 20° - 30° , these stepped footings fail to distribute ground motion to the structure properly [55].

In the proposed method, the ground slope is divided into three categories and penalized as per Table 3.4 where Z is the soil category.

Table 3.4: Penalty Scores for Ground Slope (S_{GS})

Straight	Slightly Inclined ($< 20^\circ$)	Highly Inclined ($> 20^\circ$)
0	$-5 \cdot (Z + 2)/3 \cdot S_A$	$-10 \cdot (Z + 2)/3 \cdot S_A$

3.1.1.10 Local Soil Conditions (Z)

Soil type is one of the most difficult parameters to determine since it requires expensive and time-consuming tests on the field, yet it is a major factor in seismic risk analysis. Moreover, the interaction of soil type with other parameters such as number of stories and earthquake magnitude is difficult to assess. Therefore, indicating a single constant score for each soil type should not be expected to result in a precise assessment.

In the proposed method, an interaction between the soil type and building period is considered for resonance. The soil type is categorized between $Z1$ and $Z4$, $Z1$ being hard rock/stiff soil (e.g. shear wave velocity $\gtrsim 760$ m/s) and $Z4$ being soft deposits ($V \lesssim 200$ m/s). A larger number of soil types and detailed classification is deliberately avoided since the visual determination of soil type may not be very accurate. Local soil condition parameter can be calculated using Equation (3.10). The base scores for soil type and number of stories interaction are given in Table 3.5 and Figure 3.1. This table is intended to mimic the interaction between the building and the soil, similar to the design spectra used in seismic codes. The first mode of vibration period is accepted to be approximately 0.1 times the number of stories and corner periods for $Z1$ through $Z4$ are taken from Turkish Seismic Code Table 2.4 [54].

$$S_Z = S_{\text{soil}} * S_A \quad (3.10)$$

Table 3.5: Base Scores for Soil Types and Number of Stories (S_{soil})

	1	2	3	4	5	6	7
Z1	-30	-30	-30	-20	-15	-10	-5
Z2	-30	-30	-30	-30	-20	-15	-10
Z3	-20	-30	-30	-30	-30	-30	-20
Z4	-15	-30	-30	-30	-30	-30	-30

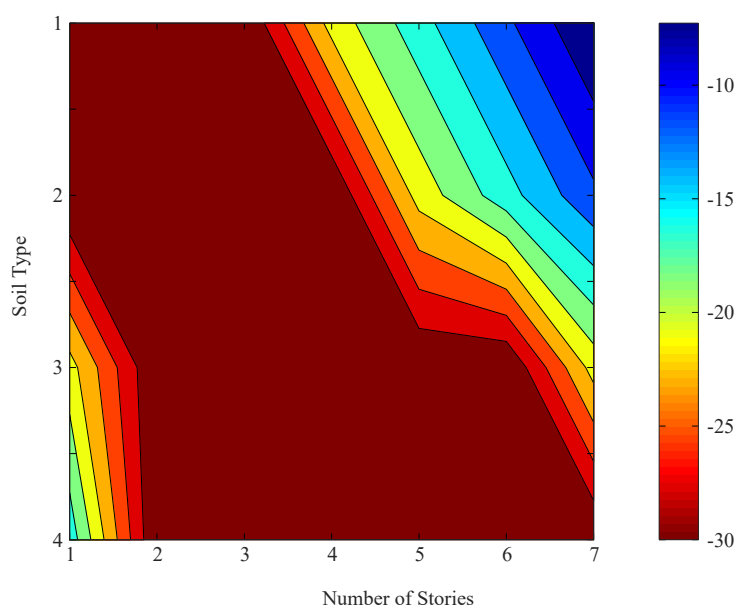


Figure 3.1: Penalty Scores for Soil Types and Number of Stories

3.1.1.11 Construction Year (Y)

The year of construction inherently includes a lot of information for a structure; the codes and specifications of that time, dominant materials and construction techniques, and any widespread common practices in structures encountered in those times. Therefore, although simple to determine, it includes a lot of factors to consider. In proposed method, the time of construction is divided into zones according to the release dates of seismic resistant design specifications in Turkey.

If this method will be implemented in other countries, the factors given here should be modified in accordance with the national code years. For example, in the United States, the initial adoption and enforcement of seismic codes are in 1941 for all structure types except tilt-up buildings (for which it is 1973). In addition, benchmark years which seismic design considerations are revised significantly is mostly around 1992 in US[2].

Major code revisions in Turkey are done in 1975, 1998, and 2007. The Turkish earthquake codes have distinct design differences in between and have different approaches for determination of total inertial force applied to the structure during an earthquake. Moreover, solid bricks were used in partition wall construction before 1975 and they performed like confined masonry during earthquakes [56]. However, modern hollow bricks dominantly used after 1975 are brittle, weak, and cannot contribute to seismic capacity. It is also known that plain reinforcement bars with a yield strength of 220 MPa were used before 1998 instead of deformed ones with a yield strength of 420 MPa and have better splicing and bonding capabilities with concrete. In addition, details for stirrups for confinement were 90° bend but became 135° after 1998, and smaller intervals were enforced towards beam-column connections. Considering all these facts, the following partial penalty function is defined, which depends on the construction year as well as the expected seismic effect in the region and the total number of stories of the evaluated structure:

$$S_Y = S_y \cdot S_A \cdot \frac{N}{3} \quad (3.11)$$

where

$$S_y = \begin{cases} -30 & \text{if } Y < 1975 \\ -40 & \text{if } 1975 < Y < 1998 \\ -15 & \text{if } 1998 < Y < 2007 \\ +15 & \text{if } 2007 < Y \end{cases} \quad (3.12)$$

3.1.1.12 Window Size (W)

Even though it has a minor effect, the size of windows is a parameter which can affect the overall seismic behavior of a structure. Too large windows effectively reduce the partition wall area of a frame, diminishing its lateral stiffness compared to other frames filled with walls. This parameter is especially more prominent in buildings with completely glazed walls as well as structures with solid brick infill walls. Unsymmetrical distribution of partitioning walls can also introduce initial eccentricity on the floor plan such as rear walls being completely filled and front facade having glazed walls or large windows.

In the proposed method, smaller windows are given a bonus whereas large ones are penalized. The level of scores is also dependent on the seismicity parameter S_A .

Table 3.6: Bonus and Penalty Scores for Window Size (S_W)

Small	Medium	Large
+5	0	$-5 \cdot S_A$

3.1.1.13 Basement (B)

Though presence of basement is not a negative parameter by itself, the condition that basement is in may give clues on the current status of concrete and reinforcement.

In the suggested approach, the condition of the basement is mainly judged according to the presence of water combined with the building age, considering the fact that the more reinforced concrete is subjected to water, the more damage it sustains. The

conditions and respective penalty scores are given in Table 3.7.

Table 3.7: Bonus and Penalty Scores for Basement (S_B)

No Basement	Dry	Humid	Partially/Fully Under Water
0	0	$-10 \cdot S_A \cdot S_{BW}/50$	$-40 \cdot S_A \cdot S_{BW}/50$

S_{BW} : duration of water presence in years

3.1.1.14 Mezzanine (M)

Mezzanine is defined as the partial mid-level story created on the entrance floor, which should be at least 5.5 meters in height [57]. Its presence greatly weakens the structure due to both increased first story height (soft story) and additional plan and elevation irregularities introduced to the system.

In the proposed method, the presence of mezzanine is penalized using the Equation (3.13).

$$S_M = -25 \cdot S_A \quad (3.13)$$

3.1.1.15 Existing Minor Damage and Past Repairs (D)

If the evaluated structure experienced earthquakes in its lifetime and/or underwent visible deformations (such as cracks on columns and partitioning walls, tilting... etc.), then it has used some of its energy dissipation capacity. Even though cracked elements were repaired, the structure is expected to perform worse than its initial design considerations unless additional dissipative and preventive measures were taken.

In the proposed method, the presence of any prior damage or signs of repairs is penalized as per Equation (3.14).

$$S_D = -15 \cdot S_A \quad (3.14)$$

3.1.1.16 Optional Parameters

The additional items in this section may not be visible in a screening process conducted only by eye; however, if they can be determined by any means (structural plans, knowledge of residents, on-site measurements. . . etc.) they provide invaluable information on the seismic performance of the building. If optional parameters are included in the evaluation process, the overall score reference is modified and the final score is normalized accordingly.

3.1.1.16.1 Structural System and Shear Wall Spatial Distribution (S_{SW}^o) The structural system of a building is one of the most important considerations to take into account during a seismic evaluation. Buildings with shear walls are known to show superior performance compared to other types of structures such as moment-resisting frames and masonry buildings. The presence of flat slab or filler-joist floor is also an important factor to be considered, since the presence of these element types may result in reduced stiffness and possible problems at slab-column connections.

The presence of shear walls is a good way to increase the overall performance of a structure. However, their planar (geometrical) distribution has major effects on the structural performance. If unsymmetrically placed, introduced eccentric-torsional response will amplify displacement demands encountered by corner columns. Although unsymmetrical placement of shear walls is not easy to determine without structural drawings, this parameter has a major role in the seismic response; therefore, it is introduced as an optional parameter. Evaluation scores are defined based on shear wall symmetry in the most critical story:

Table 3.8: Scores for Shear Wall Spatial Distribution (S_{SW})

		X		
		Symmetrical	Unsymmetrical	None
Y	Symmetrical	$+80 + S_{AQ}$	$+40 + S_{AQ}$	$+30 + S_{AQ}$
	Unsymmetrical	$+40 + S_{AQ}$	$+30 + S_{AQ}$	$+20 + S_{AQ}$
	None	$+30 + S_{AQ}$	$+20 + S_{AQ}$	$-30 \cdot S_A$

3.1.1.16.2 Presence of Strong Beam and Weak Column (SBWC^o) Almost all of the contemporary design principles for ordinary reinforced concrete buildings rely on inelastic deformations and formation of plastic hinges for energy dissipation generated by seismic demands. However, special attention should be given on the location of plastic deformations; if these hinges occur in vertical load carrying members (such as columns), an unstable mechanism will form and story collapse may occur. In order to prevent this phenomenon, modern codes enforce that in a joint, total moment capacity of columns should be at least a definite percentage greater than that of beams.

In the proposed method, if the presence of strong beam and weak column can be verified, a steep penalty is applied. This score is also modified based on expected seismic demand (Table 3.9).

Table 3.9: Penalty Scores for Presence of Strong Beam-Weak Column (S_{SBWC})

Unknown	Not Exists	Exists
0	0	$-50 \cdot S_A$

3.1.1.16.3 Fundamental Period (T^o) The natural vibration period of a structure can be measured on the field with a simple wireless accelerometer and a mobile PC or tablet device. Measuring the fundamental period of the evaluated structure is highly valuable since it enables to determine the zone on which the structure will fall in the design spectrum. For measuring the vibration period of a structure on the site, two approaches can be followed:

1. Using a smart phone's internal accelerometer directly with a special application which performs necessary signal processing,
2. Using an accelerometer and post-processing the data manually with a PC software.

The first approach has the ease of use advantage; but the accuracy, computing power and high noise levels of the cell phone accelerometers could be limiting. Even though

the second technique seems to increase the workload, considering the fact that site inspection teams are composed of at least two staff, one may go up to the top floor, deploy an accelerometer, take a minute of measurements, and obtain the fundamental period in less than five minutes. As a secondary advantage, the data file could be reused at any time.

A phone application was developed as a part of this study and made available as a beta in Google Play for Android devices [58]. Its design and inner working details are explained in Section 3.4.

In this method, fundamental period information is embedded into local soil parameters in the form of a total number of stories and earthquake zone (3.1.1.10). If the fundamental period is obtained by site measurements, it is multiplied by 10 and used instead of "Number of Stories" in the table to linearly interpolate penalty score (S_Z) from Table 3.5.

3.1.1.16.4 Stirrup Presence and Bending Angle (ST°) Stirrups provide two-dimensional confinement effect on core concrete of a column, effectively increasing its compressive and shear strength as well as enabling highly ductile behavior in the vicinity of joints. However, their presence by itself is not enough; if the ends of a stirrup are not bent 135° and directed into core section, it will easily open up under circumferential pressure, releasing any confinement effect. Moreover, if the spacing of stirrups are wide and/or the number of stirrups per member length is not increased towards joints, the structural performance of columns are reduced. For this reason, improperly detailed stirrups are only marginally better than having no stirrup at all.

In the proposed method, bonus and penalty scores for the presence and detailing of stirrups are given in Table 3.10.

Table 3.10: Bonus and Penalty Scores for Stirrup Presence and Detailing (S_{ST})

Unknown	Insufficient/No Stirrups	Bending Angle 90°	Bending Angle 135°
0	-100	-75	+25

3.1.1.16.5 Liquefaction (LI^o) Soil liquefaction is one of the most important factors that can result in collapse or toppling of the complete structure without failures. However, detailed ground investigations should be conducted in order to come up with definitive results of its possibility. The variables determining the susceptibility of a soil to liquefaction are soil type (more specifically grain size distribution), relative density, earthquake loading characteristics, overconsolidation, vertical effective stress, soil origin and age, seismic strain history, the degree of saturation, and thickness of sand layer [59].

Soil Type The weakest soil type to liquefaction is the one where deformation resistance is created by particle friction. The most common type of soil exhibiting liquefaction phenomenon is sands, yet it has been observed that clay or silt-size materials with a low plasticity index may have a degree of liquefaction as well.

Relative Density It is one of the most dominant factors controlling liquefaction. The tests and studies show that liquefaction occurs almost certainly in saturated clean sands and silty sands with a relative density less than 50%. Due to their dilation behavior, dense sands have an increased resistance to liquefaction, and the lower limit above which liquefaction is said to not occur is 75% [59].

Earthquake Characteristics The magnitude, predominant frequency, and duration of an earthquake plays an important role on the possibility of liquefaction.

Overconsolidation and Vertical Effective Stress It is established that soils under heavier loads (thus increased the level of stress) are more resistant to liquefaction. It is concluded by some researchers and investigators that saturated sands located deeper than 18 meters have a very low risk of liquefaction. [59]. Additionally, the higher overconsolidation ratio also decreases the risk by increasing the shear stress ratio needed to start liquefaction.

Soil Age and Origin Alluvial and fluvial deposits are loosely packed, thus more susceptible to liquefaction especially if they are young. It is stated that deposits older than late Pleistocene (10000 years) are unlikely to liquefy whereas late Holocene (1000 years or younger) are the most likely to liquefy [59].

Seismic Strain History It is shown in tests and research that exposure to low levels

of seismic strain in the past increases the resistance of a deposit to liquefaction whereas exposure to high levels and previous occurrences of liquefaction causes weak spots in the strata, lowering its resistance to liquefy.

Saturation Liquefaction cannot happen in dry soils, and the probability is very low in partially saturated soils. Full saturation is a prerequisite for liquefaction.

Layer Thickness In order to cause comprehensive damage at ground level, the soil layer has to be thick enough so that adequate amount of uplift pressure and water expulsion be generated to cause surface rupture and boiling [59].

Most of the parameters above can only be determined by extensive site tests and analyses, which exceed the scope of a walk-down survey. In this study, only the most important of the above variables as considered and an assumption is made such that in high seismic regions (earthquake zones 1 and 2), if there is a high level of groundwater in sandy soil, liquefaction is a risk that should be considered. Therefore, if these conditions are met, a penalty score of -50 is applied. If the relative density can be determined to be greater than 75%, it is assumed to be no risk of liquefaction whereas if it is less than 50%, liquefaction is assumed to be inevitable and further detailed seismic evaluation with soil investigations should be considered instead of a walk-down survey. If groundwater level and/or type of soil deposit underneath the structure cannot be determined, no bonus or penalty is administered.

3.1.2 Interaction of Evaluation Parameters

The relations and interaction of the proposed mandatory and optional parameters can be seen in Figure 3.2.

3.1.3 Calculating Overall Building Score

To calculate the resultant score of an evaluated structure, all the bonus/penalties determined from evaluation parameters given in Section 3.1.1 should be summed. However, a direct summation will result in a score which is hard to comprehend without knowing upper and lower bounds. Moreover, arbitrary limits for the lowest and

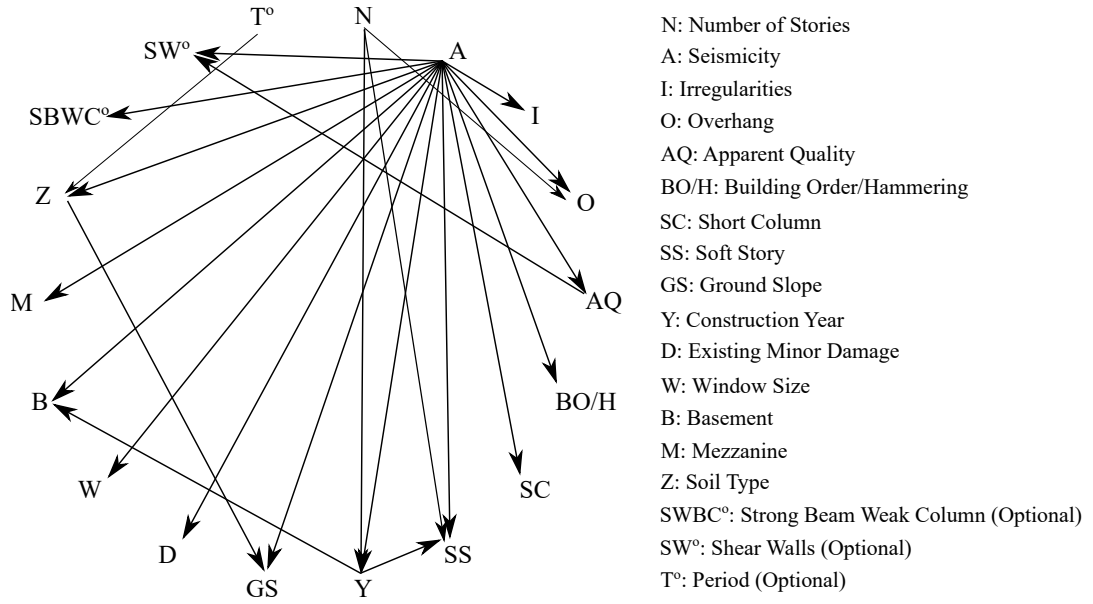


Figure 3.2: Interaction of Walk-Down Parameters

highest values that a building can attain is not user-friendly. Therefore, a normalization process is included in the computation of overall building score. There are two approaches that can be followed in the normalization process; scores can either be normalized before or after the summation. The first method has the advantage of incorporating optional parameters easier than the latter; if a parameter cannot be determined, it is not included in the calculations at all. The overall score can be calculated as:

$$S = \frac{\sum S_i - \sum S_{\min}}{\sum S_{\max} - \sum S_{\min}} \cdot 100 \quad (3.15)$$

Equation (3.15) will give the overall building score as percentage, 100 being the best and 0 the worst case scenario. The minimum and maximum values for all the evaluation parameters can be found in Table 3.11. In this table, limits for several evaluation parameters are derived according to Turkish Codes and Specifications (such as PGA limits and code revision dates) and they should be updated for implementation in other countries if necessary.

3.2 Comparison of Proposed Method and Discussion of Results

The proposed method has many additional evaluation parameters as compared to other first level methods, and there is no existing database of building stock which

Table 3.11: Minimum and Maximum Bounds for Evaluation Parameters

Parameter (S)	Minimum	Maximum
Horizontal Irregularity (IH)	-30	0
Vertical Irregularity (IV)	-30	0
Overhang (O)	-30	0
Apparent Quality (AQ)	-20	10
Building Order / Hammering (BO/H)	-15	0
Short Column (SC)	-25	0
Soft Story (SS)	-80	0
Ground Slope (GS)	-20	0
Soil Type (Z)	-30	-1
Construction Year (Y)	-93	35
Window Size (W)	-5	5
Basement (B)	-40	0
Mezzanine (M)	-25	0
Existing Minor Damage (D)	-15	0
Strong Beam Weak Column (SBWC ^o)	-50	0
Shear Wall (SW ^o)	-30	90
Liquefaction (L ^o)	-50	0
Stirrups (ST ^o)	-100	25
$\sum S^{[1]}$	-682	164

^[1]If any optional parameter (^o) is not included in the analysis, its minimum and maximum values should **not** be considered in calculating $\sum S$.

contains both the evaluation parameters' values and damage state of structures after a major earthquake. Even if there was an available database (similar to Duzce which is used for Sucuoglu method), the resulting parameter scores would be case dependent that reflects the specific earthquake excitation and building stock properties that were used for calibration, which may not be representative of all possible building properties and seismic actions elsewhere. The other alternative, which is comparing finite element model simulation results for calibration of the proposed method was also not appropriate since modeling of several evaluation parameters (such as humidity in the basement, construction year, earthquake code release years, liquefaction, window sizes... etc.) are difficult or impossible to simulate. For this reason, a statistical approach using Monte Carlo simulation for random data is assigned to parameters in order to compare the results of existing screening procedures and the newly proposed algorithm. The verification and comparison are carried out in two stages; the first stage used only the common (overlapping) parameters between the two compared methods and a general correlation was sought. The correlation is maximized by defining different cut-off values determining "pass" and "fail" cases. The ranges that yield maximum "pass-fail" and "fail-pass" are minimized. In this attempt, the cut-off score values have not reached a global minimum but converged to zero or 100 making all cases "fail" or "pass", leading to a trivial perfect correlation, and putting constraints did not amend the situation. A similar procedure was applied in the second stage as statistical-based correlation optimization work was repeated using all of the synthetically generated building evaluation parameters which each method using only its relevant ones. The second approach resulted in acceptable results with 80% to 82% correlation with the other four methods (Table 3.12). Using the same cut-off scores for the first stage also gave similar results except for FEMA. FEMA154 approach has major differences such as code revision year. FEMA is also disregarding some of the major evaluation parameters which are common in Turkey such as overhang, soft story, short column... etc. Therefore, a relatively lower match with FEMA and the new method was already expected. The correlation coefficients between Yucel and three methods other than FEMA had higher correlation rates using the same cut-off values found in the first stage and raised to 82% to 85%. The increase in the correlation was deemed to the elimination of uncommon and random parameters in the first stage.

Table 3.12: Comparison of New Method with Existing Procedures

	Stage 1				Stage 2			
	Match		Disagree		Match		Disagree	
	PP	FF	PF	FP	PP	FF	PF	FP
FEMA154	61%	7%	28%	4%	78%	3%	11%	8%
	68%		32%		81%		19%	
Sucuoglu	82%	4%	1%	14%	75%	6%	8%	12%
	85%		15%		80%		20%	
RBTY	72%	11%	4%	13%	72%	10%	4%	14%
	83%		17%		82%		18%	
Yalim	73%	9%	4%	13%	73%	9%	4%	13%
	82%		18%		82%		18%	

3.3 Limitations of the Proposed Method

The following limitations and concerns should be noted when deciding whether to apply the proposed new walk-down method to a structure or interpreting the analysis results. These limitations mostly stem from the assumptions included in the analysis calculations and can be eliminated if the underlying assumption is either not implemented or is improved.

- The method is specifically developed for reinforced concrete structures. The evaluation parameters and their scores are determined based on the observed and researched damage and failure occurrences in reinforced concrete buildings. Moreover, different types of structures have distinct properties and points to inspect during a walk-down analysis; masonry structures need wall integrities and other construction practices, steel structures need an inspection for connections and other defects. . . etc. Therefore, the proposed technique should be applied to reinforced concrete buildings only.
- The method is developed considering low-rise structures only, as all the other walk-down inspection methods. The response of the structure changes to reflect the increased effect of higher modes as the total height increases, therefore all the walk-down and preliminary methods are recommended to be used up to a certain height (or number of stories). This limit is set as 21 meters for the proposed method, which approximately corresponds to 7 stories. For taller

structures, the use of the method is not recommended.

- The method is developed considering ordinary structures, which are commonly used as residents, schools and other facilities. For special structures where the loading on the building or any other design aspect is considerably different, more detailed and specialized techniques should be applied.

3.4 PeriodFinder Android Application

In order to calculate the fundamental period of a structure in a cheap, fast and efficient manner, an Android application is developed (Figure 3.7). Modal parameter measurements are commonly applied and are a well-known area, however, all the existing implementations necessitate expensive accelerometers and data acquisition systems as well as a post-processing stage for time-frequency domain conversions. The aim was to use the smartphones which every person has in order to perform both the measurement and post-processing stage. Almost all of the modern smartphones, ranging from mid-level phones to brand flagships, include an accelerometer with three axes measurement capability today. The technical specifications of these components, however, are in correlation with the price of the phone; lower end devices tend to have lower sampling frequency, low resolution, and range whereas higher end devices can compete with dedicated accelerometers. For example, the testbed device used in the development of the PeriodFinder app (which is an LG G3 855TR) has 120 Hz sampling rate, $\pm 2g$ range, and $120 \mu g$ resolution. The fact that no additional device is required and all processing (pre and post) can be done on the phone is a tremendous advantage for site surveying teams and non-technical personnel on obtaining the fundamental period of the structure.

The application uses the built-in tri-axial accelerometer of the device and records acceleration values as fast as possible. The maximum measurement frequency varies from device to device, but generally higher end phones (flagships) can go up to 120 Hz data collection whereas medium to low-end devices are limited around 60 Hz. Due to the internal framework design of the Android operating system (OS), it is not possible to dictate sampling rate as a number; it is only allowed to select from

a list of enumerations. Even though it is possible to specify an absolute value for this parameter, it will only serve as a *suggestion* to the OS; the exact value will be determined by Android during runtime. For this particular case, the enumeration “SENSOR_DELAY_FASTEST” is selected to ensure maximum accuracy available (Figure 3.7a).

The total measurement duration is determined by the number of stories of the evaluated structure. The rule of thumb for getting an adequate number of data points is known to be 1000 seconds times the period of the structure. Using the basic assumption that fundamental vibration period of a structure is one tenth of its number of stories, total measurement duration is set as 100 times number of stories, in terms of seconds. Acceleration values are collected for all three axes, though only horizontal ones are used in the analysis. Recorded values are written to RAM of the device during recording stage, but can be exported as comma separated text file (CSV) if requested (Figures 3.7b and 3.7c).

Once the measurement stage is completed, the time series is transformed into frequency domain using Fast Fourier Algorithm. Android OS do not include a native FFT library, therefore the framework “JTransforms” is implemented. It is an open-source, multithreaded FFT library which is coded completely in Java [60]. It is claimed to be the fastest implementation of Discrete Fourier Transform, Discrete Cosine Transform, Discrete Sine Transform, and Discrete Hartley Transform in Java. The framework has the ability to work with data up to three dimensions with arbitrary sizes; there is no need to pad the data to obtain a power of 2 element count. It can transform up to 2^{63} elements in a single run and said to be optimized for real input data, which is the case in this study.

After frequency domain transformation is completed, a peak search algorithm runs on the data. It searches the maximum values in x and y axis measurements in the frequency domain, and the fundamental period of the structure is reported to the user as the largest of the two values obtained in the search. It has been seen in tests that if ambient vibrations are recorded, cell phones tend to generate high noise and peak-searching algorithms struggles in these cases because the frequency domain is not composed of clear peaks; instead, the energy seeps into every frequency (white noise)

and results in a flattened spectrum. In order to alleviate this problem, time domain pattern recognition algorithms have been studied instead of frequency domain peak search.

The basic algorithm for the pattern search is based on the assumption that the ambient vibrational response of the structure may include a single or a bunch of sinusoidal waves within its complete response, recorded as time-series, where it oscillates freely for a moment. In order to capture this instant, the following workflow is tested:

1. Estimate a range for the period of the structure from number of stories and type: This step is included to reduce the workload; if it is estimated to have a period between 0.2 to 0.6 for a structure, any search outside these bounds will be pointless. This efficiency precaution is especially important for mobile devices, which has limited power source and processing capabilities.
2. Generate perfect sinusoidal waves for the estimated range with a predefined increment: Single waves with incremented frequencies are generated for the predicted period range in Step 1. The frequency increment is selected based on required accuracy and available processing power.
3. Seek for the highest match with all of the generated waves in Step 2 within the measured time series..
4. Report the period of the sinusoidal wave with the maximum correlation as the period of the structure.

The process in Step 3 is basically one-dimensional signal recognition task, and there are tools available, such as cross-correlation. Moreover, a “sliding-MAC (modal assurance criterion)” approach is also developed.

Cross-correlation is the level of similarity between two series as a function of displacements relative to each other. It is also referred as “sliding dot product”, and it is commonly used in seeking a short signal in a longer one. Formally, cross-correlation is defined for continuous functions as [61]:

$$(f \star g)(\tau) \stackrel{\text{def}}{=} \int_{-\infty}^{\infty} f^*(t)g(t + \tau)dt \quad (3.16)$$

where f^* is the complex-conjugate of f and τ is the lag. For discrete data series, Equation (3.16) can be discretized as in Equation (3.17) [62].

$$(f \star g)[n] \stackrel{\text{def}}{=} \sum_{m=-\infty}^{\infty} f^*[m] g[m+n] \quad (3.17)$$

Sliding-MAC: Modal assurance criterion (MAC) is a statistical parameter used to assess the identicalness of two mode shape vectors. It is easy to apply to any vector and does not require any additional data. It yields a result between 0 and 1, corresponding to the correlation of vectors. Moreover, it is shown that MAC is more sensitive to large differences, whereas comparatively insensitive to smaller perturbations [63] (Equation (3.18)). The primary advantages of MAC over cross-correlation is ease of implementation and reduced computing, which is important on mobile platforms.

$$\text{MAC}_{cdr} = \frac{|\Psi_{cr}^T \Psi_{dr}|^2}{\Psi_{cr}^T \Psi_{cr} \Psi_{dr}^T \Psi_{dr}} \quad (3.18)$$

where Ψ_{cr} and Ψ_{dr} are modal vectors to be compared. Sliding-MAC approach gets a slice with the same length as the searched pattern wave from the measured time series, uses the Equation (3.18) for the search pattern and the slice, finds MAC value, and then shifts the slice one element forward for repeating the procedure again. By this way, in the end a new series indicating the consistency (linearity) between the reference wave and the measured time series is obtained.

Both of the pattern search methods are applied to several synthetic data to see their behavior and efficiency. During testing, a Gaussian white noise series is generated and a single sinusoidal wave with different frequencies and signal-to-noise ratios (SNR) is embedded within it. The two approaches are tested with the pattern wave having exact frequency first and both sliding-MAC and cross-correlation approaches yield perfect results.

In the first test, a Gaussian white noise of 10000 sampled points is generated (Figure 3.3a) with a 1 Hz sinusoidal wave having 10 dB SNR starting at point 3000 (Figure 3.3b). The sliding-MAC approach is applied with a perfect 1 Hz wave, and the result shows that this pattern is recognized in the presence of the noise (Figures 3.3c and 3.3d).

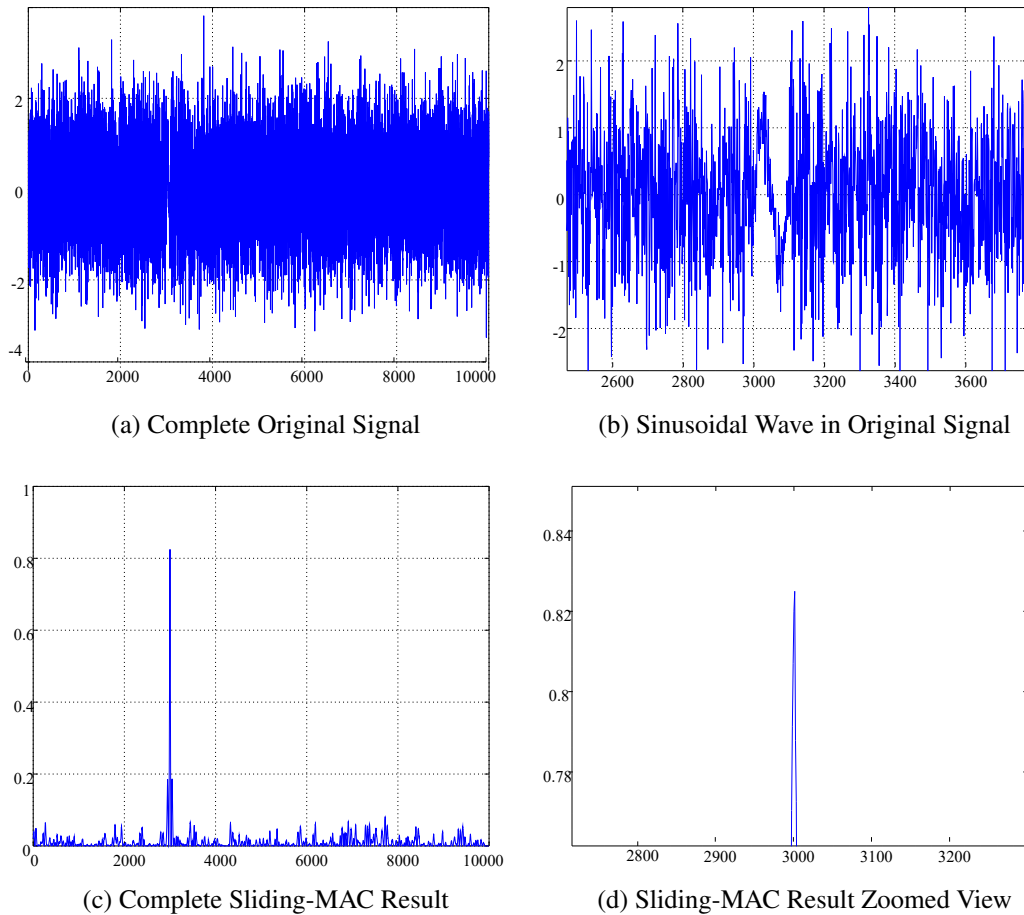


Figure 3.3: Sliding-MAC Search with Perfect Reference Wave

A similar test is repeated using cross-correlation as well. In this test, 20000 data points are generated (Gaussian white noise) with 1 Hz 10 dB SNR sinusoidal wave starting at point 8848. The results show that cross-correlation is also valid for pattern matching; algorithm accurately pinpoints the value 8848.

These tests are performed using a source sine wave with the already known frequency. In the real case, only the range of the period will be estimated and a series of potential frequencies should be tested. Due to the fact that sliding-MAC is easier to implement and necessitates less computation power, it has been chosen for the more complex searches. In testing this approach, a complete signal of 10000 data points is generated (Gaussian white noise) with a sine wave ($f=1.1$ Hz, SNR=10 dB) which starts at point 5000. In searching process, MAC series for frequencies between 0.75 and 1.25 Hz are generated and plotted. As seen in the Figure 3.4, the algorithm can identify the target frequency with around 10% error in the first try, and much less deviation in the

subsequent runs (Figure 3.4). The same procedure is repeated for $f=0.1$ Hz and $f=0.3$ Hz values, and results are plotted in Figures 3.5 and 3.6.

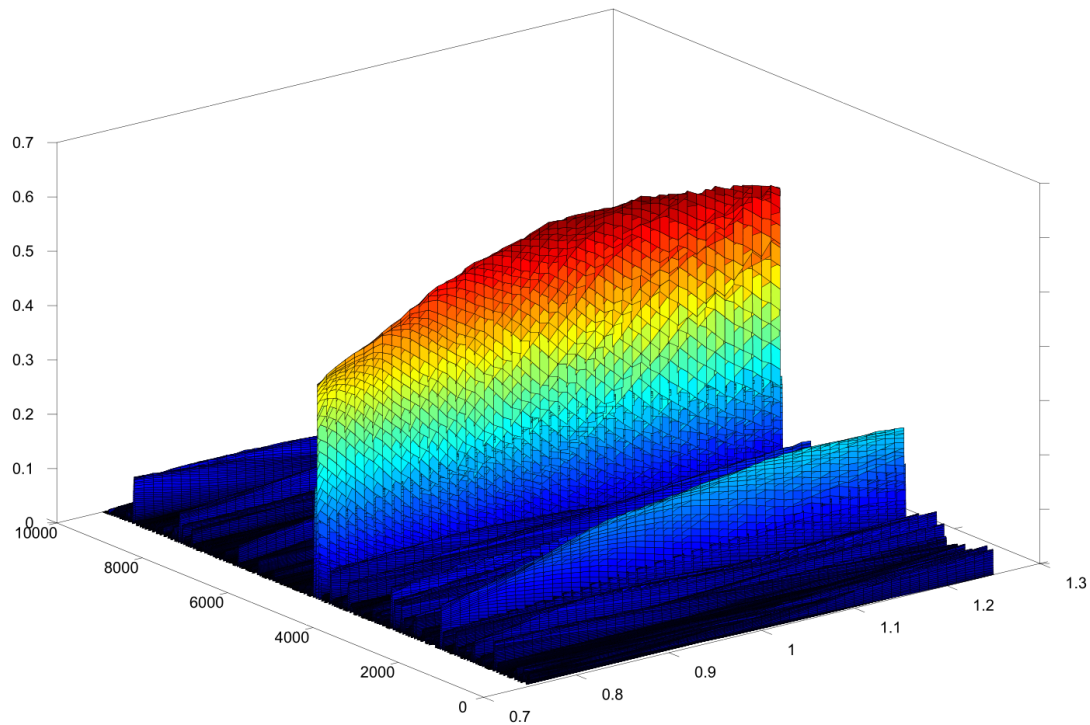


Figure 3.4: Sliding-MAC Results for Complex Search, $f=1.1$ Hz

The application is available in Google Play App store, however, it is in closed beta. Only selected accounts have access to download, yet it will be open to the public soon (Figure 3.7).

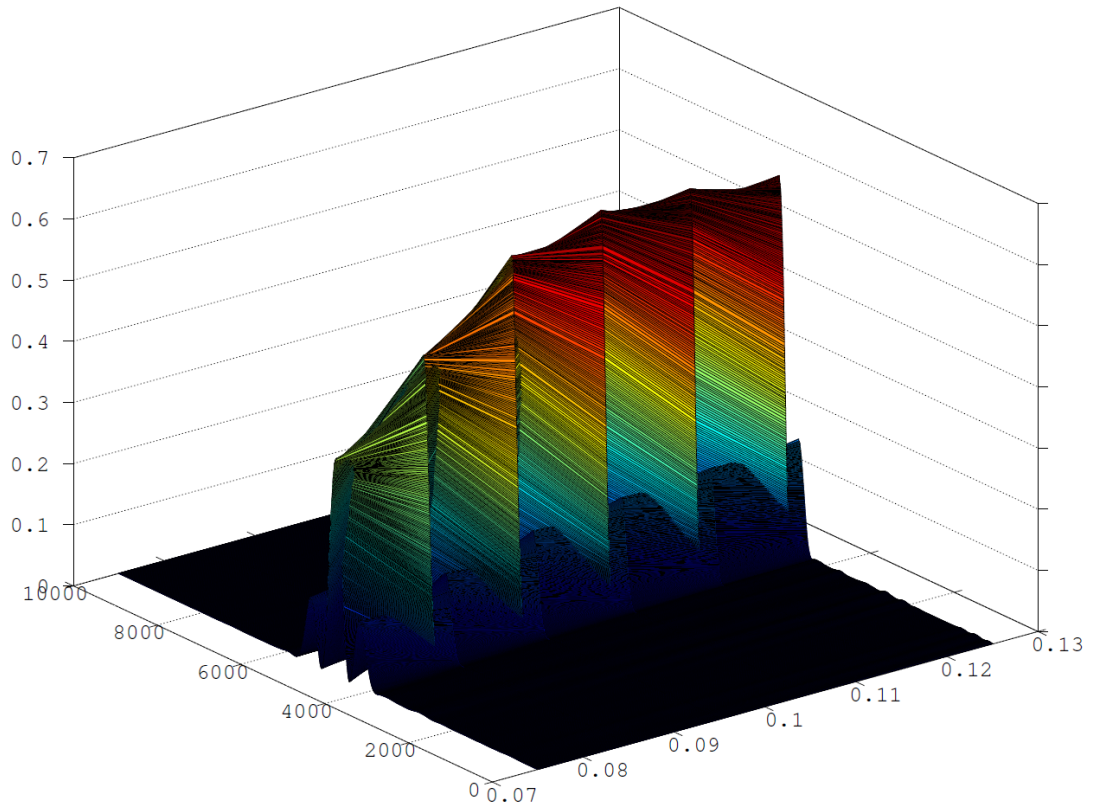


Figure 3.5: Sliding-MAC Results for Complex Search, $f=0.1\text{Hz}$

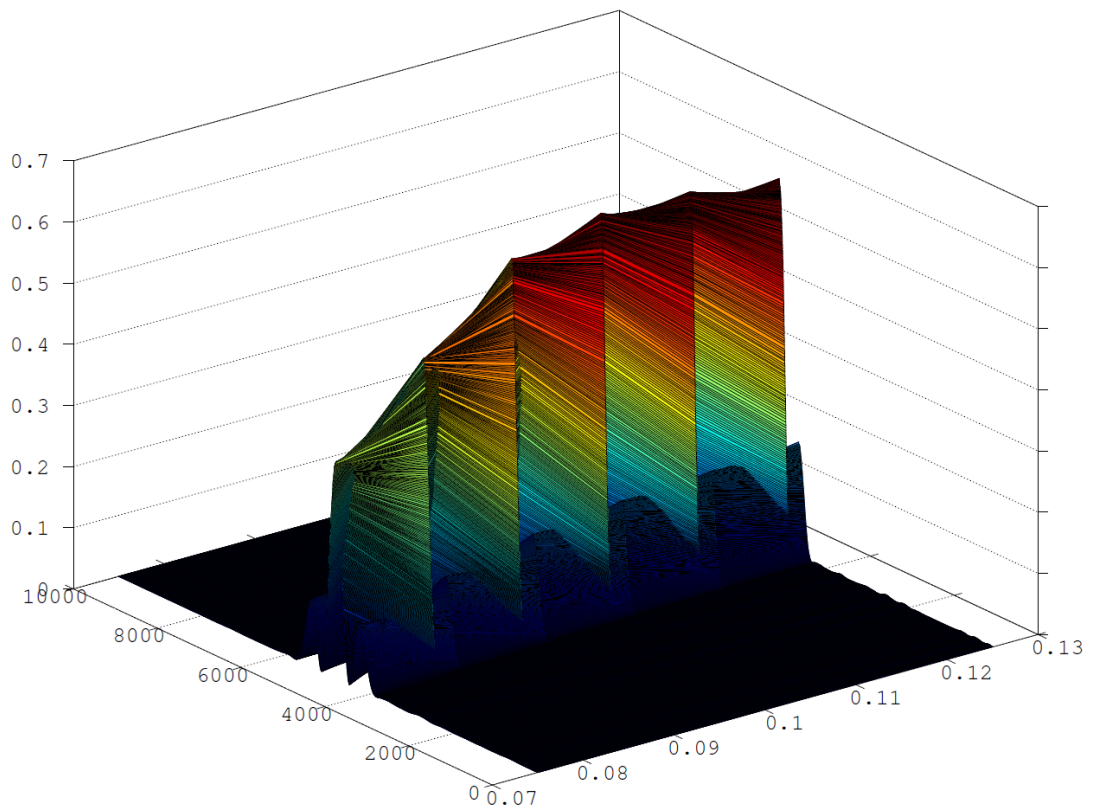
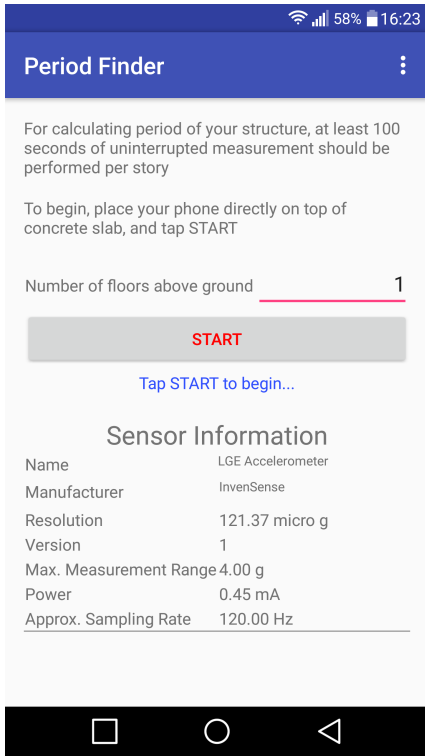
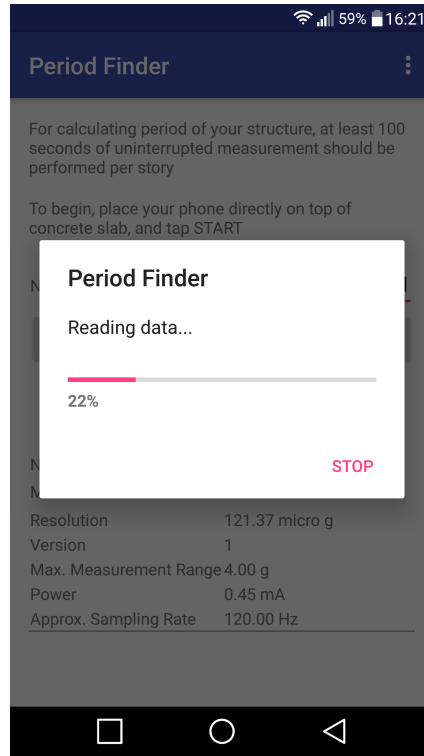


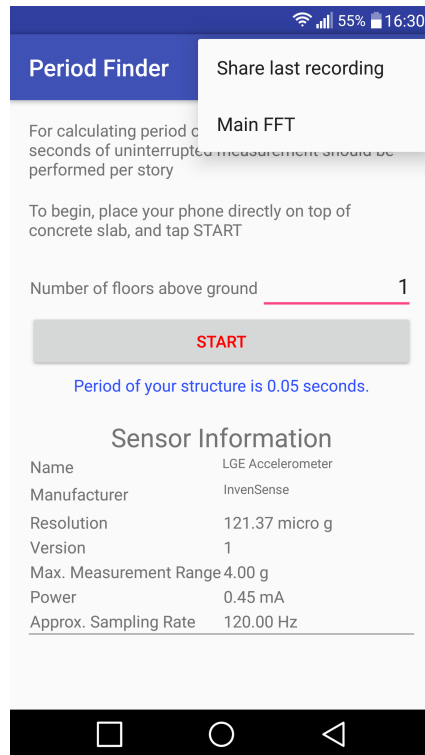
Figure 3.6: Sliding-MAC Results for Complex Search, $f=0.3\text{Hz}$



(a) Main Screen



(b) Recording Screen



(c) Result and Sharing Screen

Figure 3.7: Different Screens of the Application

CHAPTER 4

A SIMPLIFIED CAPACITY DETERMINATION METHOD

Almost all of the preliminary methods explained in Chapter 2 depend on the quantity ratio of structural elements in a building to the overall area of the most critical floor, neglecting all discontinuities and irregularities. This approach allows quick and easy calculations for condition assessment for the expense of the effect of spatial distribution of members. In this chapter, a simplified method for obtaining the capacity curve of the structure, which reflects the effect of geometry and element distribution more accurately but still easier to compute than full finite element approaches (detailed methods) will be proposed. The technique is based on simplified structural analysis of the most critical story using stiffness matrices. The approach involves no finite element process; it is solely based on constructing the pushover curve by first assembling stiffness matrix of the most critical story, then applying an incremented load while updating element stiffness values based on member nonlinear response. By this way, the effect of element locations, sizes and other structural irregularities existing on the most critical story are taken into consideration. The extra load of new computations is shown to be compensated by the increase of accuracy, therefore it can be declared that the proposed method has a degree of complexity and precision lower than a three-dimensional finite element analysis.

4.1 Algorithm for Finding Structure Capacity Curve

The computation flow of the proposed approach is as follows, and all of the steps are explained in detail within the following sections.

1. Calculate effective lateral stiffness values for vertical structural elements (columns and shear walls) .
2. Calculate two-dimensional stiffness matrix of the most critical story (MCS) for two lateral and one rotational degree of freedom (translation in x and y , rotation in z).
3. Calculate deflections for the center of mass of MCS for a unit load in the direction of analysis.
4. Using coordinate transformation, compute end deflections of vertical structural elements.
5. Convert member end displacements to internal force (shear) and then isolate the element with the highest end force.
6. Based on maximum force found in the previous step, compute the base shear that will cause the first element to yield (V_{yield}).
7. Apply the base shear calculated in Step 6 to the structure in the direction of analysis.
8. Using element force-deformation relations, calculate end forces of columns and shear walls. No element is expected to undergo plastic deformation at this stage, due to the fact that base shear is computed such that element carrying the most load is on the verge of yielding.
9. Add base shear-displacement pair obtained in Steps 6 and 8 to resultant pushover curve.
10. Increase the displacement of MCS and solve the system for base shear that will cause this deformation. Add the computed base shear–displacement pair to pushover curve.

11. Repeat Step 10 until either system becomes unstable or predefined displacement limit is reached to obtain the complete pushover curve.
12. Transform the deformations obtained for the most critical story to roof displacements to get the conventional pushover curve.

After the capacity (pushover) curve is obtained for the structure at Step 12, the performance of the evaluated building can be obtained by first determining the performance point on the curve either by capacity spectrum or displacement coefficients method, and finally comparing the ratio of yielded/failed elements (or the load they carry) to the allowable limits.

It should be noted that the proposed technique will require more information (such as the spatial distribution of members in horizontal and vertical axis) and involve more calculations than approaches stated in existing preliminary methods. However, as no finite element model creation and analysis is done, proposed method should not be considered a detailed analysis as well.

4.1.1 Calculating Element Lateral Effective Stiffnesses

4.1.1.1 Columns

The very first step of the proposed algorithm for determining the capacity curve of the evaluated structure is computing column effective stiffness values in the most critical floor. Though this is a trivial task for isolated members with theoretical boundary conditions (such as a pin or fixed ends), elements constrained in a frame show quite large deviations from this behavior due to the nature of physical beam-column joints. Many parameters such as connecting beam dimensions, story height, the total number of stories, and even loading scheme have an impact on the apparent stiffness value of a column if it is part of a framing system. Due to these reasons, it is crucial to calculate the effective stiffness of a column based on its physical properties and boundary conditions rather than using a statical formula (Equation (4.1)). In order to perform an in-situ study for each individual column in a frame, so-called “isolated ladder” approach, which is basically a substructuring technique, is used for reduced

computation effort and analysis time.

$$\text{Column Stiffness} = \alpha \cdot \frac{EI}{L^3} = \frac{\text{Column End Shear Force}}{\text{Column End Displacement}}$$

The α value in Equation (4.1) is expected to range from 3 to 12, which corresponds to different theoretical boundary conditions of pin-fixed to fixed-fixed connection respectively. Real world cases are expected to fall between these limits. In this technique, inner and outer “ladder” substructures of a general shear frame are isolated, and its stiffness matrix is calculated using several assumptions (Figure 4.1):

- Beams have inflection points at mid-length.
- Mid-length point of the beam does not have a vertical deflection (i.e. no gravity loads).
- Isolated tree substructures are two-dimensional (members connecting in out-of-plane direction have no effect on stiffness).
- Each node (beam-column connection) has a translation (horizontal) and a rotation (counter-clockwise) degree of freedom.
- Column size does not change along the vertical direction.

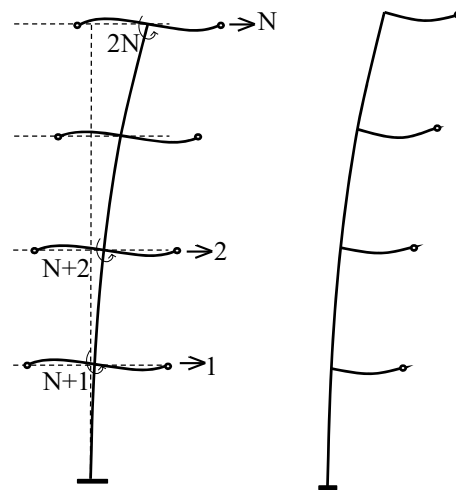


Figure 4.1: Inner and Outer 2-D “Ladder” Structures and Respective DOFs

The complete stiffness matrix is created ($2N \times 2N$ where N is the total number of stories) in such a way that the translational and rotational elements are grouped

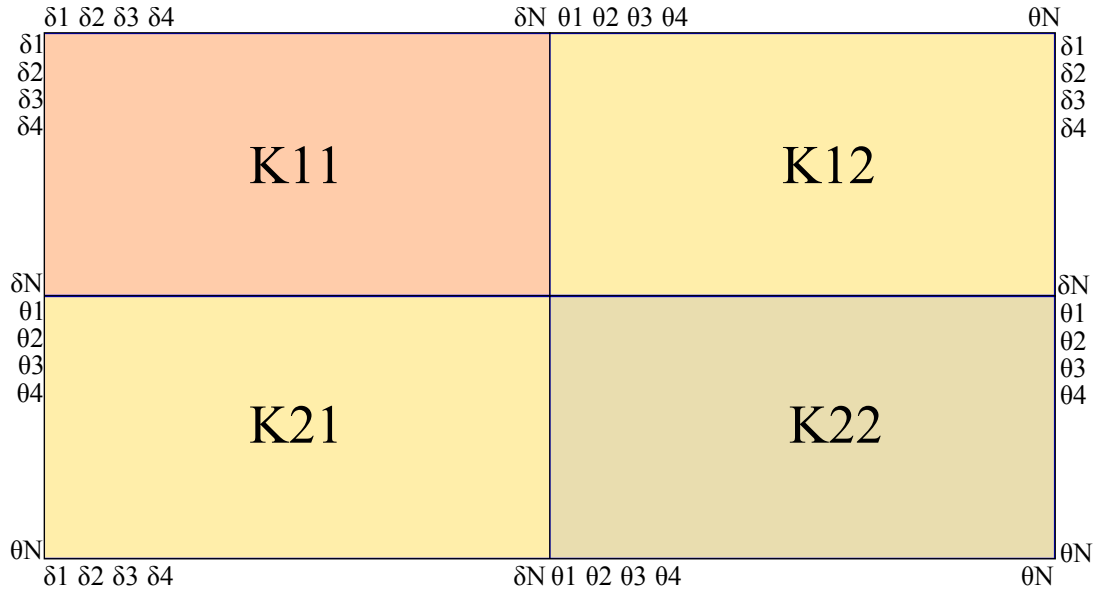


Figure 4.2: Sub-Matrices of Overall Stiffness Matrix

together (Figure 4.2), since rotational elements will be condensed out, as the system ('ladder') will only be loaded with horizontal forces.

Static condensation procedure could be applied to systems in the form of Equation (4.1).

$$\mathbb{A}\mathbb{Y} = \begin{bmatrix} A & B^T \\ B & D \end{bmatrix} \begin{bmatrix} x \\ y \end{bmatrix} = \begin{bmatrix} F \\ G \end{bmatrix} = \mathbb{F} \quad (4.1)$$

In these systems, static condensation of internal degrees of freedom is based on the substitution that first row of Equation (4.1) could be re-stated as Equation (4.2):

$$x = A^{-1}(F - B^T \cdot y) \quad (4.2)$$

Equation 4.2 is substituted into the second row of Equation (4.1), resulting in a system of the form:

$$Py = \bar{Q} \quad (4.3)$$

where $P = D - BA^{-1}B^T$ and $\bar{Q} = G - BA^{-1}F$. Thus, the vector $y \in \mathbb{R}^{N-M}$ could be calculated from a smaller system ($N - M$ instead of N). After the calculation of y , $x \in \mathbb{R}^M$ is computed by block diagonal system solution of Equation 4.2.

On this basis, the overall stiffness matrix for the isolated substructure is condensed such that only lateral loads calculated from an equivalent statical earthquake analysis approach will be applied. The loads to be applied to the substructure are determined

using Turkish Earthquake Code equivalent statical load approach [54]. As the geometry and material properties of the most critical are known, its total mass is calculated and the remaining floors are said to be identical. After application of these load vector to appropriate DOFs, their displacements are found. Finally, effective column stiffness K_e is calculated as the ratio of shear forces at column ends to drifts at the same nodes (which are basically end displacements at the ground floor) (Equation (4.4)).

$$K_e = \frac{\text{Column end force}}{\text{Column end displacement}} \quad (4.4)$$

As K_e will be a fundamental parameter in the computation of further seismic variables, the validity of the “ladder” approach should be tested.

4.1.1.2 Verification of Column Results

In order to deduce that the simplification of stiffness calculations by using a small substructure of the overall system yields results accurate enough to be considered as “correct”, several analyses are performed. In these analyses, column effective stiffness values are first computed by the approach in Section 4.1.1.1, and then by a commercial structural analysis software (SAP2000) using Equation (4.4). For comparison, the α variable in Equation (4.1) is used, which can be found by Equation (4.5).

$$\alpha_c = \frac{F_c}{\frac{EI}{L^3} \cdot \delta_c} \quad (4.5)$$

This process is carried out for several cases by selecting one parameter as varying and setting the others as their default (Table 4.1). Then the α values computed are plotted against the changing variable in their respective sections. As the right hand side of the verification procedure, the values obtained using analysis results of finite element models created by SAP2000 software (version 15.0.0) are utilized. In the modeling, one dimensional line elements are used for columns and beams. Slabs are not included directly, but their effect is considered in the model as constraints of all the nodes within a floor in displacements of both directions. Earthquake effect is applied as stated in the equivalent statical load approach of the Turkish Earthquake Code [54]; load acting on each floor is proportional to its mass and height. The column stiffness are calculated for outer and inner columns separately, using the shear forces and displacements obtained from the software after an analysis is completed.

Table 4.1: Parameters Used and Their Default Values

Parameter	Value
Modulus of Elasticity for Concrete	28000000 kN/m^3
First Story Height	4 m
Other Story Heights	3 m
Column Dimensions	0.4 m x 0.4 m
Beam Dimensions	0.25 m x 0.4 m
Compression Strength of Concrete (f_c)	20 MPa
Loading	Height proportional triangular
Number of Stories	6
Number of Bays in X Direction	3
Number of Bays in Y Direction	3

The following sections indicate that “ladder frame” method results are within an acceptable error tolerance, and can be used in further analysis techniques as an alternative to complete stiffness matrix generation of a floor.

4.1.1.2.1 Height of the First Story In most of the ordinary residential buildings which have a fewer number of floors and irregularities, the most critical story is the first one. Therefore, the effect of the first story height to the stiffness coefficient of first floor columns should be identified. In this analyses set, the first-floor height varies from 2 to 6 meters, and the results obtained are given in Figure 4.3. The linear representation of data in the first figure is not of high success (which is also indicated by its low r-square value). However, it will not be unrealistic to assume that 2 and 6 meters are not real-world applicable for ordinary residential buildings. If these two values are removed from the data set, it could be seen that the resultant graph is almost linear (Figure 4.4). Therefore, it could be concluded that the column stiffness coefficient is linearly related to the first story height for values between 2 and 6 meters (Equations (4.6) and (4.7)).

$$\alpha_{\text{inner}} = 1.0049h + 2.2108 \quad (4.6)$$

$$\alpha_{\text{outer}} = 1.0466h + 0.8673 \quad (4.7)$$

Stiffness coefficient (α) values calculated by ladder approach are very similar to SAP2000 values, with the average difference less than 10% (Figure 4.5).

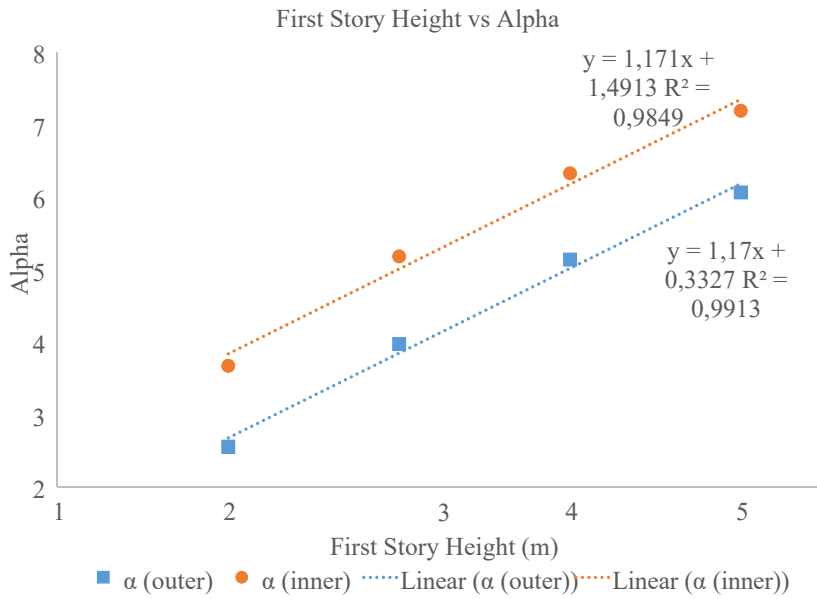


Figure 4.3: Effect of First Story Height on Stiffness Coefficient - 1

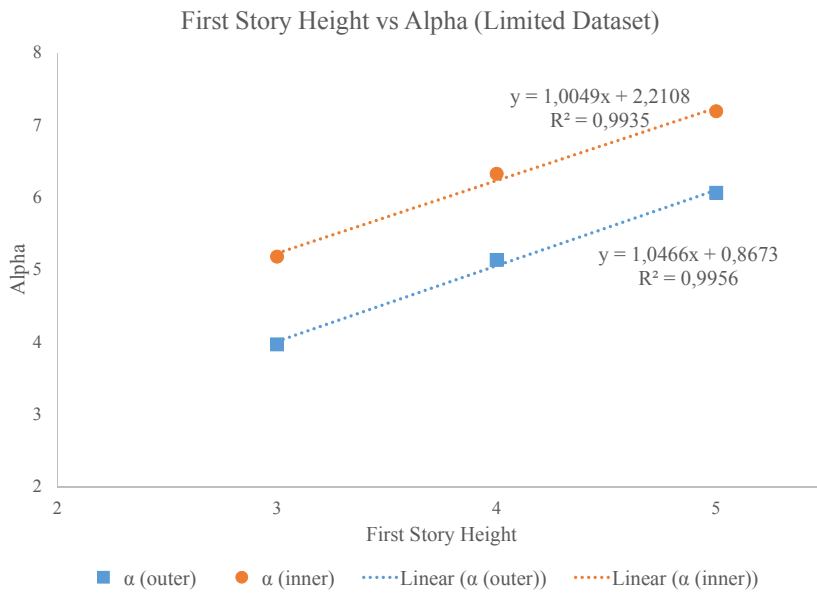


Figure 4.4: Effect of First Story Height on Stiffness Coefficient - 2

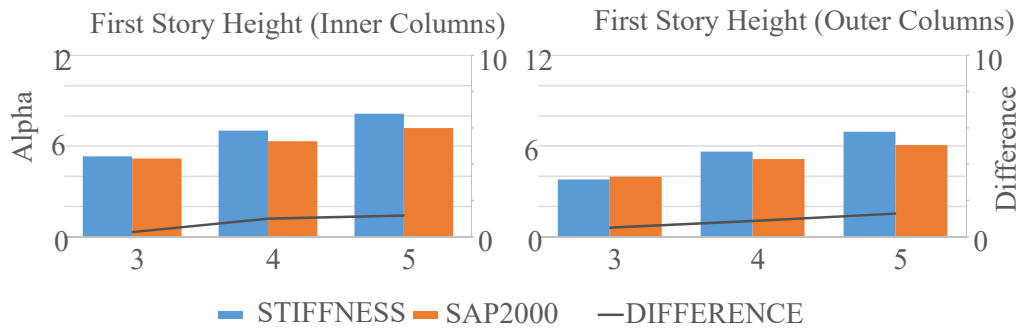


Figure 4.5: Ladder Approach vs SAP2000 Results for First Story Height

4.1.1.2.2 Total Number of Stories The total number of stories is another important parameter that determines the overall behavior of the structure under inertial loads. Buildings with many floors may require advanced studies for their response due to the increased effect of higher mode effects. However, buildings with a limited number of stories may be analyzed with simplified techniques to obtain an answer within an acceptable error tolerance.

In order to see the relation between the number of stories and the first story column stiffness coefficients, a number of analyses on buildings ranging from 4 to 20 stories are done. The increment of floor count is one between 4 to 10 stories and 5 between 10 to 20 stories. As seen in Figure 4.6, the effect of story count is asymptotic and it could be represented as an inverse function for the applicable range of the proposed method. The average difference between α values calculated by stiffness approach and SAP2000 analyses for varying number of stories are less than 10%, which could be considered as a reasonable difference for an approximation (Figure 4.7).

4.1.1.2.3 Column Size The ratio of rigidity of columns to beams which form a structural node is a major parameter that determines the distribution of element forces to the members involved. Column size directly increases or decreases this ratio, thus affects the stiffness coefficient of the target columns.

In the determination of this effect, different column sizes with areas ranging from 0.16 m^2 to 0.81 m^2 are analyzed while keeping beam dimensions constant. Columns are kept square to preserve symmetry. It is clearly seen from Figure 4.8 that column size is linearly proportional with stiffness coefficient in logarithmic scale, considering the

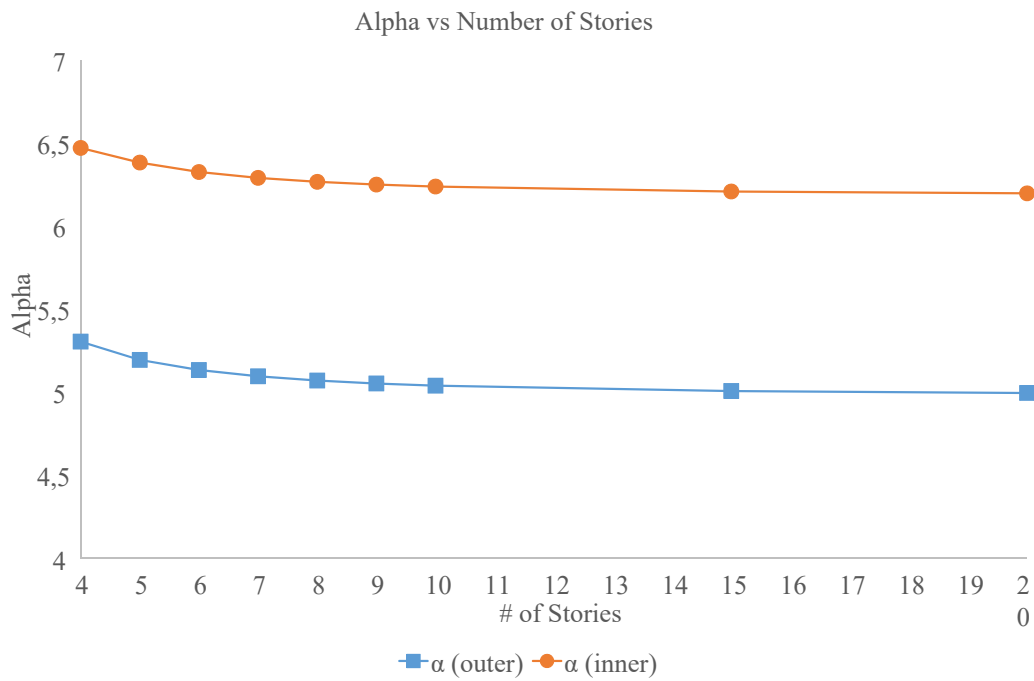


Figure 4.6: Effect of Number of Stories on Stiffness Coefficient

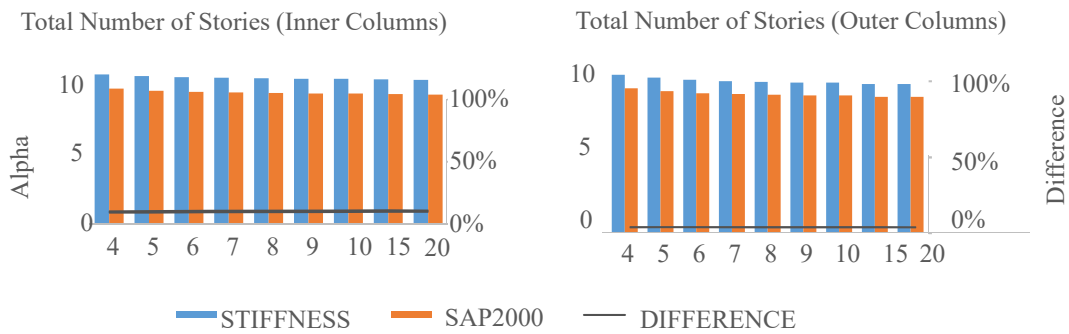


Figure 4.7: Ladder Approach vs SAP2000 Results for Total Number Of Stories

r-square values of the linear approximations. Being one of the important factors on

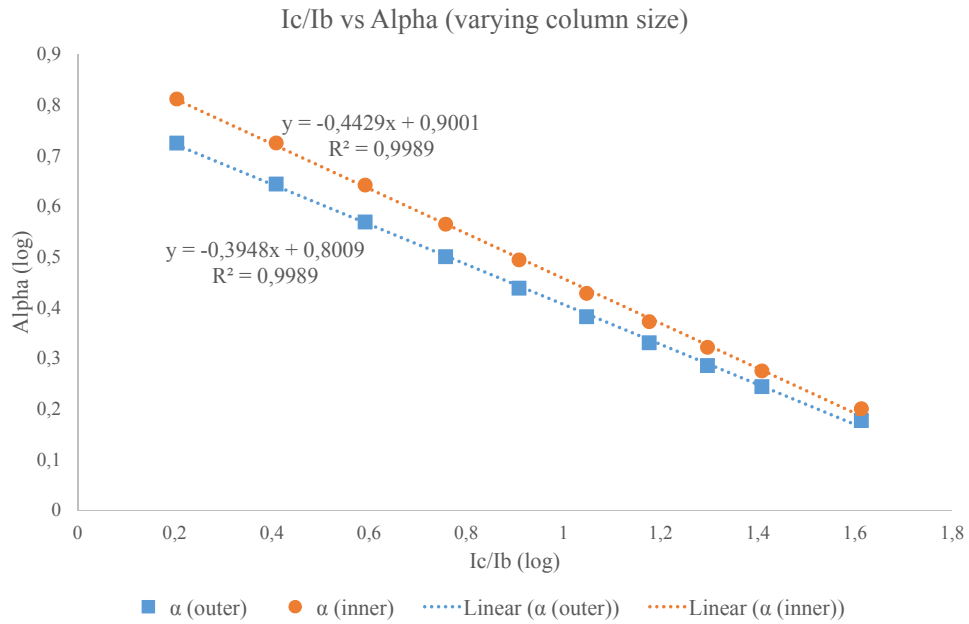


Figure 4.8: Effect of Column Size on Stiffness Coefficient

determining α coefficients, the comparison of results for varying column dimensions show an increased difference than other parameters, however these results could still be accepted as in the acceptable limit (Figure 4.9).

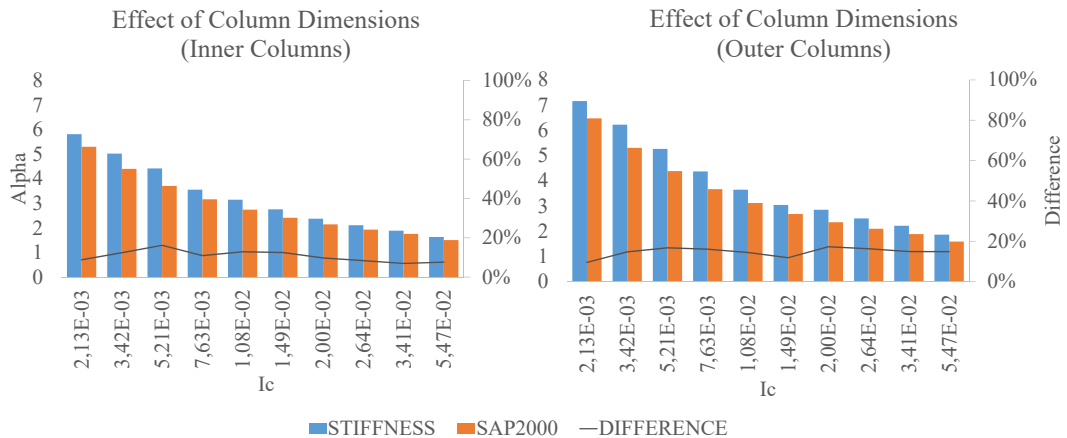


Figure 4.9: Ladder Approach vs SAP2000 Results for Column Size

4.1.1.2.4 Beam Size The ratio of the rigidity of columns to beams which form a structural node is a major parameter that determines the distribution of element forces to the members involved. Beam dimensions are inversely related with this ratio, thus

affects the stiffness coefficient of the target columns. For clarifying this influence, different analysis with changing beam dimensions are conducted. Beam area is kept varying from 0.1 m^2 to 4 m^2 by changing its width and depth.

As for the results of this analysis sequence, it is seen that if both curves are approximated using second-degree polynomials, outer columns exhibit a less fitting behavior than inner ones (Figure 4.10). If the varying input and output parameters (I_c/I_b and α) are converted to a logarithmic scale of base 10, the second-degree polynomial approximation will yield much better results (Figure 4.11). Therefore in further calculations, a log-log relationship is considered. The average difference between α

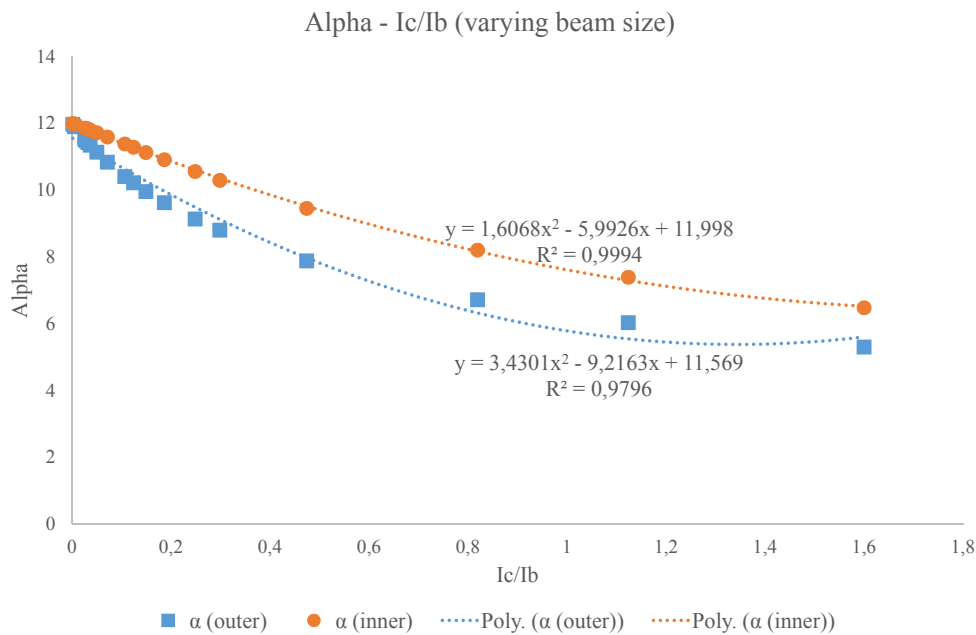


Figure 4.10: Effect of Beam Size on Stiffness Coefficient - 1

values calculated by stiffness approach and SAP2000 analyses for varying beam dimensions are highly conforming each other; maximum difference between two values is around 9% whereas the average is less than 3% (Figure 4.12).

4.1.1.2.5 Compressional Strength of Concrete The compressional strength of concrete directly affects the Young's Modulus of the material, therefore may have an impact on the stiffness coefficient. In order to search for this effect, the compressive strength of concrete in the model is changed from 4 MPa to 50 MPa, by steps of 2 between 4 and 20 MPa, 5 between 20 and 30 MPa, and 10 between 30 and 50 MPa.

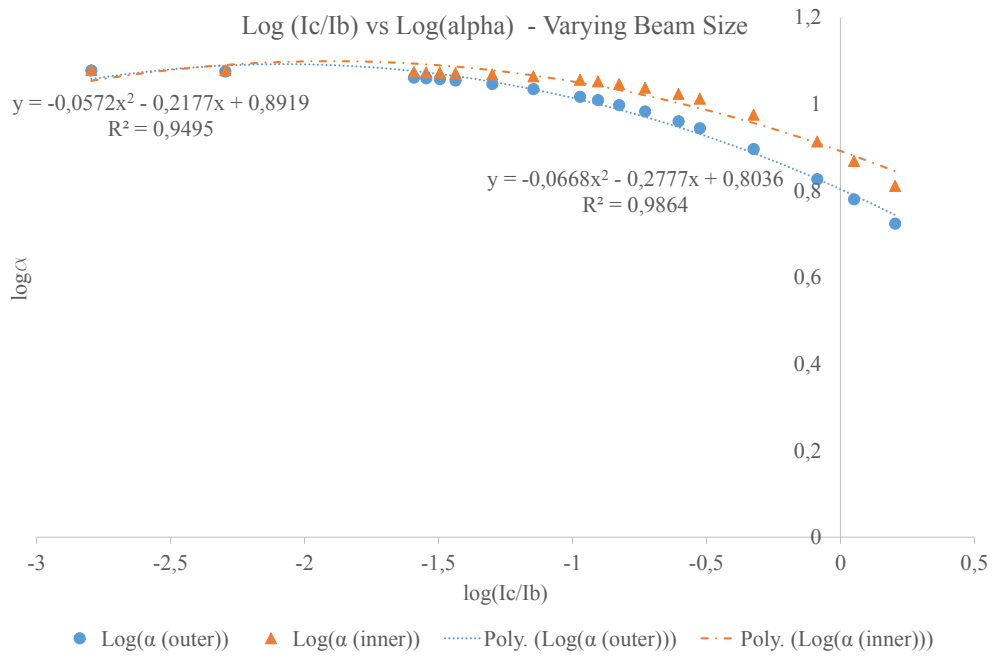


Figure 4.11: Effect of Beam Size on Stiffness Coefficient - 2

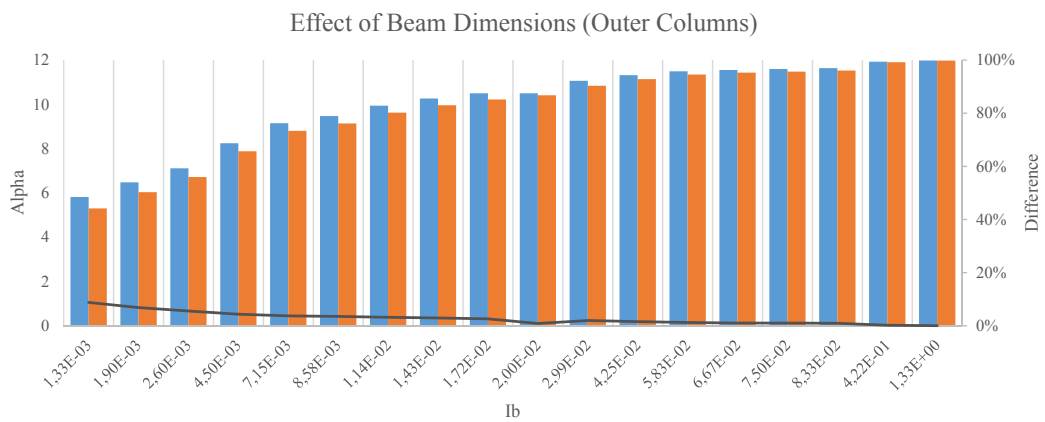
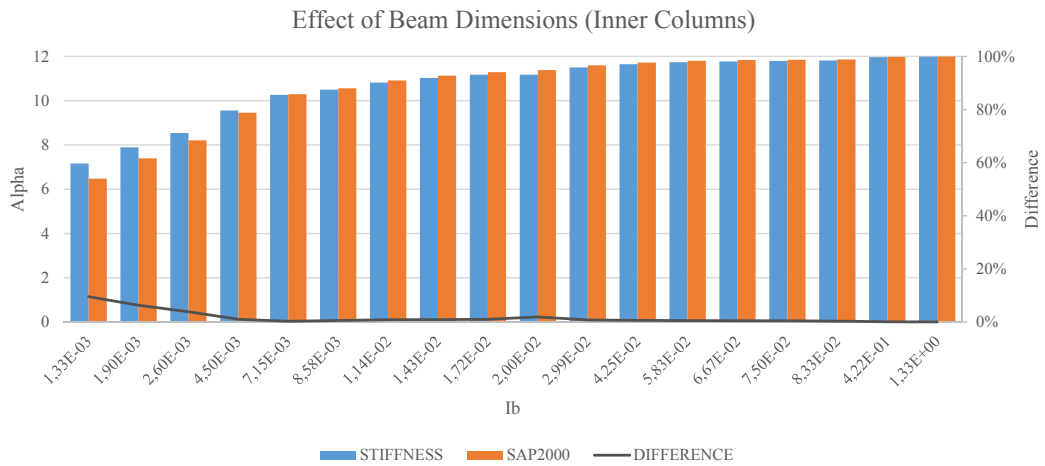


Figure 4.12: Ladder Approach vs SAP2000 Results for Beam Size

The results are summarized in Figure 4.13. As it is expected, changes in the compressive strength of concrete are irrelevant in the calculations of the stiffness coefficient, due to the fact that forces and displacements are both a function of the modulus of elasticity in the same order, and any change in this parameter cancels out in the calculations. With an average difference of 10%, it could be said values calculated

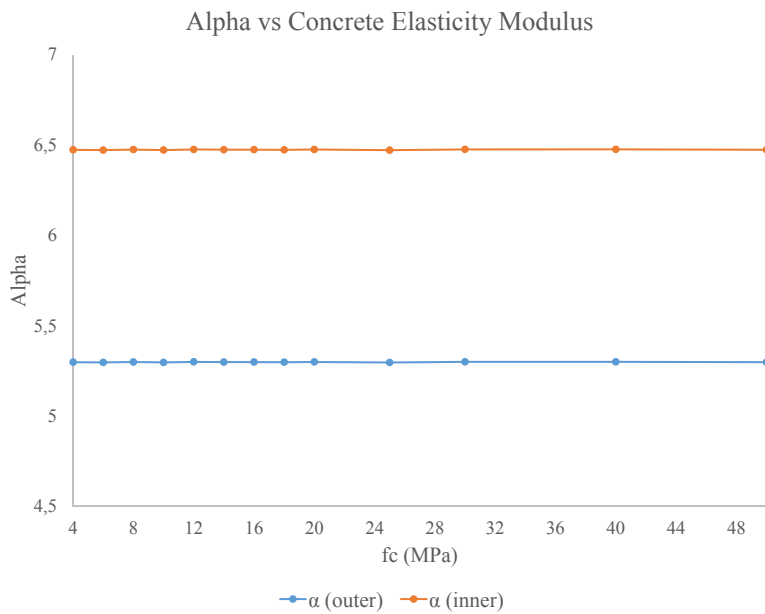


Figure 4.13: Effect of Compressive Strength on Stiffness Coefficient

by stiffness approach and SAP2000 analyses are within reasonable neighborhood of each other (Figure 4.14).

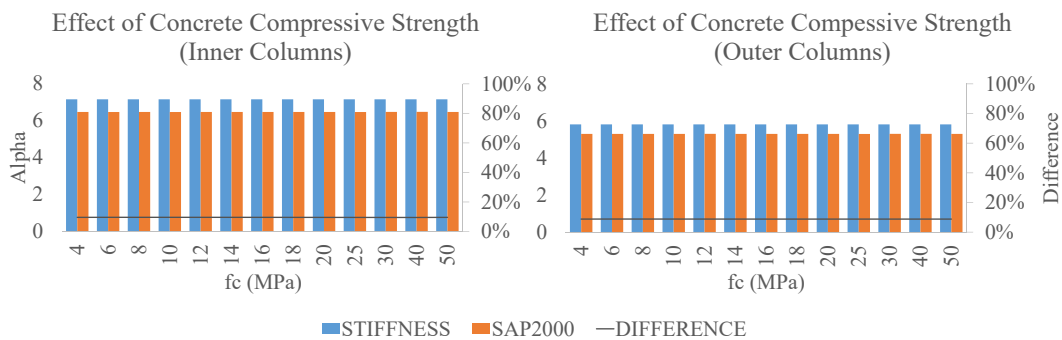


Figure 4.14: Ladder Approach vs SAP2000 Results for Compressive Strength of Concrete

4.1.1.2.6 Column Size Changes In Upper Stories As stated in the proposed algorithm (Section 4.1), the effective stiffness of a column is calculated using the response of ladder substructure it belongs, and one of the main assumptions is that column size is constant along that substructure. However, this is rarely the case in real life situations; since upper story columns carry less load than lower ones, their sections tend to diminish with height. To verify that constant section assumption does not cause excessive deviations from the actual case, several comparison analyses are conducted on different test ladder substructures. To see how the effect of section variation with respect to the number of stories between the critical floor and section change location, two different test structures are prepared. The first one includes a single floor between the critical story and the story where column sections change, and the second one includes two floors (Figure 4.15). As the number of floors be-

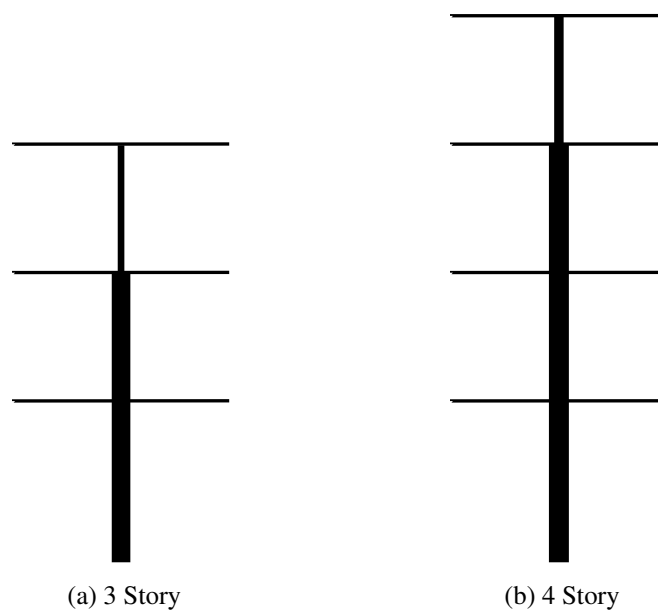


Figure 4.15: Column Size Control Structures

tween the most critical story (MCS) and column size change increases, this variation ceases to affect MCS. Moreover, the analysis results clearly indicate that even in the first case, deviation caused by assumption is less than 3% (Figure 4.16). For these reasons, no further studies are conducted, and it is verified that the assumption of “constant column size along the building height” causes no significant errors.

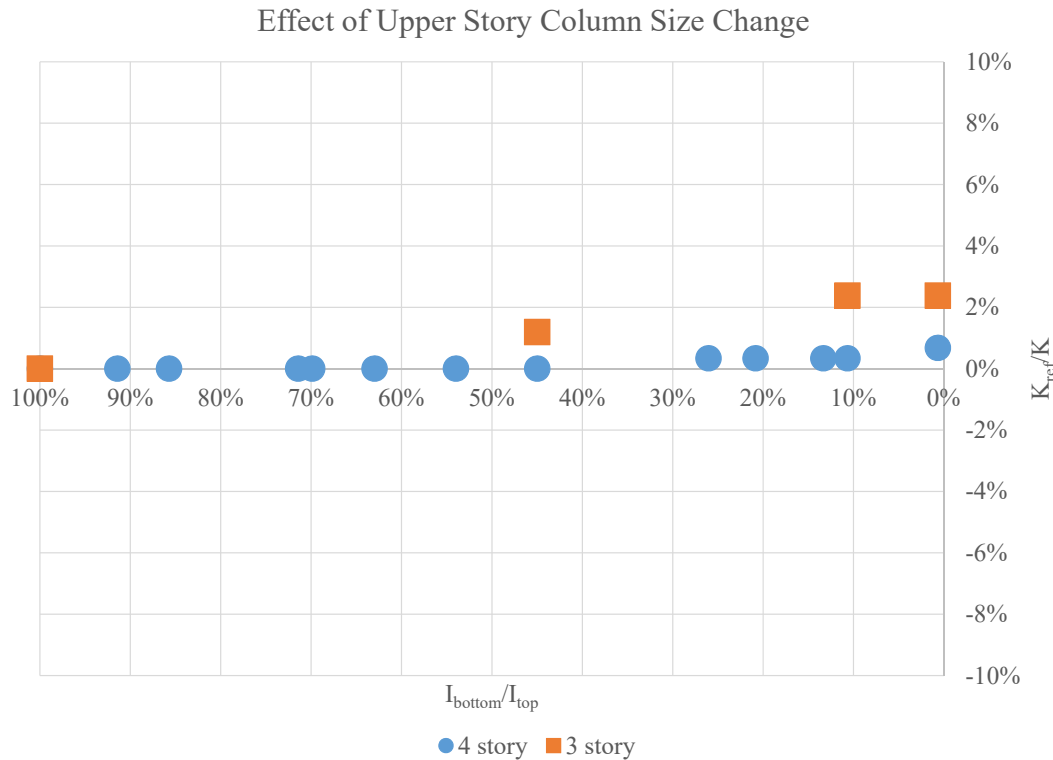


Figure 4.16: Effect of Column Size Variation Along Height

4.1.1.2.7 Discussion of Verification Results The preceding sections show that the stiffness values calculated using the suggested “ladder” approach are within a reasonable error margin of the values calculated using SAP2000, which is a commercial structural analysis and design software. The largest deviations are less than 10%, and on the average 5%, which is considered as acceptable. Moreover, the assumptions introduced are shown to cause negligible deviations from the true results.

4.1.1.3 Shear Walls

Shear walls carry almost all of the lateral loads applied to the structures since they are high-stiffness members of a structural system. Therefore, the presence of these elements requires further investigation, as their behavior is significantly different than other vertical elements (such as columns).

The dominant acting pattern of a reinforced concrete wall is highly dependent on its height; shear effects govern in lesser heights whereas flexure is more prominent in

longer elements. This phenomenon could be approximated by assuming shear and bending stiffness of a shear wall are two springs connected in series (Figure 4.17). In such systems, the overall stiffness is greatly influenced by the most flexible of the two elements; in other words, total elongation of the system is mainly due to the less stiff spring (Equation (4.8)).

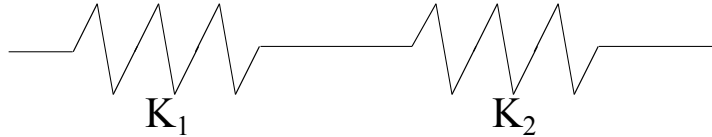


Figure 4.17: Shear Wall Stiffness Components

$$\frac{1}{k_T} = \frac{k_1 + k_2}{k_1 \cdot k_2} \quad (4.8)$$

Advancing this analogy to reinforced concrete walls, shear and flexural stiffness of a single isolated element could be calculated and combined as follows:

$$k_{\text{flexure}} = \frac{3 \cdot EI}{L^3} \quad (4.9)$$

$$k_{\text{shear}} = \frac{G \cdot b \cdot t}{1.2L} \quad (4.10)$$

$$k_{\text{total}} = \frac{k_{\text{shear}} + k_{\text{flexure}}}{k_{\text{shear}} \cdot k_{\text{flexure}}} \quad (4.11)$$

Inspecting equations (4.9) and (4.10) closely reveals that as the height of a shear wall increases, its bending stiffness decreases tremendously (as it is inversely proportional to the third power of length) whereas its shear flexibility is not affected much. As it is known that taller shear walls, which have lower k_{flexure} exhibit bending behavior, actual stiffness value should be close to the flexure stiffness. In the opposite case, shorter walls have smaller shear stiffness than flexure, therefore their deformation is governed by shear. In other words, the smaller stiffness component (shear or flexure) determines the overall behavior, which could be represented by Equations (4.8) and (4.11); k_{total} converges to the smallest of its sub-elements, k_{shear} and k_{flexure} (Figure 4.18).

Once the individual stiffness value of a shear wall is found by this method, it can be treated as a “central column” in the effective stiffness calculations.

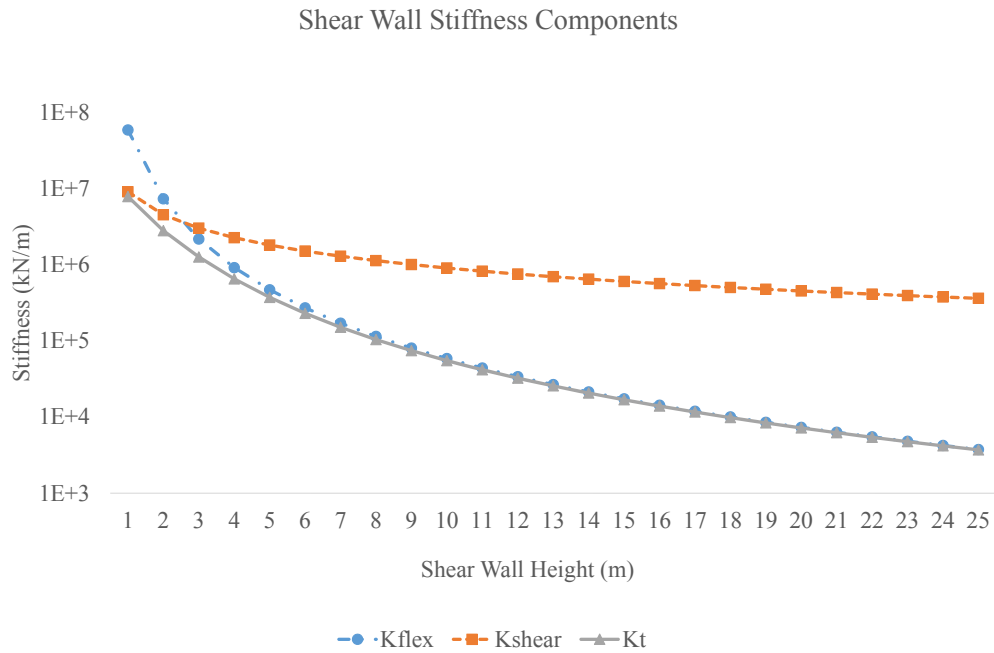


Figure 4.18: Components of Shear Wall Stiffness

4.1.1.4 Verification of Shear Wall Approach

For validating the “springs in series” approach, a total of 50 models with two different widths (1 meter and 3 meters) and changing heights (from 1 meter to 25 meters with 1 meter increment) are analyzed, and stiffness values calculated from these models are compared with the ones computed via the proposed method.

In the construction of finite element models, thin plate elements with 0.3 meters thickness are used. Walls are assumed to be isolated (i.e. no other structural components are included) and supported by fixed connections at ground level (Figure 4.19a). The load is applied to a single corner node of the top left shell element, resulting in excessive unrealistic deformations at application joint. To remedy this situation, nodes lying on the top surface are constrained to move equally in the x direction (Figure 4.19b).

In the verification process, total stiffness of a shear wall is calculated first by the suggested approach (Equation (4.11)), and then by SAP2000 analysis results (dividing applied force to top displacement). The results for both 1 meter and 3 meters wide walls indicate that the suggested approach works well; even for unrealistic conditions

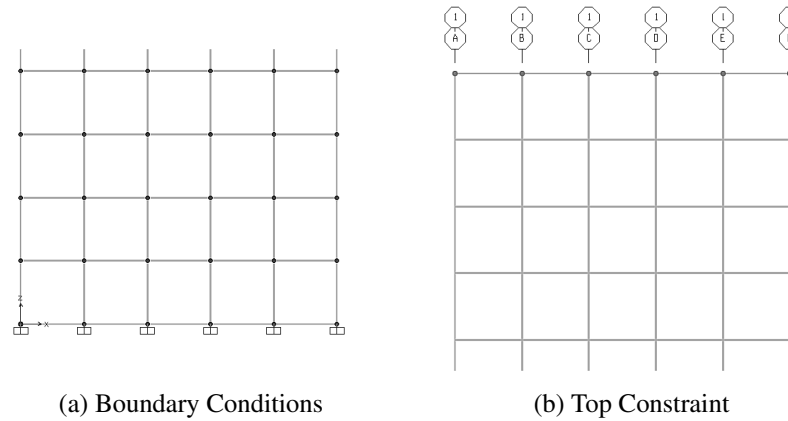


Figure 4.19: Shear Wall FEM Details

such as 1-meter wall height, the error is less than 5%. The discrepancy is much less in more applicable cases; the average error is less than 1% for walls taller than 3 meters (Figure 4.20).

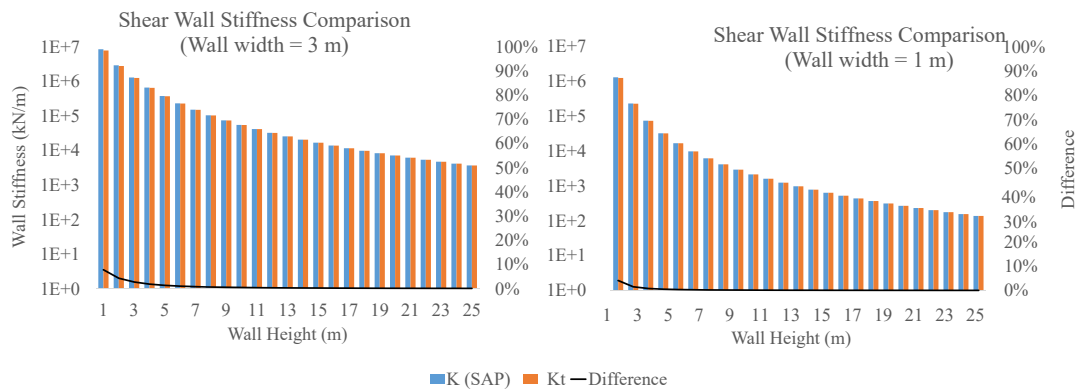


Figure 4.20: Shear Wall Approach Comparison Results

4.1.2 Creating Story Stiffness Matrix

After effective stiffness values of lateral load-carrying members in appropriate directions are determined, the overall stiffness matrix for the most critical story (MCS) is to be found using Equation (4.12). In the analysis, two lateral and one rotational degrees of freedom are considered (Figure 4.21).

The generation philosophy behind the creation of story stiffness matrix is identical to general stiffness approach; the effects (in terms of force) of unit deformation in one

DOF on others are said to be their stiffness values:

- When the system is deformed unity in x direction, all columns and shear walls create a force of $K_x \cdot 1 = K_x$ in x , therefore total stiffness in x is $\sum_{i=1}^k k_{xi}$, and a total moment of $\sum_{i=1}^k (-k_{xi} \cdot y_i)$ is required to balance torque effect of these forces. Net force in y direction is 0.
- When the system is deformed unity in y direction, all columns and shear walls create a force of $K_y \cdot 1 = K_y$ in y , therefore total stiffness in y is $\sum_{i=1}^k k_{yi}$, and a total moment of $\sum_{i=1}^k (-k_{yi} \cdot x_i)$ is required to balance torque effect of these forces. Net force x direction is 0.
- When the system is deformed unity as rotation, all columns and shear walls create a force based on their distance from the point of rotation ($\sum_{i=1}^k (-k_{xi} \cdot y_i)$ in x and $\sum_{i=1}^k (k_{yi} \cdot x_i)$ in y direction). Total moment required to balance torque effect is $\sum_{i=1}^k (k_{xi} \cdot y_i^2 + k_{yi} \cdot x_i^2)$.

The resultant stiffness matrix is given in Equation (4.12).

$$\begin{bmatrix} \sum_{i=1}^k k_{xi} & 0 & \sum_{i=1}^k (-k_{xi} \cdot y_i) \\ 0 & \sum_{i=1}^k k_{yi} & \sum_{i=1}^k (k_{yi} \cdot x_i) \\ \sum_{i=1}^k (-k_{xi} \cdot y_i) & \sum_{i=1}^k (k_{yi} \cdot x_i) & \sum_{i=1}^k (k_{xi} \cdot y_i^2 + k_{yi} \cdot x_i^2) \end{bmatrix} \quad (4.12)$$

4.1.3 Calculating Member Force-Deformation Relations

The force-deformation relations for each member will be required during computing element forces from the deformation values which will be calculated during the analysis. Once end displacements of each vertical member are found out, these deformations should be converted to element forces. The most classical approach is elastic-perfectly plastic behavior with either zero or few percents of post-yield stiffness (Figure 4.22).

One of the basic inconvenience of bilinear capacity approximations is that since the behavior is represented as two lines with a discontinuity, processing of values too close to transition point may result in convergence problems during optimization for

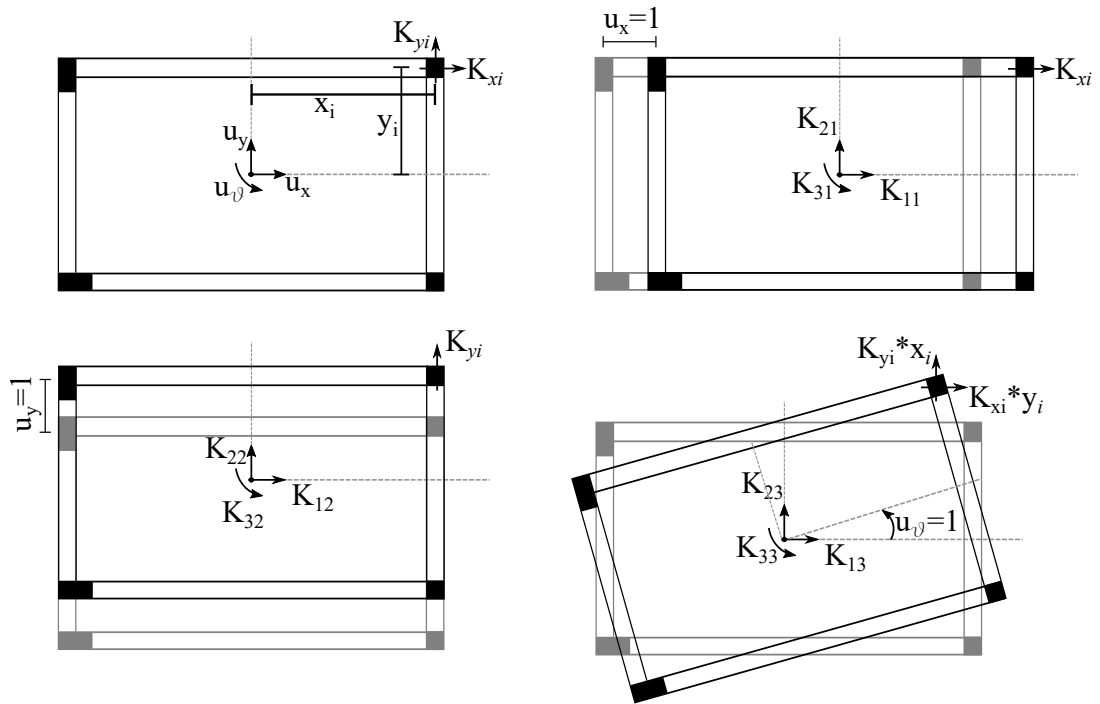


Figure 4.21: Stiffness Calculations for Most Critical Story

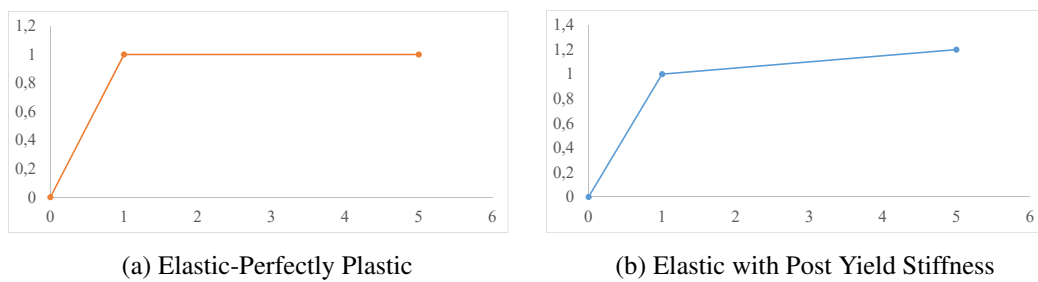


Figure 4.22: Possible Element Capacity Types

Table 4.2: Parameter Sets and Their Values

	SET 1	SET 2	SET 3	SET 4
n_1	4.0	4.0	7.0	7.0
n_2	5.5	5.5	8.5	8.5
n_3	8.5	8.5	11.5	11.5
α	0.1	0.2	0.1	0.2
K (kN/m)	4000	4000	4000	4000
d_y (cm)	0.015	0.015	0.015	0.015

story deflections. Several additional constraints such as preventing an element to return to a normal state once it yields could be added for a more stable calculation loop. Moreover, slightly changing the member capacity models will also work.

4.1.3.1 Custom Force-Deformation Equation Set

The first approach for improving stability in this study was to construct a set of equations which are continuous and differentiable at their boundaries (Figure 4.23).

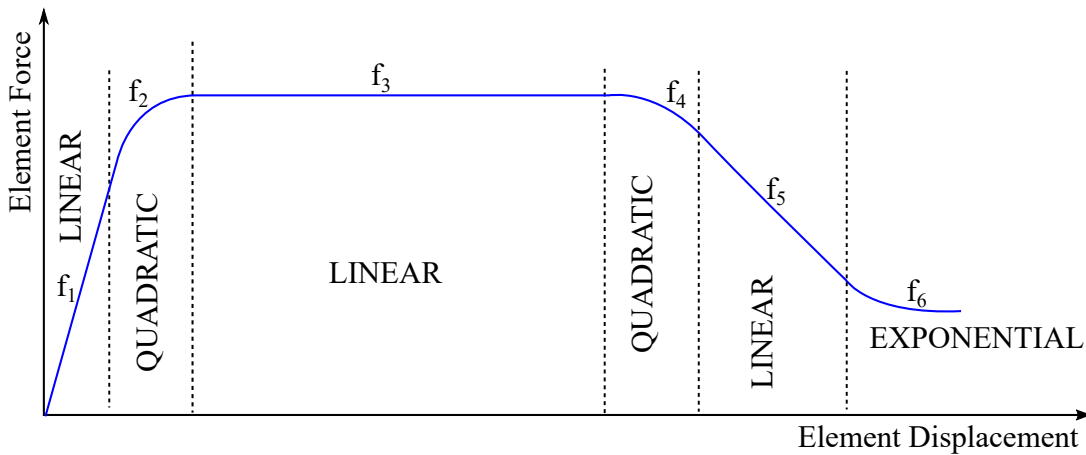


Figure 4.23: Proposed Equation Types for Regions

The complete force-deformation is obtained after conducting necessary computations by enforcing continuity and differentiability in addition to other predefined boundary values, (Figure 4.24). This set of equations is completely parametric, and is calculated for several sets of parameters (Table 4.2) as demonstration in Figure 4.25

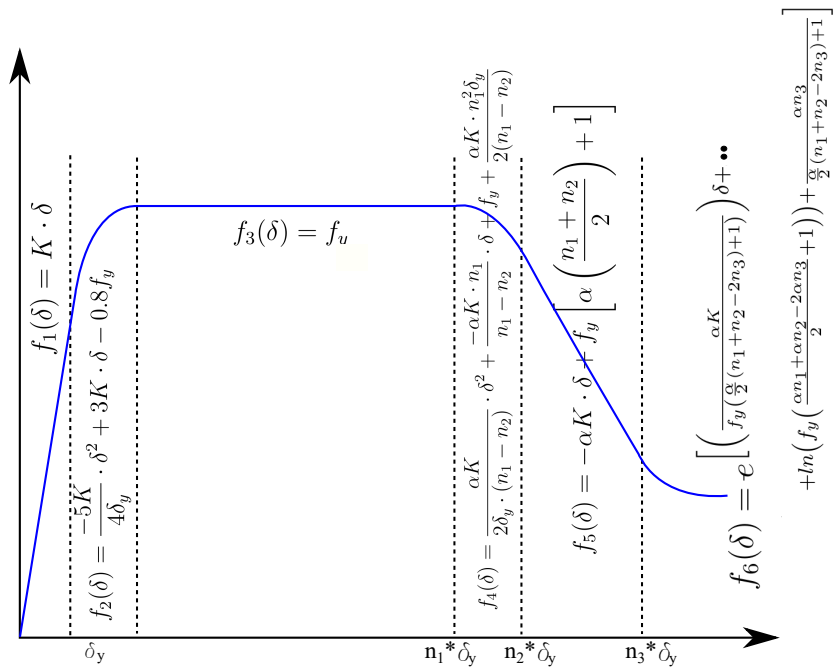


Figure 4.24: Overall Force-Deformation Relation

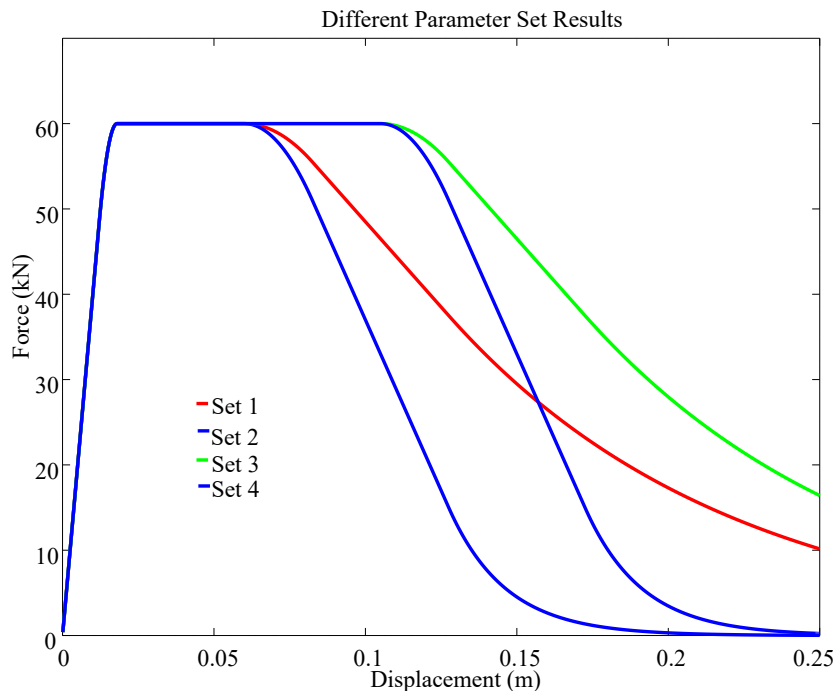


Figure 4.25: Results of Four Parameter Sets

4.1.3.2 Using FEMA356 Modeling Parameters

The Prestandard and Commentary for the Seismic Rehabilitation of Buildings has a section for general assumptions and requirements during modeling and design of buildings. In the nonlinear procedures section (C6.4.1.2.2), it gives templates for typical force–deformation relations, either in direct terms such as strain, curvature, rotation, and elongation or in terms such as shear angle and tangential drift ratio ([5]) (Figure 4.26).

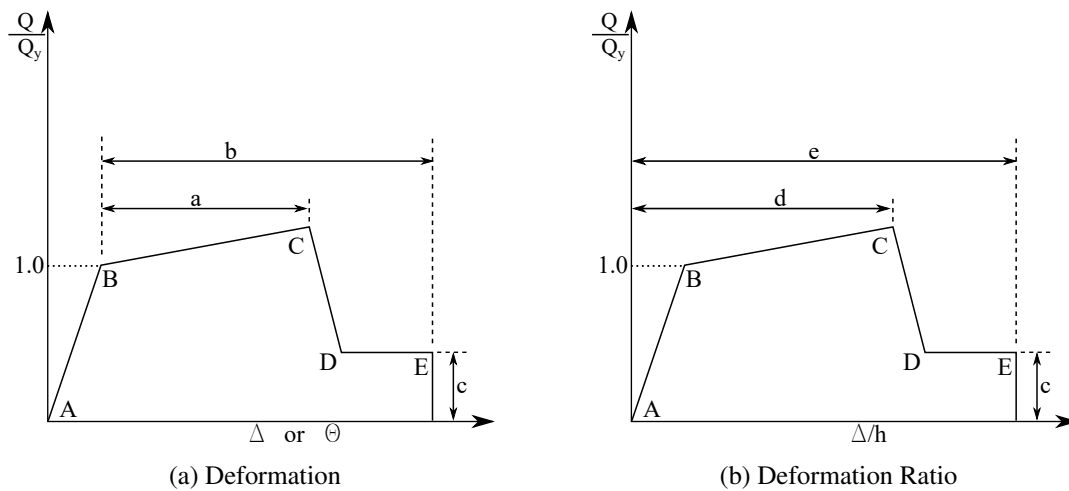


Figure 4.26: Generalized Force-Deformation Relations for Concrete Elements

In Figure 4.26a, parameters a and b refer to post-yield (i.e. plastic) deformations. The parameter c is the reduced resistance after the sudden reduction from C to D . On the contrary, in Figure 4.26b, the parameters d and e refer to total deformations measured from the origin. For both of the approaches, strength of member is assumed to drop to zero immediately after point E .

The values of these parameters (a , b , c) are defined in FEMA356 Table 6-8 based on the used capacity of a member in terms of axial and shear forces, in addition to the type of transverse reinforcement (Table 4.3).

4.1.3.3 Member Section Analysis

In order to be able to construct a load-deformation curve for a member (which will be used in determining element hinge status in the latter stages of analysis) either by

Table 4.3: Modeling Parameters for Reinforced Concrete Columns by FEMA356

Conditions			Modeling Parameters		
			a	b	c
<i>i. Columns controlled by flexure</i>					
$\frac{P}{A_g f'_c}$	Stirrups	$\frac{V}{b_w d \sqrt{f'_c}}$			
≤ 0.1	C	≤ 3	0.02	0.030	0.2
≤ 0.1	C	≥ 6	0.016	0.024	0.2
≥ 0.4	C	≤ 3	0.015	0.025	0.2
≥ 0.4	C	≥ 6	0.012	0.020	0.2
≤ 0.1	NC	≤ 3	0.006	0.015	0.2
≤ 0.1	NC	≥ 6	0.005	0.012	0.2
≥ 0.4	NC	≤ 3	0.003	0.010	0.2
≥ 0.4	NC	≥ 6	0.002	0.008	0.2
<i>ii. Columns controlled by shear</i>					
All cases			—	—	—
<i>iii. Inadequate development or splicing along the clear height</i>					
Hoop spacing $\leq d/2$			0.01	0.02	0.4
Hoop spacing $\geq d/2$			0.01	0.02	0.4
<i>iv. Columns with axial loadings exceeding $0.70P_o$</i>					
Conforming hoops over entire length			0.015	0.025	0.02
All other cases			0	0	0

custom curve or FEMA356 recommendations, its yield and ultimate strength parameters should be known. This requirement necessitates the knowledge of several section properties such as reinforcement ratio and distribution, material attributes (concrete and steel models), and clear cover. However, most of these parameters are usually unknown, since their determination requires rigorous destructive and/or non-destructive testing at the site, which may only be considered in a full-scale investigation project. Therefore, several assumptions are carried out at this stage to estimate these obscure attributes:

- Clear cover distance is said to be 25 millimeters.
- Reinforcement is assumed to be S420 steel with a modulus of elasticity of 200 GPa and yield strain of 0.00182.
- Equivalent rectangular concrete compression block approach is applied with the

assumption of $k_1 = 0.85$, which holds true up to C25 concrete, and introduces negligible errors for higher compression strength values [64].

- Total longitudinal reinforcement in columns is taken as 1% of the gross cross-sectional area, minimum value defined in Turkish Earthquake Code [54].
- The presence of intermediate steel layers is assumed to be correlated with the length of the respective edge (Equation (4.13)).

$$\text{Number of intermediate layers} = \text{floor} \left(\frac{\text{edge length}}{50\text{cm}} \right) \quad (4.13)$$

- Total reinforcement area is assumed to be divided equally to every layer (top, bottom, and intermediate) (Figure 4.27 - all dimensions are in cm).

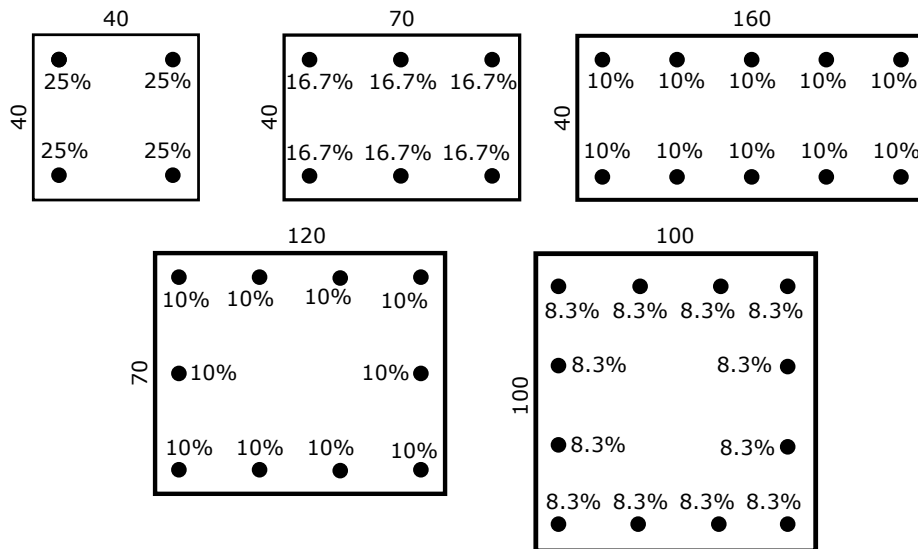


Figure 4.27: Sample Longitudinal Reinforcement Distributions

Element ultimate capacity forms a curve under varying uniaxial loading of combined axial forces and flexure, which is commonly called as interaction diagrams [64] (Figure 4.28). Every point on the curve represents the maximum axial force - moment couple the member can carry without failing; any location inside the diagram is considered safe, whereas outside regions are unsafe.

In order to obtain the force-deformation relations given in Figure 4.26, all data of interaction diagram for the section (Figure 4.28) is not necessary; only three fixed values are sufficient; yield moment, yield rotation, and ultimate moment.

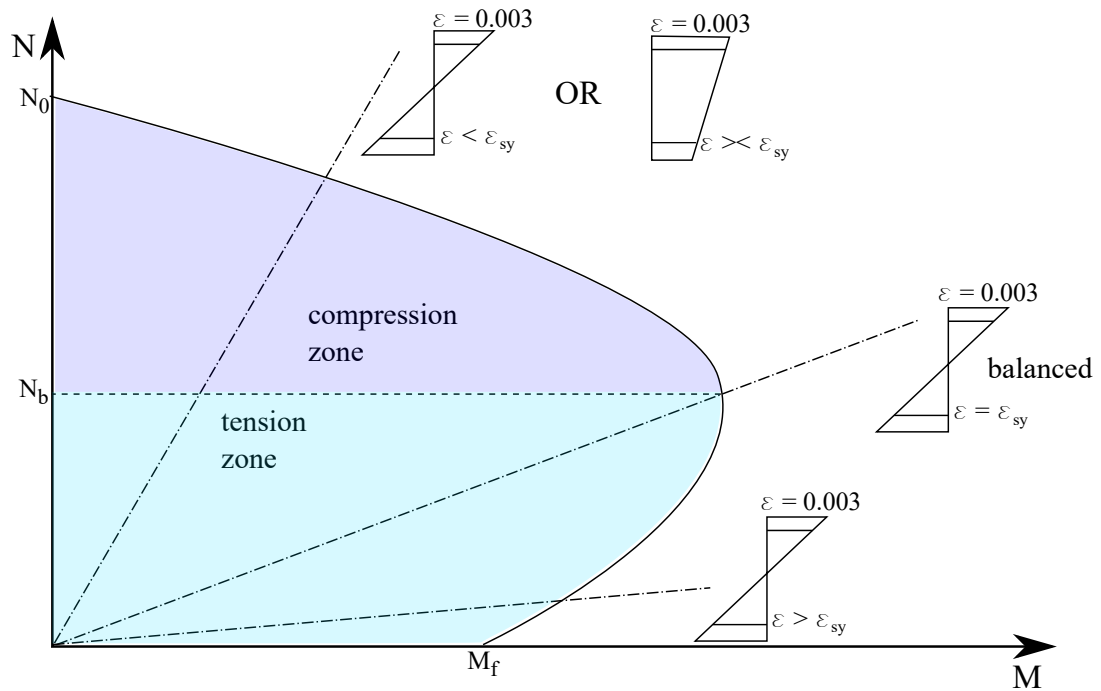


Figure 4.28: A General Interaction Diagram

4.1.3.3.1 Calculating Section Yield Capacity At the point of yield, it is assumed that reinforcement at "tension" side yields while top concrete fibers are far away from crushing strain (Figure 4.29).

The system in Figure 4.29 is impossible to solve in a closed form especially in the case of intermediate steel layers. Therefore, a trial and error search is implemented:

1. Assume neutral axis depth "c".
2. Form strain triangles, compute strains, then stresses, finally forces for steel layers and concrete (Figure 4.29).
3. Check force equilibrium:

$$N = 0.85f_{cd}A_{cc} + \sum_{i=1}^n (A_{si}\sigma_{si}) \quad (4.14)$$

4. If equilibrium is not satisfied, revise assumption of "c" by balancing excess tension or compression. If satisfied, calculate total moment of section forces around centroid to find out M_y and ϵ_c/c to compute yield curvature ϕ_y .

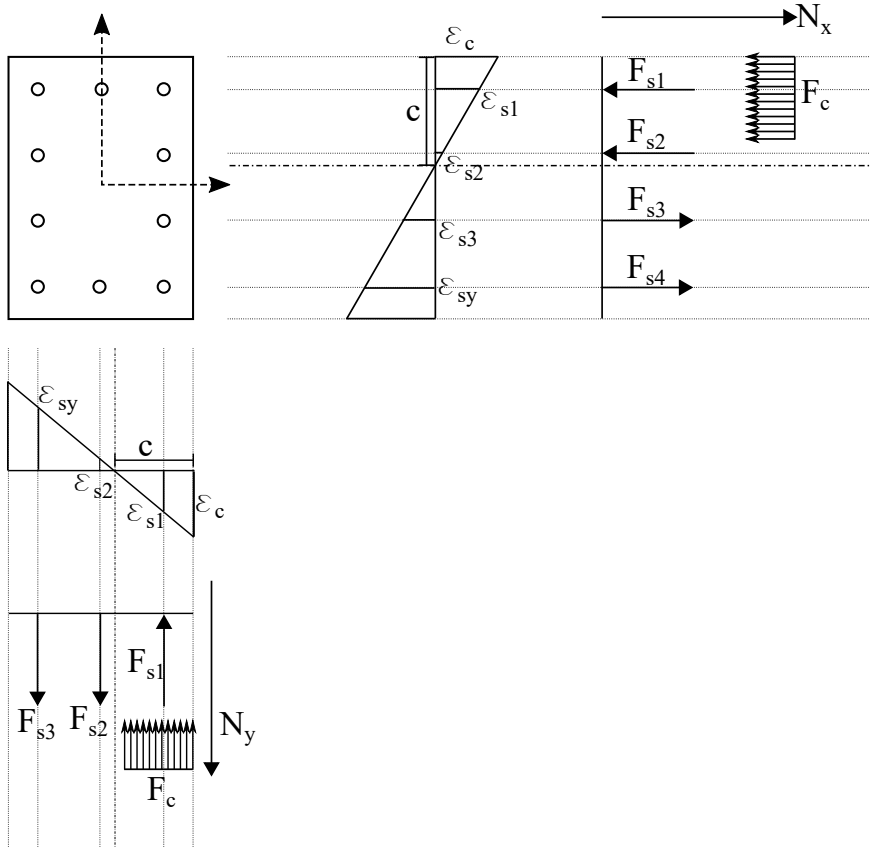


Figure 4.29: Column Sectional Response at Yield Point for Two Axes

4.1.3.3.2 Calculating Section Ultimate Capacity The ultimate point during the section analysis is where compression side strains reach the concrete crushing limit (approximately 0.003). At this instant, furthest steel strains are expected to be much higher than their yield values, and strain hardening may occur. Nevertheless, it is observed that this increase of strength in reinforcement cannot compensate the effect of crushed concrete strains, thus strain hardening can be neglected [65]. Aside from this approximation, the overall process is similar to calculating section yield capacity. Nonetheless, the solution may be simplified even further; if intermediate steel layers are not considered, approximate ultimate moment for the column can be determined as in Equation (4.15) [64] [65].

$$M_r \approx 0.5N_d \left(h - 1.2 \frac{N_d}{f_{cd}b} \right) + 0.5A_{st}f_{yd} (d - d') \quad (4.15)$$

This approximation will yield better results in higher axial load conditions due to the fact that increased loads will shift neutral axis down, causing less strain in intermediate steel layers [65].

4.1.3.3.3 Converting Moment-Curvature to Moment-Rotation The section analyses in the previous paragraphs result in yield and ultimate moment capacity of the section with respective curvature values. However, during analysis, available deformation parameter will be top end displacement of vertical members, which could be converted to chord rotations using element length and small angle approximation. Therefore, it is adjutory to relate section curvature with rotation.

At yielding instant, the element exhibits a translational deflection Δ_y caused by yield rotation φ_y under the effect of M_y , which in turn causes curvature ϕ_y (Figure 4.30). From basic stiffness and slope-deflection relations, it is known that moment and trans-

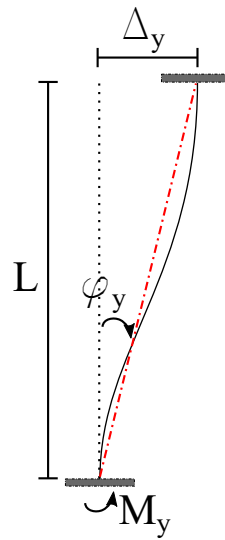


Figure 4.30: Deformations at Yielding Instant

lational deformations are related as:

$$M_y = \frac{6EI}{L^2} \Delta_y \quad (4.16)$$

Assuming small angle approximation holds valid for structural deformations, and curvature of an element under moment effect M_y is related with section EI :

$$\begin{aligned} \Delta_y &= \varphi_y \cdot L \\ \phi_y &= \frac{M_y}{EI} \end{aligned} \quad (4.17)$$

If we combine Equations (4.16), (4.17), and then solve for yield rotation:

$$\varphi_y = \phi_y \cdot \frac{L}{6} \quad (4.18)$$

For ultimate case, calculations get complicated due to the fact that plastic deformations and rotations occur. In this case, the total rotational deflection of the element is found by adding yield rotation to the plastic deformation, which in turn is a function of length where section exhibits plastic characteristics. This parameter is called "plastic hinge length", and different values are estimated to be used in the analysis where simple lumped plasticity approach is followed [66] (Table 4.4).

Table 4.4: Empirical Expressions for Plastic Hinge Length

Researcher	l_p
Baker [67]	$k \cdot d \cdot (z/d)^{0.25}$
Sawyer [68]	$0.25d + 0.075z$
Priestley and Park [69]	$0.08z + 6d_b$
Paulay and Priestley [70]	$0.08z + 0.022d_b \cdot f_y$
Sheikh and Khoury [71]	$1.0h$
Coleman and Spacone [72]	$G_f^c / [0.6f_c' (\varepsilon_{20} - \varepsilon_c + 0.8f_c'/E_c)]$
Panagiotakos and Fardis [73]	$0.18z + 0.021d_b \cdot f_y$
Bae and Bayrak [74]	$l_p/h = [0.3(p/p_0) + 3(A_s/A_g) - 1] (z/h) + 0.25$

where

A_g : Gross area of concrete cross-section

A_s : Area of tension reinforcement

d : Effective depth

d_b : Longitudinal reinforcement diameter

E_c : Modulus of elasticity for concrete

f_c : Concrete compressive strength

f_y : Reinforcement yield strength

G_f^c : Concrete fracture energy in compression

h : Overall depth

p : Applied axial force

$p_o = 0.85f_c'(A_g - A_s) + f_yA_s$: Nominal axial load capacity per ACI318-05

z : Distance from critical section to point of contraflexure

ε_c : Peak compressive strain

ε_{20} : Strain corresponding to 20% of the compressive strength

If element force-deformation relations given in FEMA356 will be used (Figure 4.26) instead of a user-defined curve (4.24), ultimate rotation values can be obtained directly from Table 4.3.

4.1.4 Applying Unit Load to Story

Once the 3×3 stiffness matrix of the most critical story is established, a unit load depending on the analysis direction is applied to it so that it is possible to estimate the yield force for the most critical story:

$$\vec{V}_x = \begin{Bmatrix} 1 \\ 0 \\ 0 \end{Bmatrix} \quad \vec{V}_y = \begin{Bmatrix} 0 \\ 1 \\ 0 \end{Bmatrix} \quad (4.19)$$

4.1.5 Calculating Member End Deflections and Forces

The end deflections of each column and shear wall based on story center of mass (CM) can be calculated by transforming displacement vector from CM to element location. As the slab translates and rotates at the same time, the displacement at any point can be calculated as in Equation (4.20):

$$\begin{aligned} \Delta_{xi} &= \delta_{xc} \mp \theta \cdot e_{yi} \\ \Delta_{yi} &= \delta_{yc} \mp \theta \cdot e_{xi} \end{aligned} \quad (4.20)$$

where Δ_i is the displacement of i^{th} column, δ_c is the displacement of CM, θ is floor rotation, and e is the eccentricity of target member with respect to CM. Sign of the right hand side of Equation (4.20) depends on the rotation and location vectors of point i (Figure 4.31). Mathematically, these signs could be computed using cross product of unit rotation and location vectors:

$$\begin{aligned} \vec{\theta} &= \{0, 0, \text{signum}(\theta)\} \\ \vec{r} &= \{\text{signum}(e_x), \text{signum}(e_y), 0\} \\ \vec{\theta} \times \vec{r} &= \{\text{signum}(\Delta_x), \text{signum}(\Delta_y), 0\} \end{aligned} \quad (4.21)$$

where signum is the sign function. As an example, the results for a positive counter-clockwise rotation ($\vec{\theta} = \{0, 0, 1\}$) yields the values in Table 4.5. Once end displacements of an element is found, its shear force can be calculated using the effective stiffness value computed in Section 4.1.1 (Equation (4.1)).

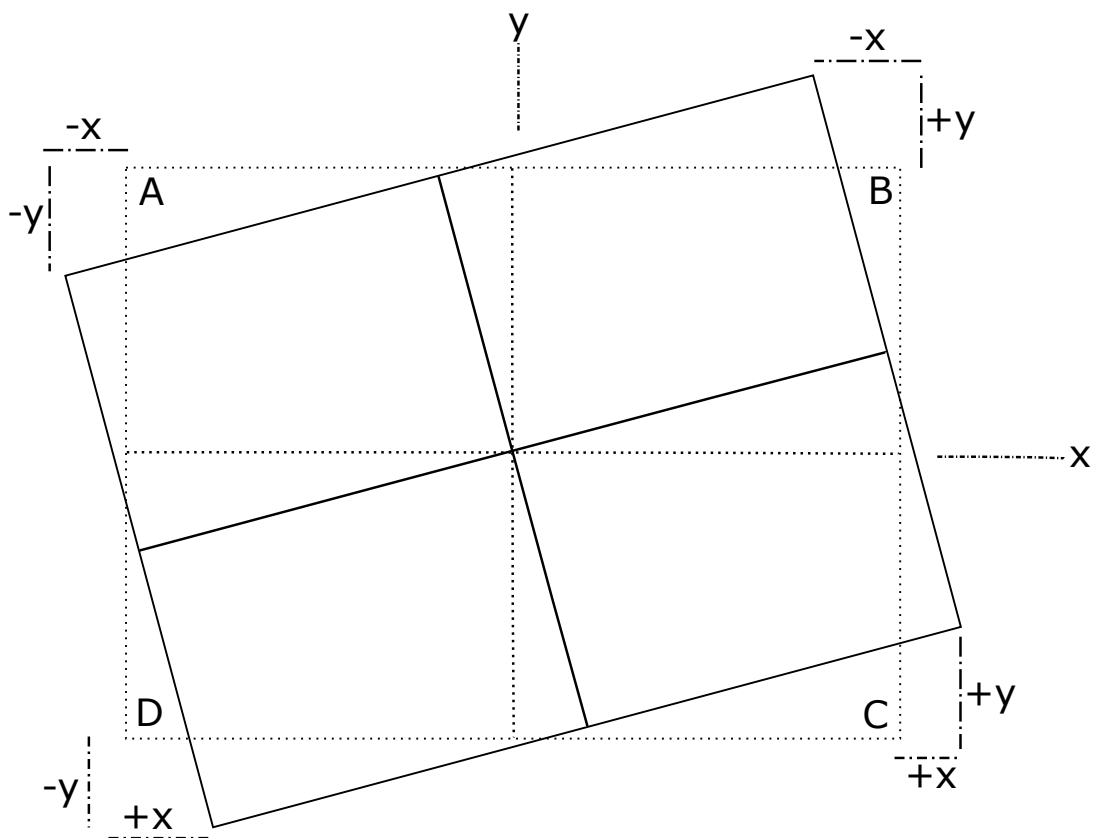


Figure 4.31: Signs of Column End Displacements

Table 4.5: Member End Displacement Equation Signs

Point	\vec{r}	$\vec{\theta} \times \vec{r}$	Displacement Equation
A	$\{-1, 1, 0\}$	$\{-1, -1, 0\}$	$\Delta_{xi} = \delta_{xc} - \theta \cdot e_{yi}$ $\Delta_{yi} = \delta_{yc} - \theta \cdot e_{xi}$
B	$\{1, 1, 0\}$	$\{-1, 1, 0\}$	$\Delta_{xi} = \delta_{xc} - \theta \cdot e_{yi}$ $\Delta_{yi} = \delta_{yc} + \theta \cdot e_{xi}$
C	$\{1, -1, 0\}$	$\{1, 1, 0\}$	$\Delta_{xi} = \delta_{xc} + \theta \cdot e_{yi}$ $\Delta_{yi} = \delta_{yc} + \theta \cdot e_{xi}$
D	$\{-1, -1, 0\}$	$\{1, -1, 0\}$	$\Delta_{xi} = \delta_{xc} + \theta \cdot e_{yi}$ $\Delta_{yi} = \delta_{yc} - \theta \cdot e_{xi}$

4.1.6 Finding First Yield Point of Structure (End of Linear Range)

Once the system is loaded with the unit load and all vertical element forces are computed using the approach given in Section 4.1.5, the member with the highest internal force is found. Considering the system will behave linearly up to the yield point, it is apparent that this element will yield first among all the others. Thus, it is possible to obtain the base shear force that will cause the first non-linearity in the system:

$$V_{\text{yield}} = \frac{F_y^e}{F_u^e} \quad (4.22)$$

where F_y^e is yield strength of the element with maximum force under unit load, and F_u^e is the force under unit load. The reason of determining yield base shear is that there is no need to pick up additional points in the elastic range of capacity curve; once the linear to non-linear transition point is established, algorithm can continue in the inelastic region (Figure 4.32) Once the yield base shear is determined, it is applied to

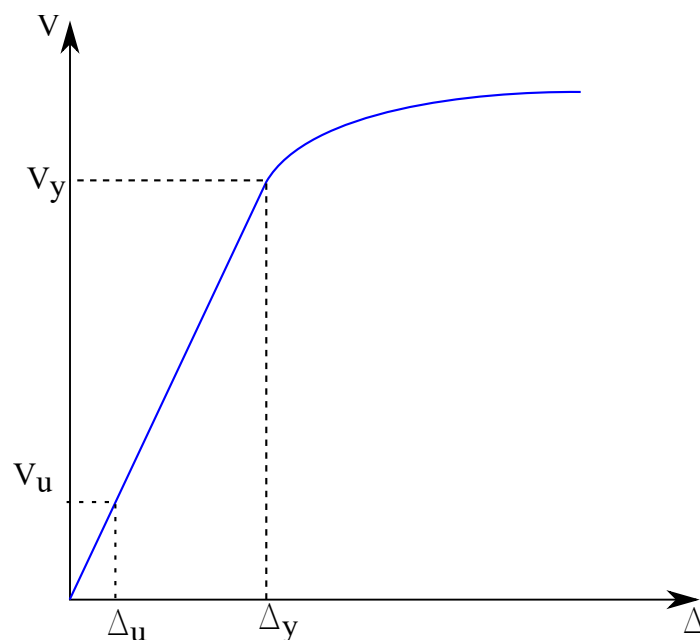


Figure 4.32: Relation of Unit Force With Yield Base Shear for Structure

the system, and the resultant force-displacement tuple is added to the overall capacity curve.

Table 4.6: System State at $\Delta_{\text{yield}} + n \cdot \varepsilon$

Known Variables	Unknown Variables
$\Delta_i = \Delta_i^{\text{yield}} + n \cdot \varepsilon$	Δ_j
$V_j = 0$	θ
$\tau = 0$	V_i

4.1.7 Constructing Inelastic Region of Structure Capacity Curve

When every element is in the linear range, it is trivial to compute force and corresponding deformation values. However, when elements start to transcend their elastic limit, it is impossible to solve the system using simple matrix manipulations. As internal element forces are a function of base shear, which in turn should be equal to the sum of these element forces, an iterative solution approach has to be followed. Moreover, since capacity curve generation relies on displacement based analysis, the base shear that is required to result in target displacement is another unknown parameter. Due to all these reasons, a minimization algorithm should be implemented.

First of all, global yield displacement calculated in previous step (Δ) is increased with a unit amount (ε) in the direction i . And then, force equilibrium is used to calculate the unknown variables; the deflections in other axis and base shear (Table 4.6). Once base shear is determined, the displacement Δ_i is increased further at each step, together with base shear calculations, until it reaches the ultimate limit. In the end, the overall capacity curve for the most critical story will be obtained (Figure 4.33).

4.1.7.1 Optimizing For Force Equilibrium

When the column inner forces are determined for the first time, equilibrium will be satisfied automatically since individual element deflections are calculated from the total base shear. If no member shows nonlinearity (i.e. yields), then there is no further necessity of balancing forces. However, if there are members whose internal forces exceed their capacity, then the force they carry are reduced to their limit. In this case, equilibrium will be disturbed, and there will be excess forces to be re-distributed to

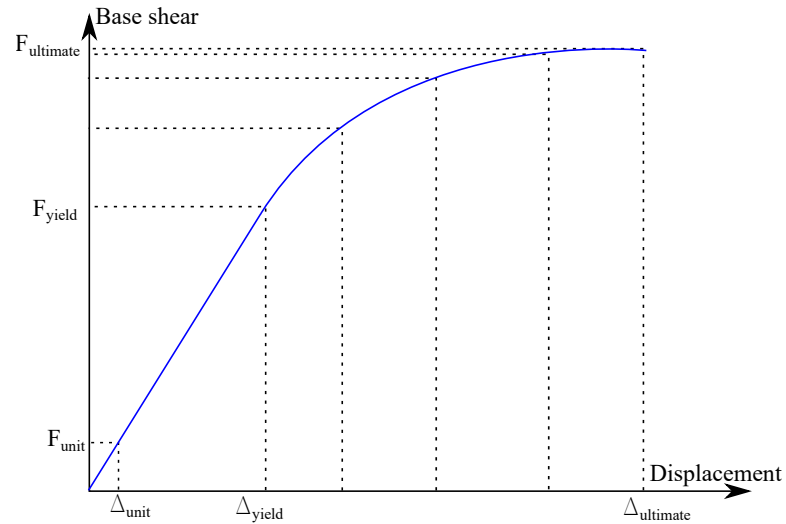


Figure 4.33: Resultant Capacity Curve

other elements. In order to achieve this, the optimum deformations (Δ_x , Δ_y , Θ) of slab center that returns element forces balancing total base shear should be found. This is a definition for an optimization problem which can be stated as in Equation (4.23).

$$\arg \min_{\Delta_x, \Delta_y, \Theta \in \mathbb{R}} (V_j^2 + \tau^2) \quad (4.23)$$

where V_j is the base shear in secondary direction (which is a function of Δ_x , Δ_y , and Θ), and τ is base torque.

There are different approaches for the solution of this case, such as unconstrained optimization algorithms (Steepest descent, Newton's method, Marquardt's method... etc.), numerical techniques (Nelder-Mead simplex method... etc.), and meta-heuristic approaches (particle swarm optimization, big bang - big crunch optimization... etc.).

4.1.7.1.1 Numerical Unconstrained Optimization Methods They are the oldest available approaches for solutions to optimization problems and many algorithms of this type share similar characteristics:

- They are based on derivative information of different orders. Differentiation of the objective function yields insight on the direction where it gets minimum fastest. Therefore, the cost function should be differentiable in several orders.
- Since they obtain their search path from the objective function itself, they are

usually fast methods and very efficient for cases where derivative information is easily available.

- Due to the reasons stated above, they cannot be applied directly to non-differentiable, discrete, or discontinuous problems.

Their basic working principle is:

$$x^{k+1} = x^k + \alpha^k s^k \quad (4.24)$$

where

x^k : current design point at iteration k

x^{k+1} : new design point at iteration $k + 1$

s^k : search direction at iteration k

α^k : step size at iteration k

The main divergence between different implementations of methods are in determination of the search direction s .

The most common numerical unconstrained optimization methods are as follows:

Bisection Method Alternatively referred as interval halving or dichotomy method, it is a root-finding technique via bisecting the selected interval into sub-intervals continuously. It is a relatively slow method in terms of convergence rate, therefore most of the times it is used as a basis for determining an initial guess for more advanced approaches.

Steepest Descent Method Also called "gradient descent", this approach assumes that the maximum descent in objective function values will be parallel to its gradient ([75]):

$$s^k = -\nabla f(x^k) \quad (4.25)$$

Since most objective functions are considerably flat around their extremities, this approach usually ends up with a characteristic slow zig-zagging behavior with small step sizes. This results in slow convergence to the target; its rate of convergence is considered to be inferior to many other methods in cases of

poorly conditioned convex problems. Moreover, for non-differentiable functions, gradient methods are ill-defined.

Newton's Method This method is the application of the Newton-Raphson method to the derivative of a function which should be differentiable to second order to find the roots of the second derivative, which are stationary points of that function [76]. In other words, it utilizes the second derivative to estimate the ascent or descent of the objective function, then incorporating this information into search direction s :

$$s^k = - [\nabla^2 f(x^k)]^{-1} \cdot \nabla f(x^k) \quad (4.26)$$

However, this does not always guarantee a decrease in the function; if the first multiplicative of right-hand side of Equation (4.26) is positive-definite, the direction s have to be descent. If not, s may either be descent or ascent. The main advantage of this algorithm is that it limits the zig-zag behavior near the target point, but it works poorly in locations away from it. Moreover, it suffers from the conditions that limit the success of overall numerical methods.

Marquardt's Method Also known as "Levenberg-Marquardt Algorithm" or "Damped Least Squares Method", this approach is an interpolation between Newton's method and steepest descent method [77]. Steepest descent works well when the initial point is far away from extremities, whereas Newton's method is better in the close neighborhood of the optimum value. Thus in Marquardt method, the steepest descent is initially followed, and then Newton's method is applied. The transition from one algorithm to other is dependent on the nature of the objective function, and should be adaptive; i.e. it has to depend on the history of obtained intermediate solutions.

4.1.7.1.2 Metaheuristic Algorithms From a language point of view, *heuristic* means *to find or discover by trial and error*. *Meta-* prefix adds *beyond* or *higher level* meaning, and in combined the word **metaheuristic** is used to denote algorithms that perform better than blind random search approaches. The term itself was created by Fred Glover [78]. Later, its official definition is given as:

"A master strategy that guides and modifies other heuristics to produce solutions beyond those that are normally generated in a quest for local optimality." [79]

Two leading constituents of all metaheuristic algorithms are generating diverse solutions to explore as much search space as possible and focus the search in a local region if a good solution is found there. These two items are called exploration and exploitation (or sometimes referred as diversification and intensification) [80].

There are a number of metaheuristic methods, and most of them are created by observation of natural phenomena:

Simulated Annealing is based on metal annealing processing, and it has the ability to escape from being trapped in local optima [81]. Essentially, this is a technique of search along a Markov chain which is expected to converge under appropriate conditions.

Genetic Algorithms (GAs) Being one of the most popular evolutionary algorithms, GAs are developed by John Holland in the 1960s. The heart of the technique is to encode solutions as arrays of bits or character strings (chromosomes) and then manipulating these strings by genetic operators. The selection is based on their fitness to find a solution to the problem [82].

Differential Evolution (DE) Developed by Storn and Price, it is an extension of genetic algorithms, extending GAs by carrying out operations over each component in terms of vectors [83].

Ant Colony Optimization First introduced by Dorigo in the 2000s, this approach is based on the fact that ants use pheromones to divert the colony to a target, marking the trail to and from it [84]. These pheromones are not permanent, yet they are augmented by the increased number of ants following the route, which in turn creates a positive feedback mechanism.

Bee Algorithms These are based on the foraging behavior of bees, and a few variants exist in the literature such as honeybee algorithm, artificial bee colony, bee algorithm, virtual bee algorithm, and honeybee mating algorithms. Ant and bee algorithms are better suited for discrete and combinatorial optimizations.

Particle Swarm Optimization (PSO) Suggested by Kennedy and Eberhart in 1995 [85], this technique depends on swarm behavior of collective animals such as bird flocks and fish shoals. From publishing, PSO attracted a high level of attention and currently considered as an ever-expanding research domain in the field of swarm intelligence. There are more than two dozen variants, as well as hybrid approaches that combine PSO with other methods.

Big Bang-Big Crunch (BB-BC) Considering the evolution of the universe as a model, BB-BC method creates a set of randomly distributed particles and then collapses these to single points by either minimum cost or center of mass approaches [86].

Cuckoo Search One of the most recent nature-originating approaches, this method is based on the parasitic brooding behavior of some cuckoo species [87]. Later, it is enhanced by Lévy flights (instead of random isotropic searches) [88], and it is claimed that it may perform more efficiently than PSO or genetic algorithms [87].

Among all the numerical and metaheuristic methods listed above, an improvised incremental technique and a modified steepest search method are selected based on several reasons:

- **Ease of implementation:** These methods are highly adaptable to computer applications.
- **Ability to process discontinuities:** When the objective function has discontinuous or non-differentiable sections, modified steepest search may fail to converge. In these cases, the incremental technique will be utilized.
- **High rate of convergence:** Since every new configuration of the system ($\Delta_{\text{yield}} + \varepsilon \times i$) will be based on a previously solved step, the convergence will be achieved within few trials; there is no need to search the whole solution space. In other words, since the balance is disturbed by a very small increment, the new minimum point is expected to experience a diminutive shift.

4.1.7.2 Implementing Custom Incremental Search Method

The technique is based on a step by step incremental search of solution space in the direction where objective function decreases. The very basic algorithm is as follows:

1. Select a base point.
2. Increment base point in one direction (either positive or negative) by a predefined step size.
3. Compare objective functions at new and base points:
 - (a) If new OF is less than the previous OF, the direction of iteration is correct, assume new point as a base and go to step 2.
 - (b) If new OF is greater than old one, the direction of iteration is incorrect. In this case, increment base point in the opposite direction of step 2 by a predetermined fraction of initial increment step (for example; if the base point is increased by 10% at first, it should be decreased by 8%). Assume this new point as a base and go to step 2.

For every new point of the structural capacity curve in the inelastic region, the only deformation in the primary direction (called i) is known (Table 4.6). The other two deformations are to be determined, and this multiple dimensions issue is handled by swapping variables at each successive step; odd numbered steps increment one variable while even numbered ones deal with the other one. The initial guess for the new capacity point is assigned to be the last computed point on the curve (p : previous step):

$$\Delta^{(0)} = [\Delta_i^p, \Delta_j^p, \theta^p] \quad (4.27)$$

1. At step s , increment the first unknown displacement Δ_j by an amount ξ_j in the direction γ_j :

$$\Delta^{(s)} = \left[\Delta_i^{(s-1)}, \underbrace{\Delta_j^{(s-1)} + \gamma_j \cdot \xi_j}_{\Delta_j^s}, \theta^{(s-1)} \right] \quad (4.28)$$

2. Calculate objective function (OF) for step $s - 1$ and s :

$$\begin{aligned}
V_j &= \sum F_j \\
\tau &= \sum (F_i \cdot e_j + F_j \cdot e_i) \\
\text{OF}^{(s-1)} &= [V_j^{(s-1)}]^2 + [\tau^{(s-1)}]^2 \\
\text{OF}^{(s)} &= [V_j^{(s)}]^2 + [\tau^{(s)}]^2
\end{aligned} \tag{4.29}$$

where $V_j^{(s)}$ is the total base shear in direction j at step s , and $\tau^{(s)}$ is the torque applied to structure at step s . Since the system is excited only in i direction, both of these variables should be zero.

3. Compare objective functions at step s and $s - 1$:

- If OF does not change sign and $\text{OF}^{(s)} < \text{OF}^{(s-1)}$, algorithm is moving in the direction of solution. Then go to step 4 for next variable.
- If OF does not change sign and $\text{OF}^{(s)} > \text{OF}^{(s-1)}$, algorithm is moving in the opposite direction of solution. Therefore reverse the related direction variable, keep step size the same ($\lambda = 1$), then calculate new point for current step s (Equation (4.30)).
- If OF changes sign, algorithm has passed the solution point. In this case, reverse the related direction variable, decrease the step size by a predefined percentage $\lambda < 1$, then calculate new point for current step s (Equation (4.30)).

$$\begin{aligned}
\gamma'_j &= -\gamma_j \\
\xi'_j &= \lambda \cdot \xi_j \\
\Delta^{(s)} &= [\Delta_i^{(s-1)}, \Delta_j^{(s-1)} + \gamma'_j \cdot \xi'_j, \theta^{(s-1)}]
\end{aligned} \tag{4.30}$$

With this new $\Delta^{(s)}$, continue to next step 4.

4. Starting step $s + 1$, increment second unknown deflection θ by an amount ξ_θ in the direction γ_θ from the point computed in step s :

$$\Delta^{(s+1)} = [\Delta_i^{(s)}, \Delta_j^{(s)}, \theta^{(s)} + \gamma_\theta \cdot \xi_\theta] \tag{4.31}$$

5. Calculate objective functions for steps s and $s + 1$ per Equation (4.29).

- If OF does not change sign and $OF^{(s+1)} < OF^{(s)}$, algorithm is moving in the direction of solution. Then go to step 1.
- If OF does not change sign $OF^{(s+1)} > OF^{(s)}$, algorithm is moving in the opposite direction of solution. Reverse the related direction variable, keep step size the same ($\lambda = 1$), then calculate new point for current step $s + 1$ (Equation (4.32)).
- If OF changes sign, algorithm has passed the solution point. In this case, reverse the related direction variable, decrease the step size by a predefined percentage $\lambda < 1$, then calculate new point for current step s (Equation (4.32)).

$$\begin{aligned}
\gamma'_\theta &= -\gamma_\theta \\
\xi'_\theta &= \lambda \cdot \xi_\theta \\
\Delta^{(s+1)} &= \left[\Delta_i^{(s)}, \Delta_j^{(s)}, \theta^{(s)} + \gamma'_\theta \cdot \xi'_\theta \right]
\end{aligned} \tag{4.32}$$

6. Check objective function against error tolerance value ψ .

- If $OF^{(s+1)} < \psi$, target point is found; add this point to capacity curve.
- If $OF^{(s+1)} > \psi$, go to step 1, and continue with step $s + 2$.

4.1.7.3 Implementing Custom Steepest Descent Algorithm

Steepest, or sometimes referred as "gradient" descent is a first-order optimization algorithm. It has roots in the fact that if a multi-variate function is defined and differentiable around a point, then it decreases fastest in the negative gradient of itself (Figure 4.34 and Equation (4.33)).

$$x_{n+1} = x_n - \gamma_n \nabla F(x_n) \Rightarrow F(x_0) \geq F(x_1) \geq F(x_2) \geq \dots \tag{4.33}$$

Gradient descent method can be applied to systems with any number of dimensions (even with infinite-dimensional ones). In the algorithm scope, the target displacement in current axis (Δ_i) is known, and unknown variables are displacement in other axis and the rotation (Δ_j, θ). During the customized descent algorithm, first one dimension is traced for the minimum, and then when it is found, the second variable comes

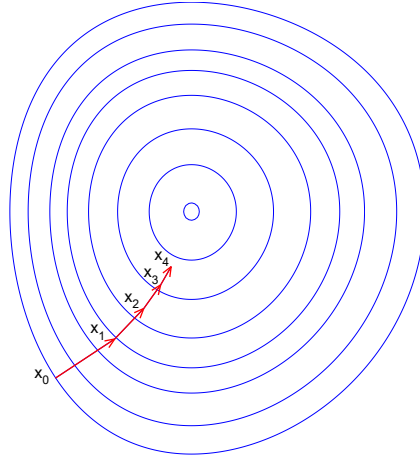


Figure 4.34: Level Sets for a Steepest Descent Solution

into play. The objective function to be minimized is set as $V_j^2 + \tau^2$, since the system is excited from primary axis only (loads in other directions should be zero).

1. For the known target displacement $\Delta_i = \Delta_{\text{yield}} + \varepsilon \times n$, initial guesses for Δ_j and θ are values of these variables at yield point.
2. Using these initial guess displacements, calculate element deflections and forces; then compute the objective function:

$$\begin{aligned}
 V_j &= \sum F_j \\
 \tau &= \sum (F_i \cdot e_j + F_j \cdot e_i) \\
 \text{OF}_1 &= V_j^2 + \tau^2
 \end{aligned} \tag{4.34}$$

3. Increment Δ_j by a step ζ , and then calculate objective function OF_2 using new Δ_j .
4. If OF_2 is less than tolerance, then move to search of θ . If not, form a line that passes through points OF_1 and OF_2 , then find where this line crosses horizontal axis (which will be new guess for Δ_j) (Figure 4.35):

$$\Delta_j^{(3)} = - \frac{\text{OF}_1 \cdot (\Delta_j^{(1)} - \Delta_j^{(2)}) - \Delta_j^{(1)} \cdot (\text{OF}_1 - \text{OF}_2)}{\text{OF}_1 - \text{OF}_2} \tag{4.35}$$

5. Calculate OF_3 using $\Delta_j^{(3)}$. If OF_3 is less than tolerance, move to search of θ . If

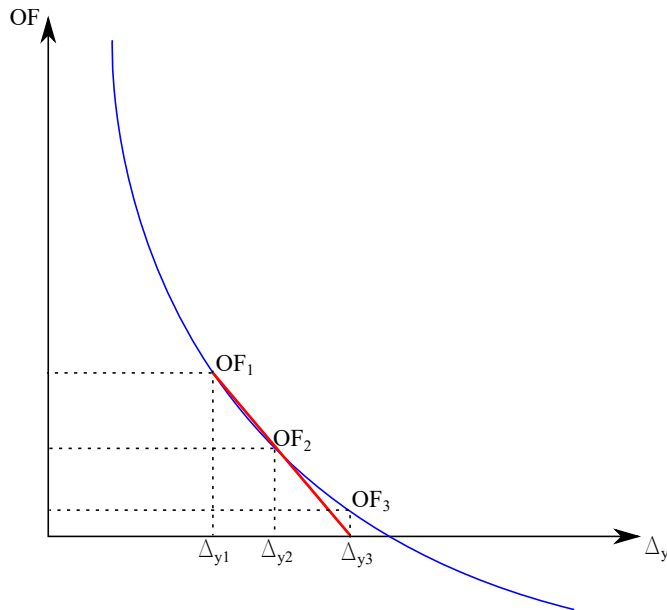


Figure 4.35: Finding Next Guess

not, form a line passing through new point and the previous one (discarding the guess older than single generation), then repeat the last step.

6. Once sufficient precision is achieved in Δ_j , start optimizing θ ; begin with θ_{yield} , increment it by ζ , perform modified steepest descent to find final value.
7. Using the resultant displacement vector found in previous steps, calculate base shear in target direction, and add this data tuple to capacity curve.

4.1.8 Converting Critical Story Displacements to Roof Displacements

Once the force-displacement curve is obtained for the ground level (usually the most critical story), the deformations can be converted to roof displacements to be compatible with the conventional performance decision techniques (which are explained in the next section) if necessary. The main assumption in the suggested conversion method is the overall structural response is dominated by the first mode of the structure. Therefore, if higher mode effects are estimated to be stronger than anticipated, this method should be revised accordingly.

The assumed expected deformation patterns of frame and shear wall types of structures for the first mode are given in Figure 4.36.

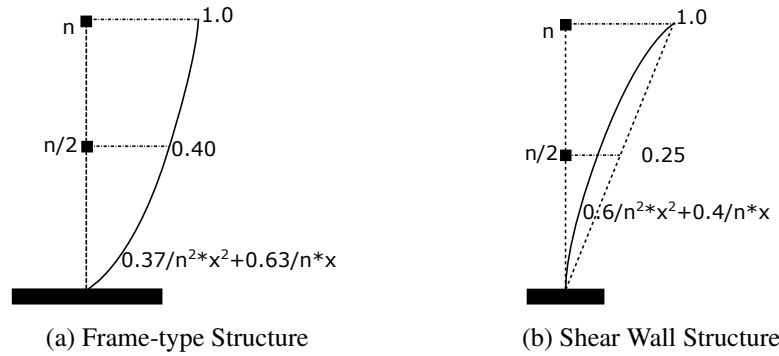


Figure 4.36: Displacement Patterns for Different Structure Types

According to these modal shapes, the roof displacements can be estimated as per Equation (4.36) for structures with frames only and with shear walls.

$$\Delta_{\text{roof}} = \phi_1^{-1} \times \Delta_{\text{first story}} \quad (4.36)$$

where ϕ_1 is the modal value of the first story associated with the first (fundamental) mode of the structure.

4.2 Deciding Overall Seismic Condition

The proposed algorithm yields the conventional pushover curve which relates the roof displacement to base shear force in a fast and relatively easier way compared to standard three-dimensional pushover analysis (Figure 4.33). After this capacity curve is obtained, the performance of the structure can be assessed using common methods already defined in different codes and specifications.

4.2.1 Finding Performance Point

The capacity curve of a structure summarizes the performance of a building for a range of demand (represented as base shear); basically, it is an envelope of responses for a spectrum of seismic effects. In order to obtain the response for a specific effect (which is referred as performance point), the intersection of demand curve with capacity should be determined. The most common methods to be followed for this purpose are capacity spectrum method (Section 2.2.3.1) and displacement coefficients method (Section 2.2.3.2), both of which are first explained in detail in ATC40 [1]. In

this study, displacement coefficients method is preferred due to its simpler nature and easier implementation.

4.2.1.1 Displacement Coefficients Method

It is an extension of the equal displacement rule with several modification factors and yields the displacement demand directly. The main advantage is that it does not require conversion of the curve to spectral coordinates (acceleration-displacement response spectrum or ADRS). This method works best with structures which are regular or slightly irregular; the presence of any torsional or higher mode effects should be noted carefully.

In the process, first of all, the capacity curve should be converted to a bilinear representation, where the effective stiffness (K_e) should intersect the original curve at $0.6V_y$ (Figure 4.37). This item may require a trial and error stage because V_y value is unknown until the K_e line is drawn, and it is not certain the intersection will take place in $0.6V_y$.

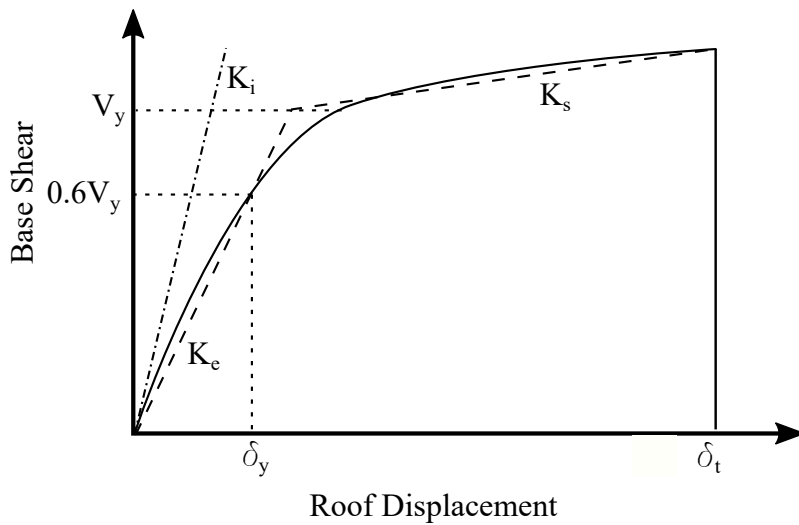


Figure 4.37: Bilinear Capacity Curve for Displacement Coefficients Method

The effective fundamental period of the structure is determined using the initial and effective stiffness values of the structure (K_i and K_e) as well as the elastic period (T_i) (Equation (4.37)).

$$T_e = T_i \sqrt{\frac{K_i}{K_e}} \quad (4.37)$$

Then the target displacement value (δ_t) can be calculated as in Equation (4.38):

$$\delta_t = C_0 C_1 C_2 C_3 S_a \frac{T_e^2}{4\pi^2} \quad (4.38)$$

The Equation (4.38) is basically a modified version of equal displacement rule, where modifications are used to convert an elastic single degree of freedom demand to an inelastic multi-degree of freedom response.

C_0 is the modification factor for establishing the relation between the spectral displacement and likely building roof displacement. It can be calculated by either first modal participation factor at roof level, calculated by modal analysis or a shape vector corresponding to the deformed shape of the structure at target displacement, or from Table 4.7.

C_1 is the modification factor for establishing the relation between expected maximum inelastic displacement to the elastic response. It is calculated as per Equation (4.39), where T_0 is the corner period of the spectrum representing the constant acceleration to constant velocity translation and R is the ratio of inelastic strength demand to calculated yield strength coefficient (Equation (4.40)).

$$C_1 = \begin{cases} 1.0 & \text{if } T_e \geq T_0 \\ [1.0 + (R - 1)T_0/T_e]/R & \text{if } T_e < T_0 \end{cases} \quad (4.39)$$

$$R = \frac{S_a/g}{V_y/W} \times \frac{1}{C_0} \quad (4.40)$$

C_2 is the modification factor to establish the effect of hysteresis shape on the maximum displacement response. It is determined as per Table 4.8.

C_3 is the modification factor to establish the increase in displacements due to second order effects. For structures with positive post yield stiffness, it is set to 0. For negative values, it is calculated by Equation (4.41), where R and T_e are defined above and α is the ratio of post-yield stiffness to elastic stiffness in the bilinear representation.

$$C_3 = 1 = \frac{|\alpha|(R - 1)^{3/2}}{T_e} \quad (4.41)$$

S_a is the demand spectral acceleration determined from either a design or a response spectrum.

Table 4.7: Values for Modification Factor C_0 [1]

Number of Stories	Modification Factor ¹
1	1.0
2	1.2
3	1.3
5	1.4
10+	1.5

¹ Intermediate values should be calculated using linear interpolation.

Table 4.8: Values for Modification Factor C_2 [1]

Performance Level	$T = 0.1$ second		$T \geq T_e$ second	
	Type 1 ¹	Type 2 ²	Type 1 ¹	Type 2 ²
Immediate Occupancy	1.0	1.0	1.0	1.0
Life Safety	1.3	1.0	1.1	1.0
Collapse Prevention	1.5	1.0	1.2	1.0

¹ Ordinary moment-resisting frames, concentrically braced frames, tension-only braced frames, unreinforced masonry walls, or any combination of these.

² All frames not assigned to Type 1.

4.2.2 Calculating Seismic Performance Level

Once the performance point has been determined for the estimated seismic effect, the condition of all vertical members at that point can be specified by going back to pushover calculations and extracting the step at performance point. Details of this step (end forces, end displacements which can be converted to rotations and then section curvature) yield the condition (whether it is in elastic or inelastic range), as well as the end shear force of each and every column. For establishing the performance level of the structure from this stage, either the process stated in any code or a newly proposed simplified can be used. In the following sections, the Turkish Earthquake Code approach and the new simplified method are explained.

4.2.2.1 Turkish Earthquake Code Approach

The Turkish Earthquake Code specifies a post-processing approach to determine the seismic performance level for both linear and nonlinear analyses. The linear anal-

ysis post-processing relies on comparing the elastic forces with capacities of each member, deducing their effective statuses in a quasi-nonlinear manner. Since the proposed capacity determination method considers element nonlinearities, the second post-processing approach, which is a direct comparison of strain limits, can be implemented. These limiting values are given in Table 4.9.

Table 4.9: Strain Limits for Columns in Turkish Earthquake Code

Performance Level	Concrete (ε_{CU})	Steel (ε_S)
Minimum Damage	0.0035	0.01
Safety Limit	$0.0035 + 0.010(\rho_s/\rho_{sm}) \leq 0.0135$	0.04
Collapse Limit	$0.0040 + 0.014(\rho_s/\rho_{sm}) \leq 0.0180$	0.06

The possible performance levels that a structure can attain with their respective conditions and criteria are as follows:

Immediate Occupancy Performance Level For a building to be considered at this level, no columns should exceed minimum damage level, and only 10% of beams can be between minimum damage and safety limit. If any element is expected to encounter brittle failure, they should be retrofitted.

Life Safety Performance Level For a building to be considered at this level, at most 30% of primary beams should be between safety and collapse limits in addition to the following criteria:

- The total shear force contribution of columns between safety and collapse limit to the overall story shear force should be less than 20% (Except for top story, where the limit is 40%).
- The total shear force contribution of columns where both ends (top and bottom) exceed minimum damage level to the overall story shear wall should be less than 30%.

Collapse Prevention Performance Level For a building to be considered at this level, the following criteria should be met:

- Only 20% of primary beams can go beyond collapse limit.

- The total shear force contribution of columns where both ends (top and bottom) exceed minimum damage level to the overall story shear wall should be less than 30%.

Collapse Performance Level Any structure that does not conform to the levels defined above are considered to be in collapse performance level.

4.2.2.2 A Simpler Approach

The method explained in Section 4.2.2.1 yields direct performance level of a structure, however, it requires analysis results for each story including beams in addition to columns and shear walls. Moreover, detailed sectional properties such as existing confinement condition and its design limits should be known. In this section, a new approach is suggested for estimating expected performance level with less data and the pushover calculations of the proposed capacity determination method, which only considers vertical elements in the most critical story.

Immediate Occupancy For a structure to be considered at this level, all the columns should be in the linear range, and the performance point on the pushover curve should be at least 10% less than the start of inelastic behavior.

Collapse Prevention For a structure to be considered at this level, the total shear force contribution of vertical members which exceed minimum damage level to the overall story shear force should be less than 20%.

Risk of Collapse Any structure that can not conform to collapse prevention performance level is assumed to be in the “risk of collapse” region, and necessitate further detailed analysis.

In the performance level list, the item “Life safety” is omitted considering the fact that assumptions and approximations used in the proposed capacity determination method makes trials of precise performance level determinations obsolete.

4.3 Verification and Comparison Analyses for Proposed Capacity Determination Method

In order to verify the capacity curves obtained using the proposed method, the commercial structural analysis software SAP2000 is used. Different types of structures (symmetrical and unsymmetrical in the plan) with varied structural systems (moment resisting frames and shear wall types) are analyzed using both the new method and SAP2000, and the resultant push-over curves are compared in the following sections.

4.3.1 Finite Element Modeling Notes

In all the models created by SAP2000, columns and beams are modeled with standard line elements whereas shear walls are approximated with “central column” approach. In this method, a line element having a width identical to the modeled shear wall is used instead of area elements. The wall behavior is accomplished by almost infinitely rigid beams connecting to the central column at each story, enabling a response similar to a shear wall in terms of displacement pattern. This simplified approach is commonly used for analysis and design of regular and simple structures. Slabs are not included in the models by any element type, however, their effect is incorporated with the implementation of diaphragm constraints on z-axis per story. Infill walls are not considered as the standard pushover analysis procedure.

Two different types of hinges are defined; a P-M1-M2 interacting for columns and P-M interacting for beams. These hinges are assigned to all members at their starts and ends (a relative length of 0 and 1). The reinforcement pattern, which is an essential parameter for generated hinge properties, is defined identically to the reinforcements generated by the proposed method, as explained in the previous chapters.

The loading scheme is triangular and proportional with height; and applied to the geometrical center of the structure (though the location is not of importance due to the diaphragm constraints defined at each individual z-level). For symmetrical structures, loads are defined on a single axis only (x-axis). For unsymmetrical buildings, the triangular load pattern is applied on both horizontal axes (x and y).

The analysis type is defined as “nonlinear static” starting from the unstressed structure. Pushover curve is obtained by displacement controlled analysis, and a number of results to be saved is defined as between 10 and 100 (default values). The remaining nonlinear parameters are left as defaults. For symmetrical structures, only a single analysis case is defined on the x-axis. For unsymmetrical buildings, analysis cases are applied on both horizontal axes.

The material properties are set as identical with the parameters used in the proposed method solutions.

4.3.2 Symmetrical Structures With No Shear Walls

Ordinary shear frames without any shear walls are quite a common structure type and have the simplest response due to their non-complex structural system. Several of this type are analyzed, ranging from a very simple box with 4 columns per story to a more realistic building with 7 floors. All structural elements in these models are identical in terms of dimensions and materials (all columns are 0.5m x 0.5m, all beams are 0.5m x 0.375m and C25 concrete is used).

4.3.2.1 Symmetrical Structure 1

This is the very first structure used for comparison, and it is kept as simple as possible to be able to identify potential problems in the algorithm and the bugs in the developed software (Figure 4.38). It is a 4 story box with 4 columns at each story, and 4 beams connecting these columns. The results obtained by the proposed method and SAP2000 analyses for the first story and the roof floor are given in Figure 4.39. As seen from the figure, the results are almost identical as expected.

4.3.2.2 Symmetrical Structure 2

This structure is also very simple and used to check the software and the method in an easy manner (Figure 4.40). It has four stories and composed of two connected structures given in Section 4.3.2.1. The results obtained by the proposed method

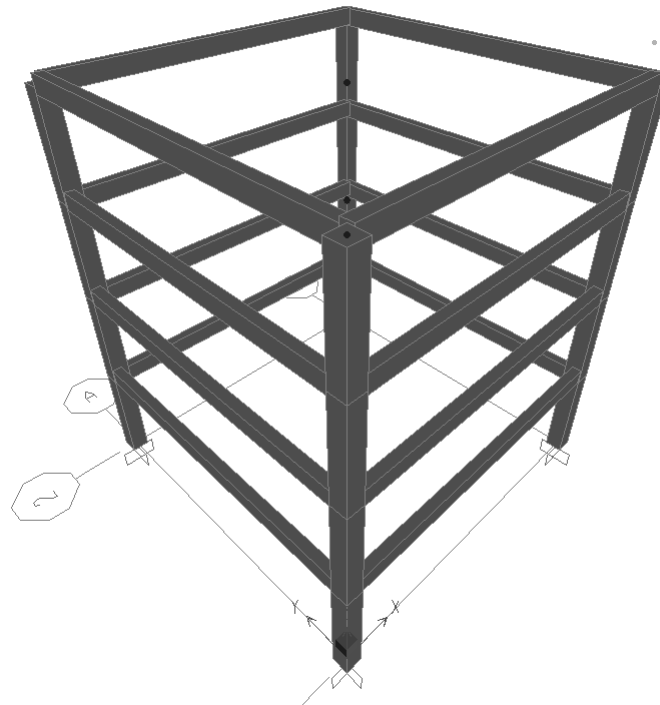


Figure 4.38: Symmetrical Verification Structure 1

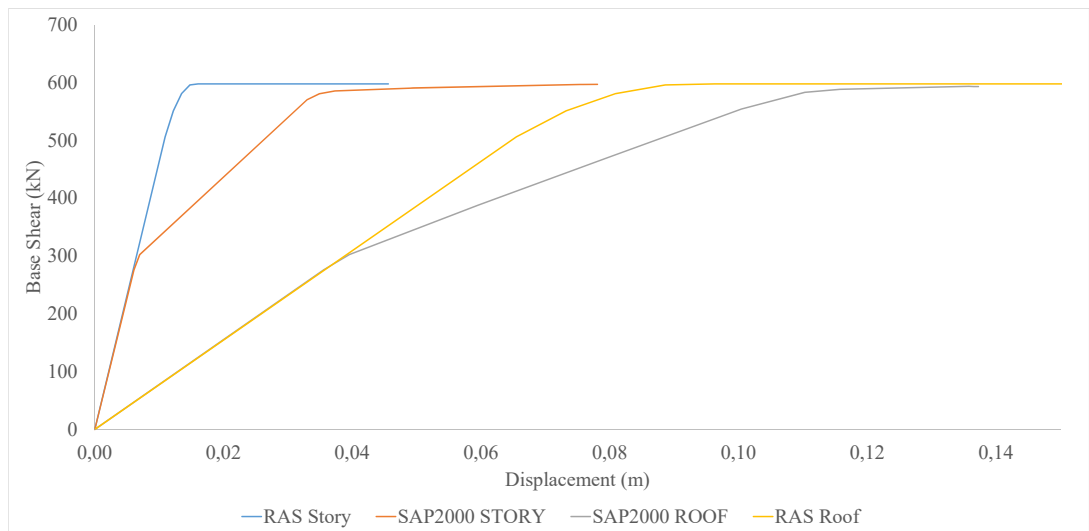


Figure 4.39: Analyses Results for S1

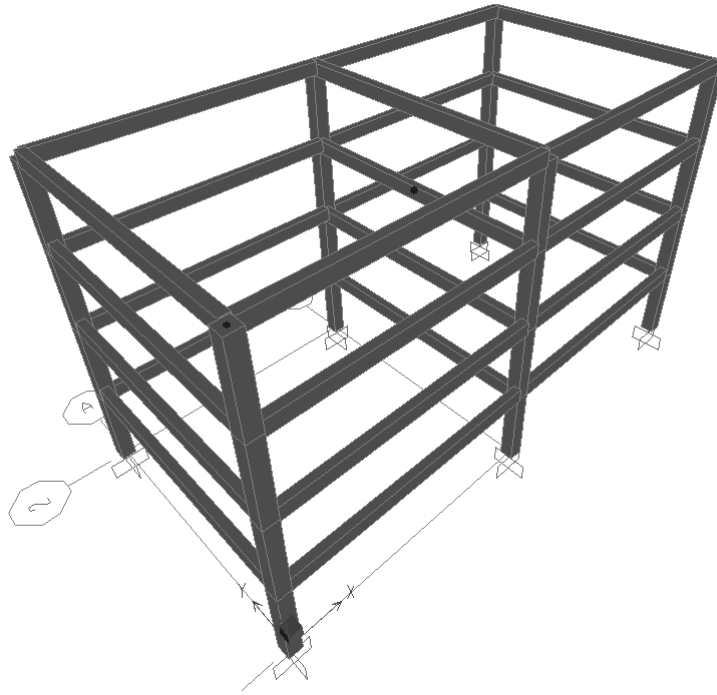


Figure 4.40: Symmetrical Verification Structure 2

and SAP2000 analyses for the first story and the roof floor are given in Figure 4.41.

4.3.2.3 Symmetrical Structure 3

The structure is given in Figure 4.42. It is a 4 story building and the results obtained by the proposed method and SAP2000 analyses for the first story and the roof floor are given in Figure 4.43.

4.3.2.4 Symmetrical Structure 4

The structure is given in Figure 4.44 is a frame building with two bays in both x and y directions. The results obtained by the proposed method and SAP2000 analyses for the first story as well as the roof level are given in Figure 4.45.

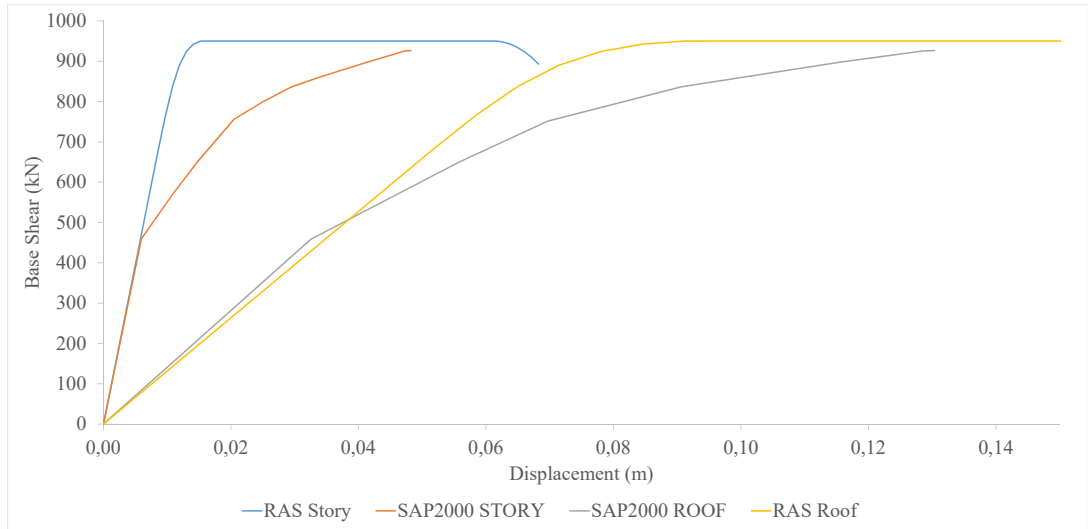


Figure 4.41: Analyses Results for S2

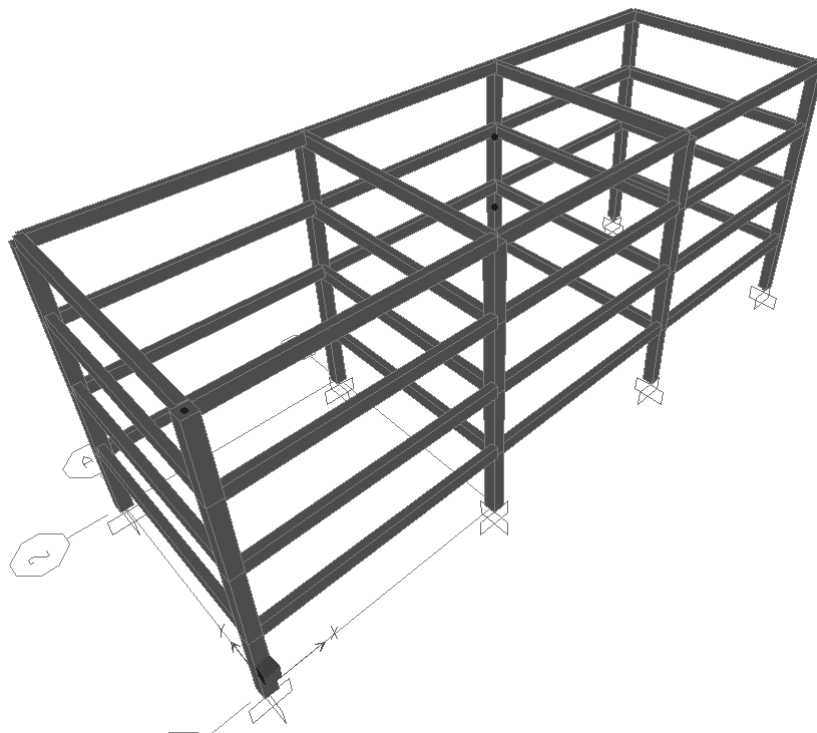


Figure 4.42: Symmetrical Verification Structure 3

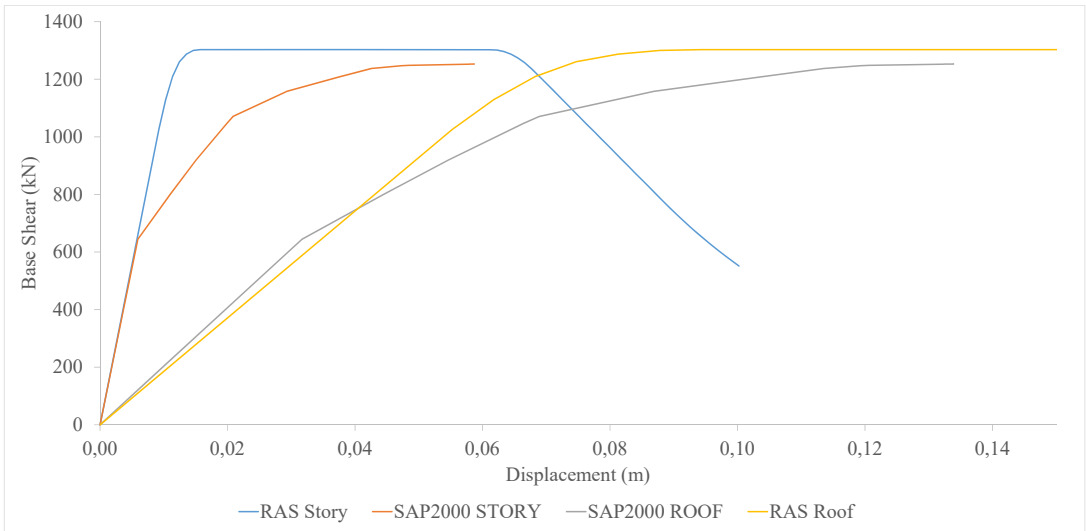


Figure 4.43: Analyses Results for S3

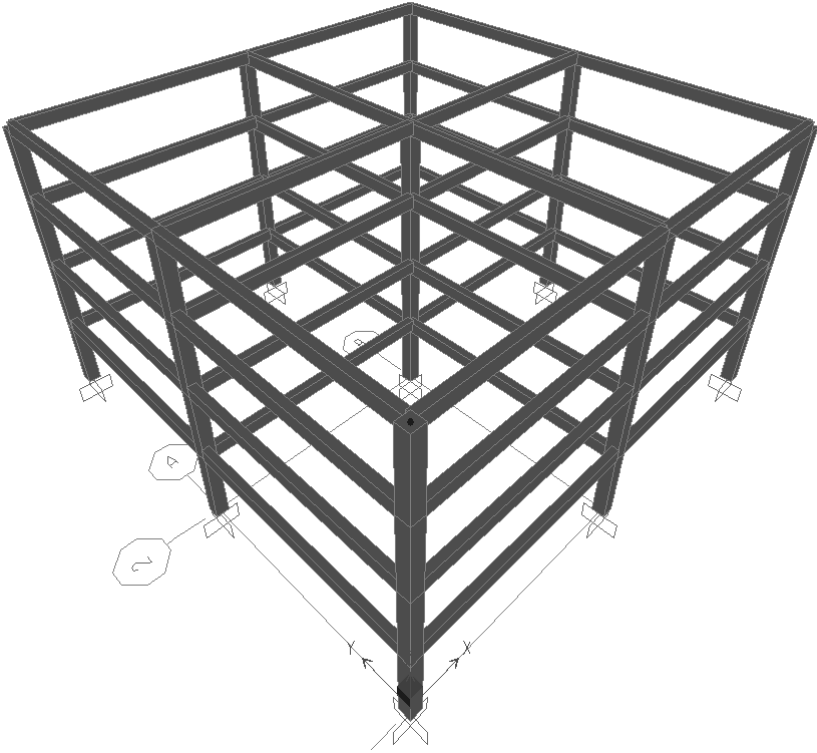


Figure 4.44: Symmetrical Verification Structure 4

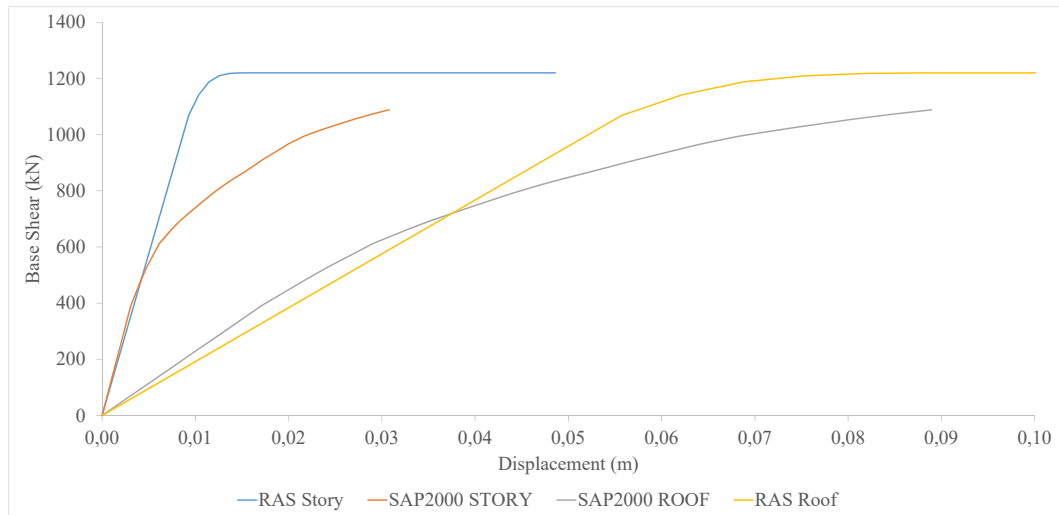


Figure 4.45: Analyses Results for S4

4.3.2.5 Symmetrical Structure 5

The structure is given in Figure 4.46. It is a frame building with three bays in x and two bays in y directions with a total of 4 stories. The results obtained by the proposed method and SAP2000 analyses for the first story and the roof floor are given in Figure 4.47.

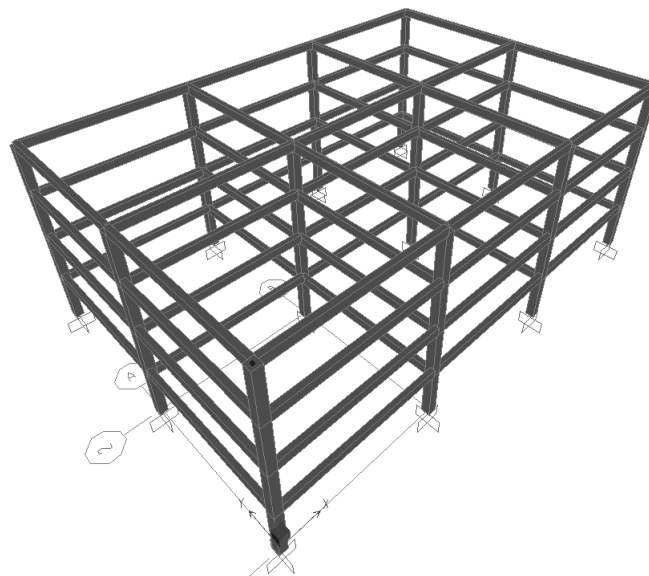


Figure 4.46: Symmetrical Verification Structure 5

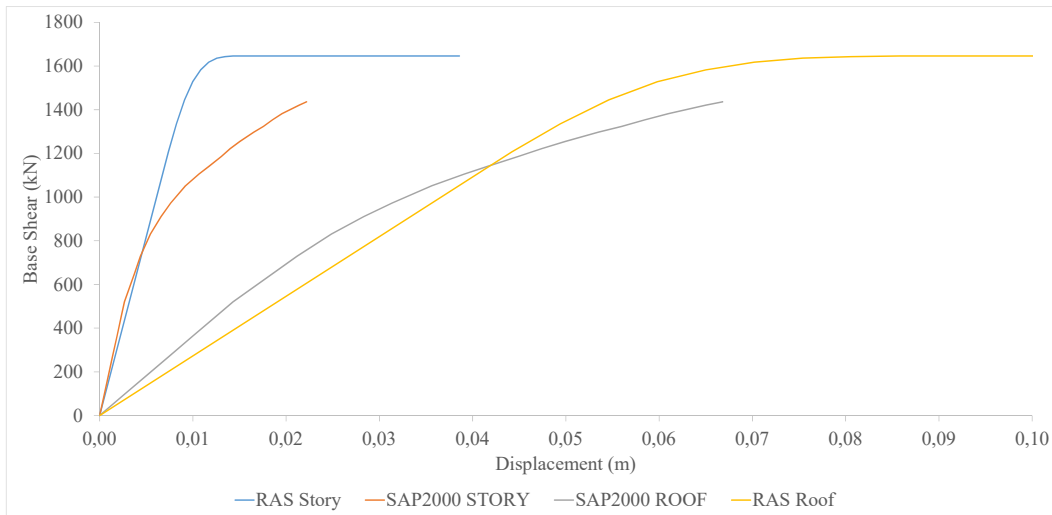


Figure 4.47: Analyses Results for S5

4.3.2.6 Symmetrical Structure 6

The structure is given in Figure 4.48. It is a frame building with five bays in x and four bays in y directions with a total of 7 stories. It has base area dimensions of 50 meters by 40 meters, and the most complex symmetrical structure analyzed. The results obtained by the proposed method and SAP2000 analyses for the first story and the roof floor are given in Figure 4.49.

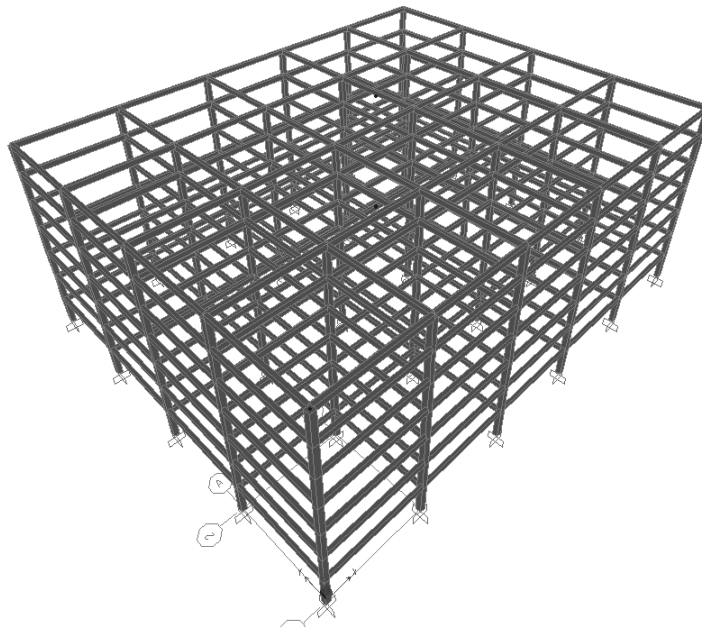


Figure 4.48: Symmetrical Verification Structure 6

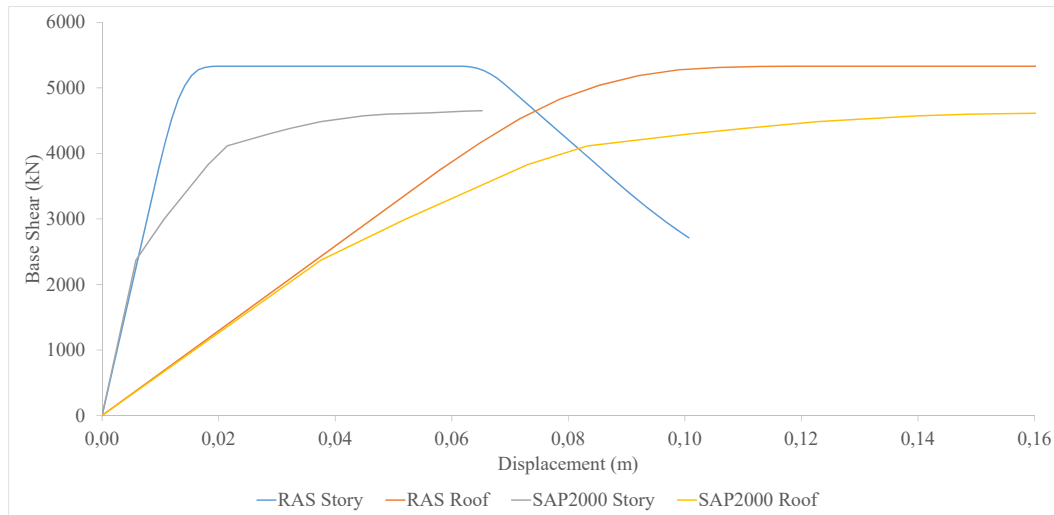


Figure 4.49: Analyses Results for S6

4.3.3 Unsymmetrical Structures With No Shear Walls

In this section, the response of the proposed method to buildings with unsymmetrical properties is checked.

4.3.3.1 Unsymmetrical Structure 1

The evaluated structure has a small horizontal irregularity and different column dimensions within the same story (Figure 4.50). The columns along the upper edge are not square like the others, but of rectangular shape with dimensions 0.75m x 0.5m and aligned such that their strong direction coincides with the x-axis. The capacity curves obtained are given in Figure 4.51.

4.3.3.2 Unsymmetrical Structure 2

Instead of analyzing a series of simple structures as in the case of symmetrical examples, a direct complex structure is used. The evaluated building has five bays in x and 4 bays in the y axis. All columns and beams are identical and the unsymmetric (torsional) behavior is achieved by plan irregularity (Figure 4.52). The results for pushover analyses in both x and y axes are given in Figure 4.53.

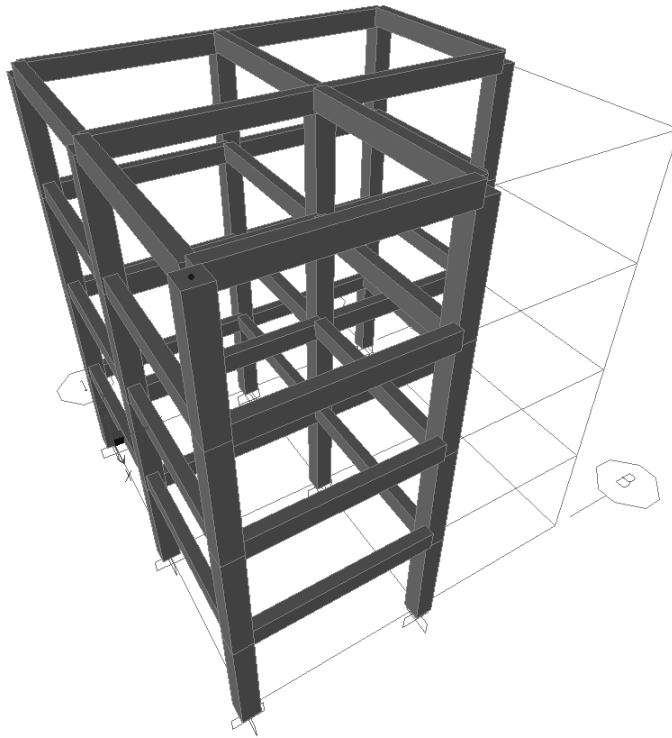


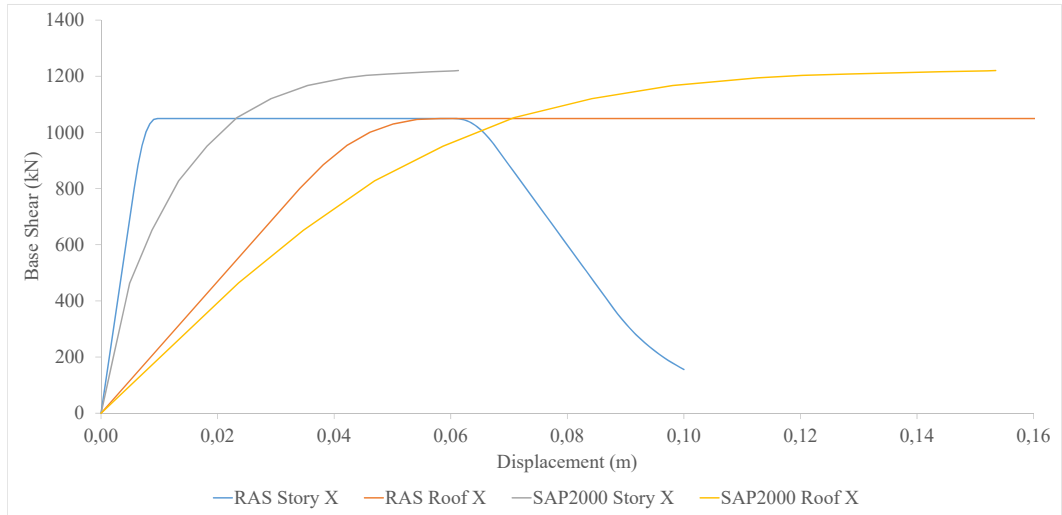
Figure 4.50: Unsymmetrical Verification Structure 1

4.3.4 Structures with Shear Walls

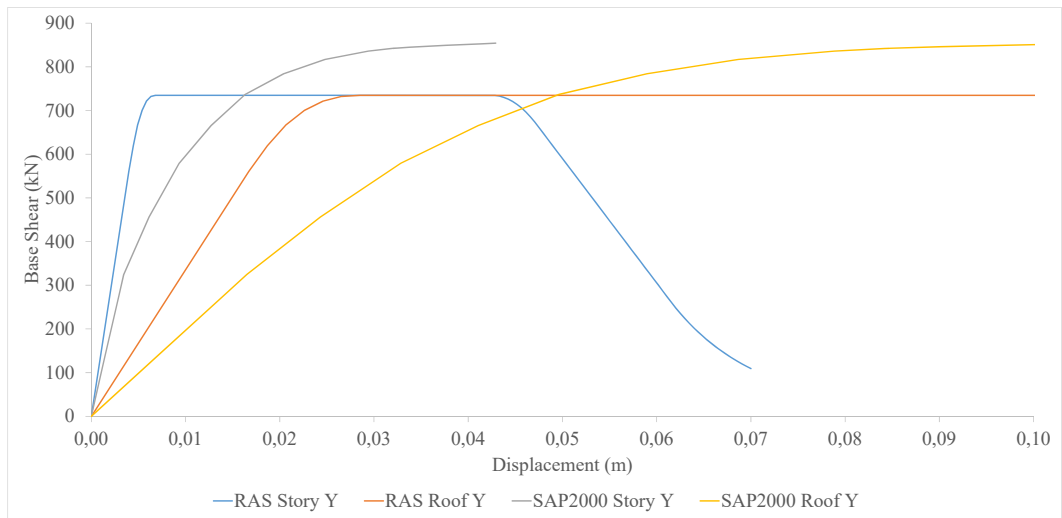
As the final stage of verification, two structures with shear walls are analyzed using both the proposed method and SAP2000 software.

4.3.4.1 Shear Wall Structure 1

This is a very simple structure, and the simplicity is deliberately selected for the ease of tracing errors in both the algorithm and the code during analysis in the presence of shear walls. The building is a 2 bay structure in both axis, and the shear walls are aligned in X direction only (Figure 4.54). The capacity curve obtained in the primary axis (where the shear walls behave as wall members instead of columns) is given in Figure 4.55.



(a) Analyses Results for U1 in x-axis



(b) Analyses Results for U1 in y-axis

Figure 4.51: Analyses Results for Unsymmetrical Structure 1

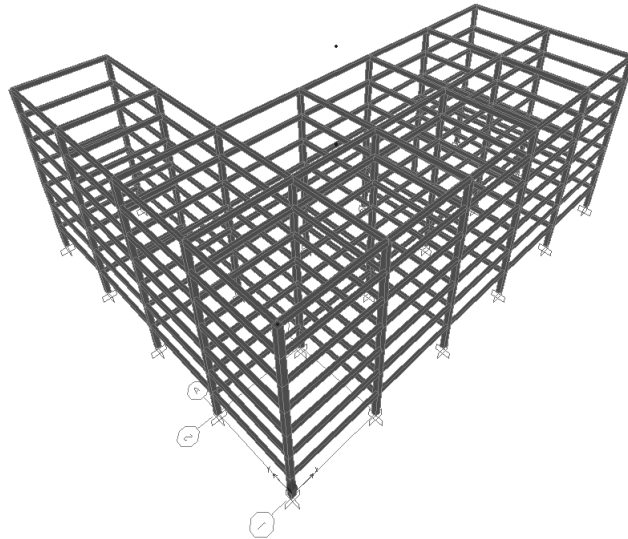


Figure 4.52: Unsymmetrical Verification Structure 2

4.3.4.2 Shear Wall Structure 2

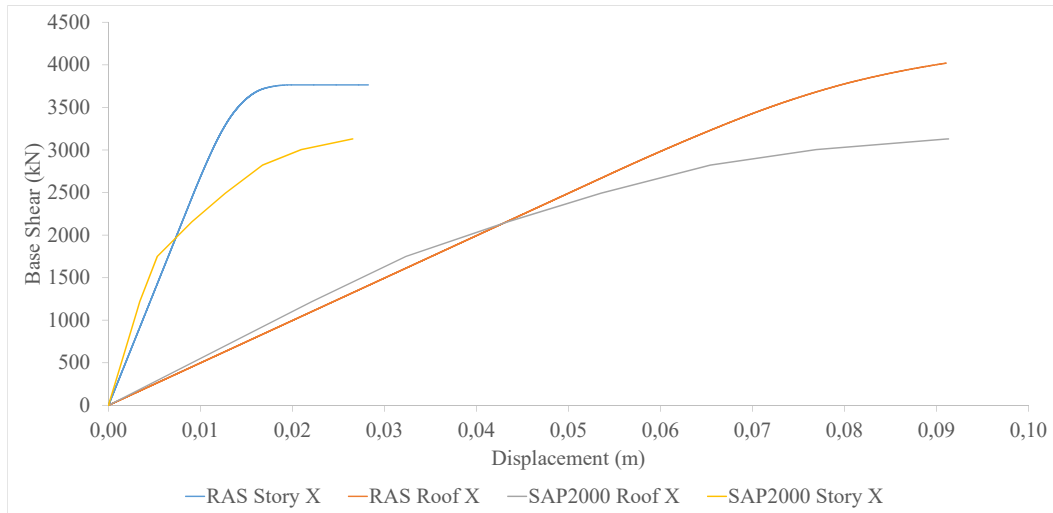
This is the most complex structure analyzed for comparison purposes and it is selected to represent a real life case. The building has five bays in both x and y-axes, a core wall around the center, and individual shear walls along the outermost corners (Figure 4.56). The structure has a 30m x 30m base area, and all the columns are identical. The resultant capacity curves obtained are given in Figure 4.57.

4.3.5 Comparison of Verification Analyses Results and Discussions

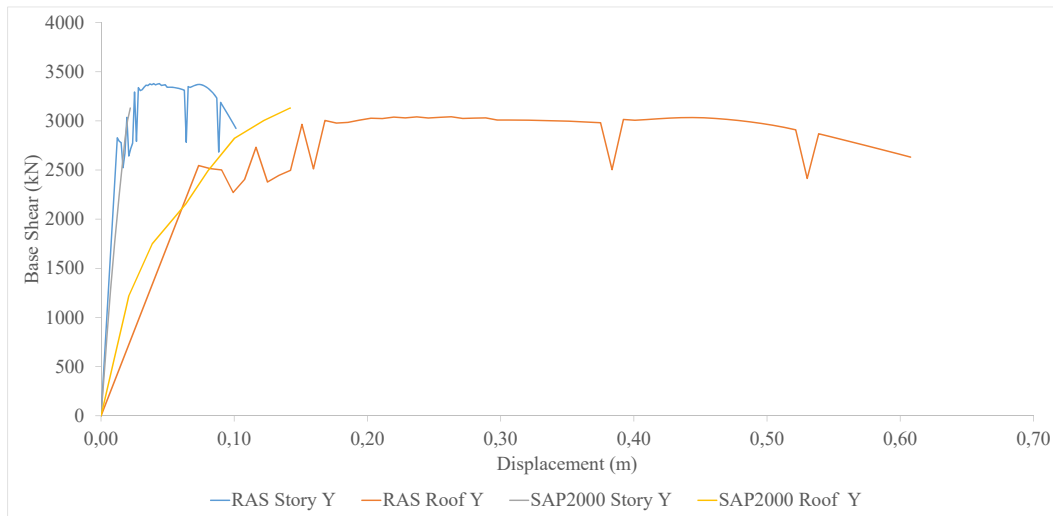
Comparison of the capacity curves in terms of maximum base shear and the first displacement value for this force considering all the analyses given in Section 4.3 are tabulated below in Table 4.10.

From the Table 4.10 and Figures from 4.39 to 4.57, it is seen that the proposed method can determine the maximum base shear the structure can endure with a reasonable accuracy for symmetrical and slightly unsymmetrical structures. The errors are decided to be within tolerable limits considering the analysis is a stiffness-based, one story approach.

One of the important points to note in the capacity curve comparisons in Figure 4.39



(a) Analyses Results for U2 in x-axis



(b) Analyses Results for U2 in y-axis

Figure 4.53: Analyses Results for Unsymmetrical Structure 2

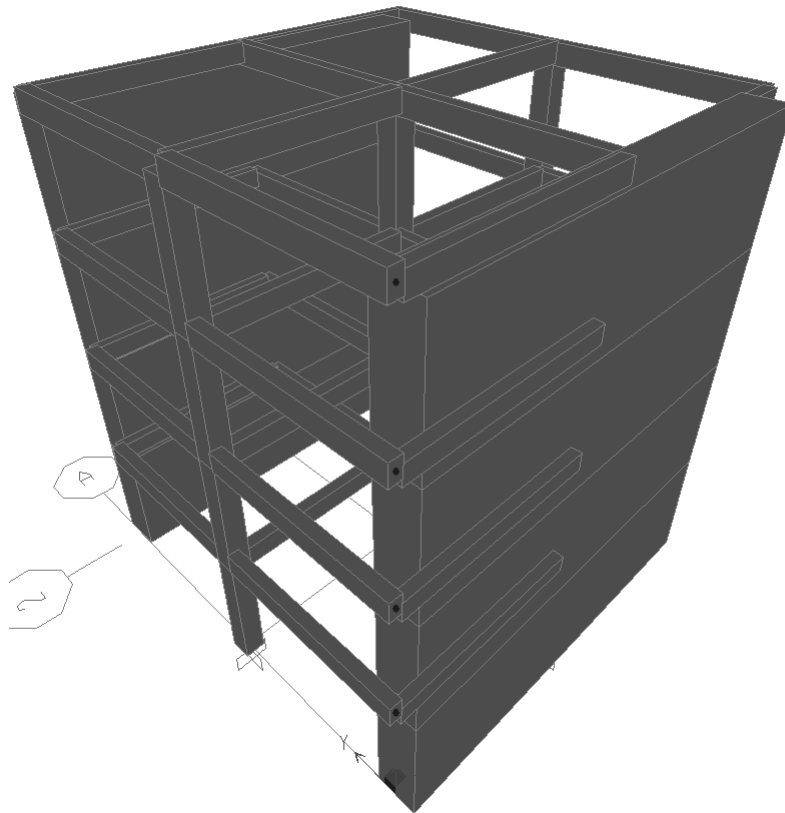


Figure 4.54: Shear Wall Structure 1

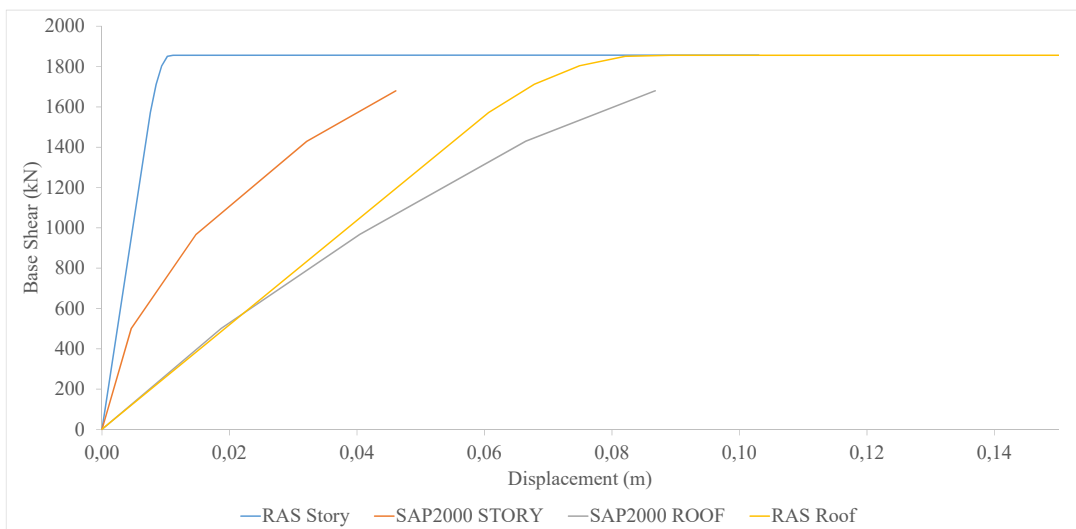


Figure 4.55: Analyses Results for Shear Wall Structure 1

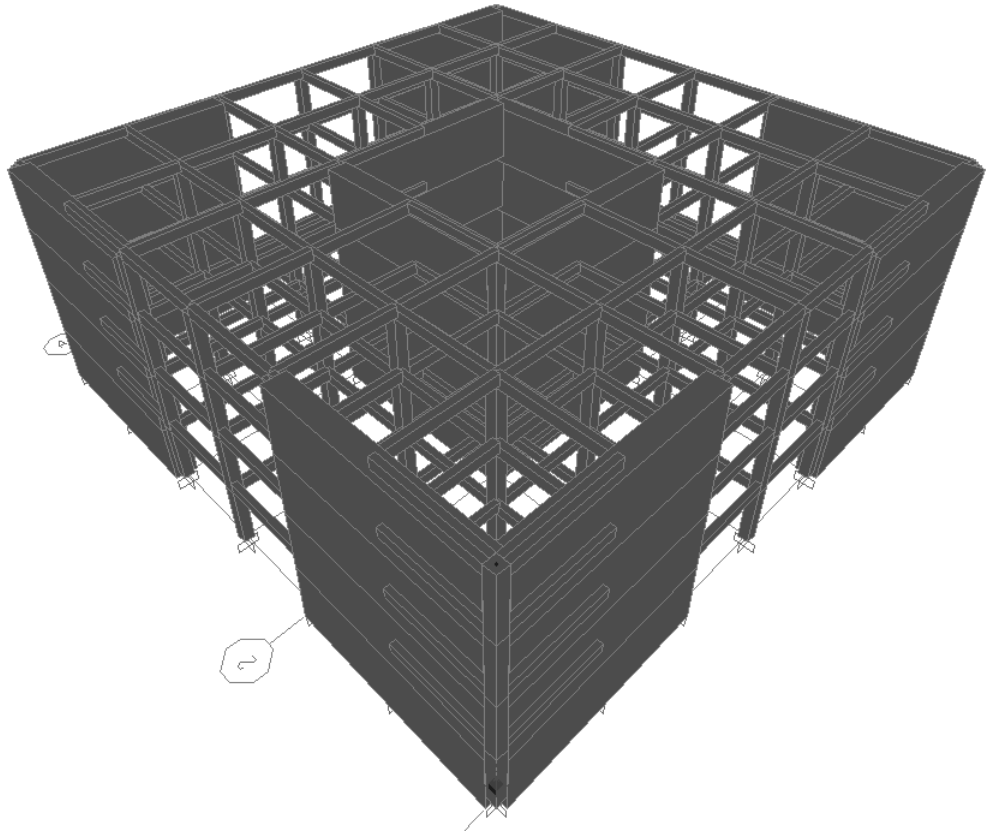


Figure 4.56: Shear Wall Structure 2

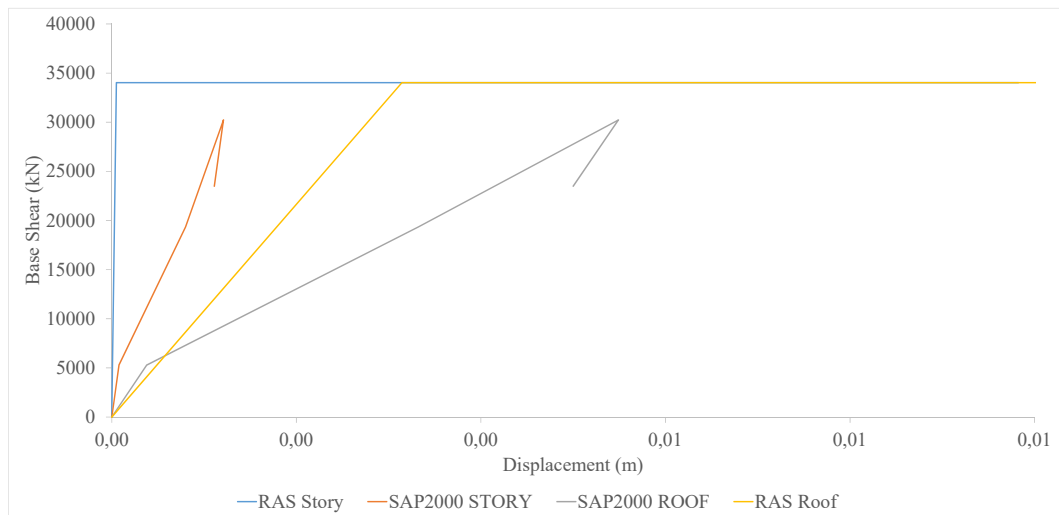


Figure 4.57: Analyses Results for Shear Wall Structure 2

Table 4.10: Comparison of Verification Analyses Results

		Maximum Base Shear (kN)		
		RAS	SAP2000	Difference (%)
Symmetrical	1	598	590	1.4
	2	950	926	2.6
	3	1303	1253	4.0
	4	1219	1088	12.0
	5	1646	1440	14.3
	6	5330	4651	14.6
Unsymmetrical	1 (X)	1049	1253	18.9
	1 (Y)	720	850	15.3
	2 (X)	3764	3129	20.3
	2 (Y)	3371	3130	7.7
Shear Wall	1	1860	1680	10.7
	2	34020	30228	12.5

through 4.57 is that the starting point of yielding for the entire structure and the displacement pattern during yielding phase shows slight deviations from SAP2000 analysis. This phenomenon is expected to stem from mainly two reasons:

- Plastic hinges are assigned to the ends of both columns and beams during the modeling process of test structures in SAP2000. Test buildings are designed as code-compliant, therefore the beams yield before the columns, initiating the decrease in the initial stiffness of the structure. However in the proposed method, beams are considered for their stiffness effect only, and plastic hinge formation is allowed solely on columns. Consequently, in SAP2000, the yielding of the structure begins before the proposed method where beam yields are not taken into account. This results in the deviation in the start of the yielding point between RAS and SAP2000 results.
- In the analysis, a custom set of continuous equations are used as the force-deformation relations for the columns. This equation set does not have any strain hardening and includes residual strength for elements after the ultimate point. However, standard bilinear relations with “unloading element after ul-

imate point” is used in SAP2000 models. Even though this difference will not result in the deviation between starting points of yielding behavior, it will manifest itself in the late regions of the inelastic section.

4.4 Limitations of the Proposed Method

The following limitations and concerns should be noted when deciding whether to apply the proposed new capacity determination method to a structure or interpreting the analysis results. These limitations mostly stem from the assumptions included in the analysis calculations and can be eliminated if the underlying assumption is either not implemented or is improved.

- The method is applicable to only reinforced concrete structures. The other common structural types either have their own concerns during analysis or require a completely different approach; masonry structures do not have beams and columns and require wall analysis, steel structures have connections and buckling issues that should be addressed separately, and timber constructions have other points to be considered.
- The method is advised to be applied to structures with the first mode dominant response, which are either completely symmetrical structures or ones having only minor irregularities. Even though the irregularities caused by vertical member differences are considered in the analysis, the “first mode dominant modal pattern” used in converting story deformation to roof displacements (Section 4.1.8) is valid for structures whose response is governed mostly by the first mode. Therefore, if the method is applied to a structure with increased higher mode effects, the error values are expected to increase at the roof level. Therefore, the loss of accuracy should be taken into account when using the new method on high-rise buildings, highly irregular structures and other conditions where higher order modes start to manifest their presence on the overall response.
- The method assumes a rigid body motion for the slab; the deformations within the slab are said to be none. This diaphragm behavior holds unless there are

large openings in the slab or presence of high irregularity combined with very thin slab thickness. Therefore, for structures with large slab voids or buildings where inter-slab deformations are expected, the accuracy of the proposed approach is anticipated to diminish.

- The new method is based on the response of the most critical story, which most of the times is identified as the first story. However, if it is anticipated that the most critical story corresponds to higher floors, the necessary modifications should be applied in the determination of vertical member effective stiffness values and converting story deformations to roof level displacements.
- The presence of shear walls are approximated as “springs in series” analogy in the proposed method. This approximation yields acceptable results for structures having shear walls in addition to columns in their frames. However, for structures that are composed of only shear walls (such as tunnel formwork constructions), this approximation may result in increased errors due to the contrasting behavior of reinforced concrete walls compared to columns. Therefore, the method should be applied to structures composed of only shear walls with caution.
- The yield and ultimate capacity of columns are a function of the axial load on top of them in addition to several other parameters. In the implementation of the proposed algorithm, this load is calculated for every column using tributary area approach, assuming 1 t/m^2 load. However, in cases where the expected load is greater than this value (such as archive or other storage facilities, structures with tanks inside. . . etc.), the application should be done keeping the increased loading in mind.

CHAPTER 5

DEVELOPMENT OF AN ON-LINE CONDITION ASSESSMENT SYSTEM

It is now an industry standard to create complex finite element models of structures for detailed analysis in many aspects such as seismic response, modal properties, and load-resistance mechanisms with the ever increasing computing power of central processing units and storage limits for read-access memory and hard disks of computers. Adding the advanced capabilities of graphic rendering hardware and software to this arsenal, it is also possible to create beautiful output images for the analysis results. For this reason, there are quite a bunch of analysis software available in the market, each of which claims to specialize in one or more distinct features. However, none of these programs make use of the broadband high-speed Internet connection available even for the mobile platforms. This aforementioned software almost completely focuses on sophisticated models of a single structure for many different loading combinations and effects, which is a suitable approach for office-based detailed design and assessment procedures. Nevertheless, there is a need for a more mobile analysis system which has the capability of connecting site teams for simpler computations and assessment techniques. In this way, the office and site staff will be able to communicate instantly and relatively faster evaluations could be done at the ground zero (i.e. the location of the target structure). One of the main objectives of this study is to develop such a system with all the inter-connected components for leading to more efficient and faster structural assessment of large zones with many buildings. In addition, with the use of visual aids and an extensive help mechanism, it may be possible to create a system where nontechnical people can perform walk-down or even preliminary level analyses. By this approach, first level assessment stages can be delegated

to residents of structures, leading to very fast and efficient prioritization of detailed analyses for a large building stock. Furthermore, if this system is introduced to an adequate portion of the population, earthquake risk awareness may be spread with ease, turning the attention of the public to key points of seismic resistant design.

5.1 Overview of the System

Similar to all large-scale on-line networks, a web-based assessment system should be divided into several main components for better management and sustainability. In turn, these bigger sections have to be composed of smaller modular parts to ensure extensibility as well as ease of debugging and development. Considering abstraction is the key to managing complexity, the system should be implemented as small scale as possible. Through this approach, both adding new components and managing the existing parts will be straightforward.

The target system is planned to have the following major components:

- Graphical user interface (GUI)
- Data access layer (databases and accessing components)
- Analysis engine
- Reporting engine

5.2 Graphical User Interface

The graphical user interface (GUI) is the component that allows users to interact with the electronic devices with the help of graphical icons and audio-visual indicators, thus considered as one of the most important parts of a software. As opposed to text-based interfaces where users need to learn specific keyboard commands to be typed, GUIs have much less steep learning curves, and “WIMP” approach (“window, icon, menu, pointing device”) is almost a universal standard paradigm for personal computers. WIMP heavily relies on high-level interfaces with the mouse, keyboard, and

screen, thus higher quality interfaces can be created [89] [90]. After the introduction of powerful mobile devices (tablets and smartphones), newer actions such as pinching and rotating (which are unsupported by one pointer and mouse) are also included in interaction methods, which is called the post-WIMP user interfaces [91]. These contemporary elements allow better navigation and use as they match with human cognitive, perceptual, manipulative and social abilities [92].

The platform on which GUI will be used heavily influences the design choices, especially for the client application because of several reasons. First of all, each platform has its own set of native controls (text boxes, buttons, dropdown menus... etc.). Therefore, aside from several frameworks (such as Xamarin) and implementations (such as Java Virtual Machine), every interface should be designed separately for each target platform for optimum visual and user experience. Secondly, available screen size for different platforms changes significantly; therefore dimensions of controls and window layouts should be planned accordingly. Having too many elements on a 4-inch screen with a very small font may render the usability nearly impossible. Third, the input capabilities and methods of platforms vary greatly. Most of the time, desktop environments do not have touch input and image acquisition components (such as a camera) whereas mobile systems do not include pointer and input devices such as mouse and keyboard. Therefore, minimizing the actions that are uncomfortable for the user to accomplish in the target platform is a prime requirement for success. Because of these reasons, individual interfaces have to be developed for the desktop, the web, and mobile environments for the client application.

5.2.1 Standalone Software vs. Web Application

The major decision to be made before starting to code the application is deciding whether it will be a standalone software to be installed with a distributable installer or a web application accessible via browsers. Both approaches have their advantages and disadvantages, which will be discussed in the next sections.

Even though losing its market share and total usage time in the last decade to touch-screen mobile competitors, desktop computers still constitute the main branch of engineering analysis and design hardware due to their high computing power, currently

unmatched multi-threading capabilities and ease of use. Consequently, an installable client for a standard PC is a precondition.

Considering the fact that most of civil engineering design and analysis programs as well as mainstream office software work on Microsoft Windows operating system (OS), it is decided to disregard other common OS such as Macintosh OS (MacOS), Solaris, and popular Linux distributions (Ubuntu, Mint, Red Hat, Debian, Fedora, Puppy... etc.). For Windows OS, there are two main alternative graphic libraries for user interfaces; old “Windows Forms (WinForms)” and new “Windows Presentation Foundation (WPF)”. The former one provides access to native Windows user interface common controls by wrapping the extant Windows API in managed code [93]. It uses GDI+ (a Windows API and a core operating system component responsible for the creation of graphical objects and their transmission to output devices like monitors and printers) and released around the 2000s. Even though it is one of the most common control libraries used, Microsoft announced in 2014 that WinForms is in maintenance mode with no new features being added but bugs found will still be fixed. WPF is released in 2006 as a part of .NET Framework 3, and rather than relying on older GDI subsystem, it uses DirectX. Moreover, it has many advanced functionalities such as anti-aliasing, high DPI rendering, better data-binding, animations and story-boarding, styles and themes, application commands... etc.

For mobile platforms, two main dominant shareholders (namely iOS and Android) are completely incompatible. Unless few frameworks that claim to port the application to any platform (such as Xamarin) are used, interface design should be carried out separately for every platform. The Android environment is Java based whereas iOS uses either Swift or Objective-C. Their UI philosophy and enforced policies are also very dissimilar, making a unified user interface experience across platforms a very tedious task to accomplish.

The main advantages of a standalone software to a web application is off-line availability. Users do not need internet access to use the program; it can work on any location, independent of connectivity. However, this advantage comes with several fundamental caveats. First and foremost, software platforms (Windows, iOS, Android... etc.) are completely incompatible; for every target operating system, an in-

dividual UI should be created from scratch. Second, version tracking and control is extremely hard; publishing updates and new versions have no effect unless the user manually upgrades to a newer version. For these reasons, web application path is chosen instead of a standalone software.

5.2.2 Web Application Properties

To overcome the main disadvantages listed in Section 5.2.1, it is decided to create a web application. The licensing and delivery model is selected to be “Software as a Service (SaaS)”. In most basic terms, SaaS is licensing a software on a subscription basis, and centrally hosting it. SaaS has been incorporated into the strategy of some leading enterprise software companies [94]. Most of the SaaS projects are based on multitenant architecture; a single instance of the software runs on the server and serves multiple *tenants* (users). To ensure scalability for high demand, the application may be run on several servers as well (“horizontal scaling”). The developed application is classified as vertical SaaS, answering the needs of a specific industry instead of being industry-independent.

The most important advantage of web approach is *accelerated feature delivery*; which is being able to update the application more frequently compared to conventional software. This is possible thanks to several factors:

- Central hosting, which enables to decide and execute the update by the provider, not the client.
- Singular configuration, which makes development testing faster.
- No backdated version support because there is always a single version.
- Access to all customer data, which enables expediting design and testing.
- Access to user behavior via web analytics and other monitoring tools.

Some other advantages that lead to acceptance and spread of SaaS systems are listed below:

- Increasing availability and affordability of broadband internet.
- Standardization of web development technologies (CSS, JavaScript, HTML) and abundance of improved web application frameworks (Ruby on Rails, ASP.NET, Laravel... etc.).
- An increasing number of web-based UI applications.
- Standardization of HTTPS protocol, enabling lightweight security affordable and usable for daily applications.
- Utilization and acceptance of integration protocols like REST and SOAP.

Like the traditional systems, cloud-based software applications suffer from a variety of disadvantages and challenges as well. Some of these items can be overcome with design changes, whereas there is no solution for the others:

- Data security on vendor servers should be established to prevent any leaks or thefts.
- Since the application is hosted on a remote server, there will always be a latency in response times of the environment.
- Multitenant architectures limit customization for large scale clients.
- If large files are involved, their transfer over the web may be a tedious task.

5.2.3 Technologies and Services Used

Web technologies made great advancements in the last decade, conforming the hardware and connectivity improvements. Internet page development moved from resource hogging, unresponsive, almost static screens to light and responsive media with many additional tools such as geolocation, asynchronous request/responses, and device-aware designs. Moreover, it is now possible to command hardware connected to the device (such as camera, microphone... etc.) directly from browser without any additional plug-ins. In the past, extra components were required to be installed (such as ActiveX plug-ins) in order to accomplish the same control, yet these extensions

were unstable and contained security threats and vulnerabilities. The modern counterpart, HTML5 API's for multimedia and other hardware control are much more stable, easier to implement, universally supported (on PC and mobile platforms), and more secure.

5.2.3.1 Programming Language

For the overall system, the language selected is C#. It is a multi-paradigm programming language encompassing strong typing, imperative, declarative, functional, generic, object-oriented and component-oriented programming disciplines. It was developed by Microsoft within its .NET initiative and later approved as a standard by Ecma (ECMA-334) and ISO (ISO/IEC 23270:2006).

5.2.3.2 Web Application Framework

In the web application sections of the system, ASP.NET MVC is used. It is an open-source server-side web application framework designed for web development to produce dynamic web pages. It was developed by Microsoft to allow programmers to build dynamic websites, web applications, and web services. ASP.NET is in the process of being re-implemented as a modern and modular web framework, together with other frameworks like Entity Framework. The new framework will make use of the new open-source .NET Compiler Platform (codename "Roslyn") and be cross platform. ASP.NET MVC, ASP.NET Web API, and ASP.NET Web Pages (a platform using only Razor pages) will merge into a unified MVC 6. The project was called ASP.NET vNext but later renamed as ASP.NET Core.

5.2.3.3 Web Application Architecture

The architecture implemented is Model-View-Controller (MVC) version 5. It is a software architectural pattern mostly (but not exclusively) for implementing user interfaces. It divides a given software application into three interconnected parts, so as to separate internal representations of information from the ways that information is

presented to or accepted from the user.

Traditionally used for desktop graphical user interfaces, this architecture has become extremely popular for designing web applications (Figure 5.1).

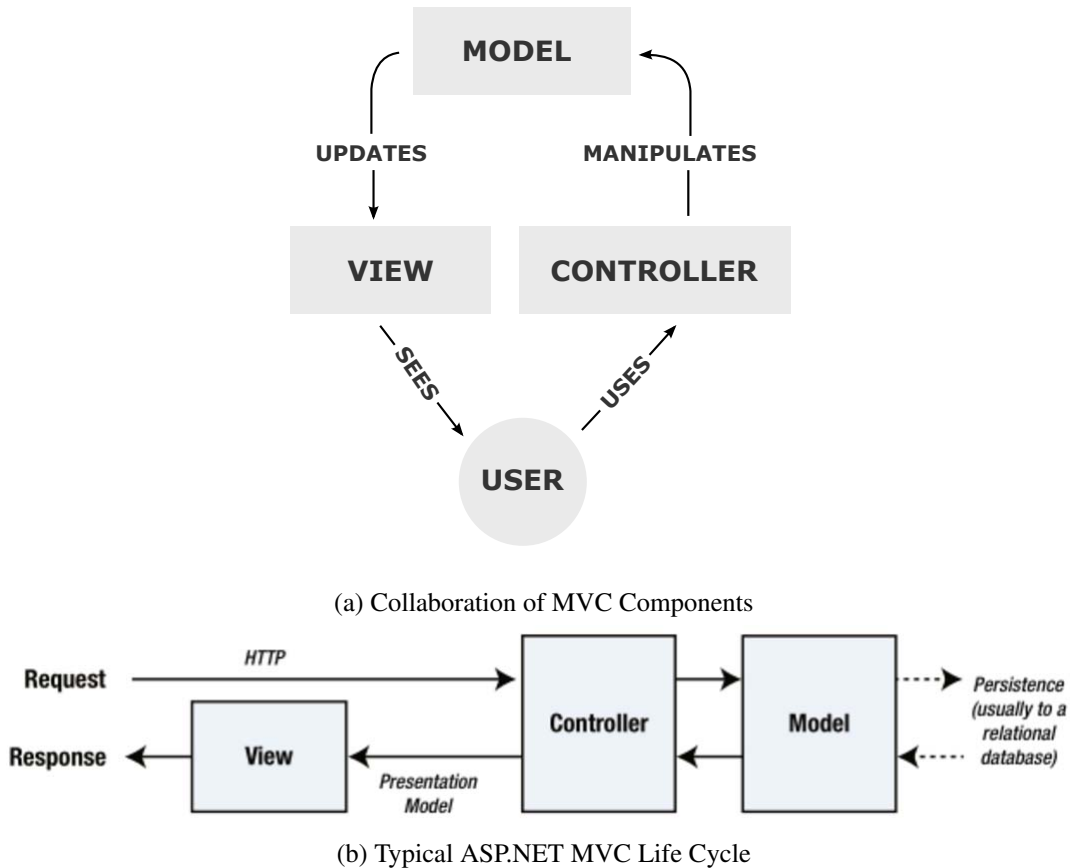


Figure 5.1: Generic and ASP.NET MVC Implementations

5.2.3.4 Page Style and Design

Instead of static text decorations and properties, contemporary web sites make use of Cascading Style Sheet (CSS) technology combined with HTML markups, which is merely a catalog of when and how an element should look on which devices. Though one could create his own design from scratch, there are many well-designed templates on Internet, both free of charge and premium. The developed system makes use of **Bootstrap** front-end framework, a free and open source collection of tools. It contains HTML and CSS-based design templates for typography, forms, buttons, navigation

and other interface components, as well as optional JavaScript extensions. It aims to ease the development of dynamic websites and web applications. It was originally named as Twitter Blueprint and meant to be used internally by Twitter. However, later it was embraced by development community very fast, and released as an independent open source project in 2011. It is compatible with the latest versions of all major browsers, including its most prized responsive web design properties. This feature enables adjusting the layout of a web page dynamically, based on the device used in viewing the page. Individual elements can be resized or hidden based on the width of the browser, leading to the optimum user experience on every screen size available in the market.

5.2.3.5 Authentication and Authorization

For authentication of registered users and granting authorization to different levels, *Microsoft Identity* is used. It is a new API from Microsoft to manage users in ASP.NET applications. The mainstay for user management in recent years has been ASP.NET Membership, which has suffered from design choices that were reasonable when introduced in 2005 but has aged badly. The biggest limitation is that the schema used to store the data worked only with SQL server and was difficult to extend. The schema itself was overly complex, which made it harder to implement changes. There were few attempts on improving Membership such as “Simple Membership” and universal providers. But even with these, the fundamental issues of depending on relational data and difficult customization remained. To address both problems and provide a more modern user management platform, Microsoft has replaced Membership with Identity. It is flexible and extensible, but still immature, and features that are taken granted in a more mature system can require a surprising amount of work. Identity is a part of OWIN - Open Web Interface for .NET. It is an abstraction layer that isolates a web application from the environment that hosts it. OWIN is an open standard, and its implementation for Windows platform is called Project Katana. OWIN/Katana isolates the ASP.NET technology stack from the rest of .NET framework. OWIN developers select the services they require for their application, rather than consuming an entire platform as happens with ASP.NET. Individual services, known as middleware, can be developed at different rates, and developers will be able to

choose between providers for different services. It is still in its early days; it may be possible to build Web API and SignalR applications without System.Web and IIS process requests, but that is about all.

5.2.3.6 Data Access Layer

Entity Framework (EF) is an open source object-relational mapping (ORM) framework for ADO.NET, part of .NET Framework. The Entity Framework is a set of technologies in ADO.NET that support the development of data-oriented software applications. Architects and developers of data-oriented applications have typically struggled with the need to achieve two very different objectives. They must model the entities, relationships, and logic of the business problems they are solving, and they must also work with the data engines used to store and retrieve the data. The data may span multiple storage systems, each with its own protocols; even applications that work with a single storage system must balance the requirements of the storage system against the requirements of writing efficient and maintainable application code.

The Entity Framework enables developers to work with data in the form of domain-specific objects and properties, such as customers and customer addresses, without having to concern themselves with the underlying database tables and columns where this data is stored. With the Entity Framework, developers can work at a higher level of abstraction when they deal with data and can create and maintain data-oriented applications with less code than in traditional applications. Because the Entity Framework is a component of the .NET Framework, Entity Framework applications can run on any computer or server on which the .NET Framework (starting with version 3.5 SP1) is installed.

As explained before, EF creates its database based on the relations defined in model class definitions (key attributes, navigation properties. . . etc.) on the first deployment. There are multiple database initialization strategies that can be followed in code-first approach. This selection of strategy is very important; when the underlying model structure changes, there are different policies that EF can follow in order to update the database to match its model counterpart. These policies depend on the

initialization strategy selected at the beginning. The appropriate policy should be defined very carefully since wrong decisions will almost certainly result in losing data irrecoverably. There are four different database initialization strategies:

CreateDatabaseIfNotExists: This is the default initializer, and it will create the database if none exists as per the configuration. However, if the business model changes and the application are run with this initializer selected, it will throw an exception.

DropCreateDatabaseIfModelChanges: This initializer drops (deletes) an existing database and creates a new one if underlying business models change. However, all the data in the old database will be irrevocably lost, and usually, it is not a good approach for real life scenarios.

DropCreateDatabaseAlways: The initializer drops an existing database every time the application is run, irrespective of changes in business model. This is usually used in development stages only.

Custom DB Initializer: Almost in all real life cases, the above strategies do not satisfy the demands, and a custom initializer is written.

In real life scenarios, the requirement is that the database should be created only if there is none before, and it should be updated without any data loss to match the business model changes. There is no predefined strategy which conforms to this need, therefore a custom initializer is almost always defined from *NullDatabaseInitializer*, which disables data initialization for the given context type. Instead, “migrations” are used in database creation and upgrade events. “Migration” is a set of SQL transactions that are executed when the database schema does not match business models. This is an advanced feature set, therefore it requires several steps to be enabled and configured to work as intended. In the end, EF creates a migration folder which includes a configuration file and an individual SQL command file for each migration which updates the database schema reflecting changes of model classes. In this web application, there are two different contexts (users and structures) and two databases, therefore each migration context is activated and tracked individually.

One other important item to be discussed under Entity Framework section is the implementation of connection resiliency and retry logic. Applications connecting to a database server have always been vulnerable to connection breaks due to back-end failures and network instability. However, in a LAN-based environment working against dedicated database servers, these errors are rare enough that extra logic to handle those failures is not often required. With the rise of cloud-based database servers and connections over less reliable networks, it is now more common to connection breaks to occur. This could also be due to defensive techniques that could databases use to ensure fairness of service, such as connection throttling, or due to instability in the network causing intermittent timeouts and other transient errors. *Connection resiliency* refers to the ability for EF to automatically retry any commands that fail due to these connection breaks.

Connection retry is taken care of by an implementation of the *IDbExecutionStrategy* interface. These implementations will be responsible for accepting an operation, and if an exception occurs, determining if a retry is appropriate and retrying if it is. There is a total of four execution strategies available in EF:

DefaultExecutionStrategy It does not retry any operations, it is the default for any database other than SQL server.

DefaultSqlExecutionStrategy This is an internal execution strategy that is used by default. It does not retry at all, however, it will wrap any exceptions that could be transient to inform users that they might want to enable connection resiliency.

DbExecutionStrategy This is suitable as a base class for other custom execution strategies. It implements an exponential retry policy, where the initial retry happens with zero delays and the delay increases exponentially until the maximum retry count is hit. It has an abstract *ShouldRetryOn* method that can be implemented in derived execution strategies to control which exceptions should be retried.

SqlAzureExecutionStrategy It inherits from *DbExecutionStrategy* and will retry on exceptions that are known to be possibly transient when working with SqlAzure.

Since the system is hosted on Azure cloud services, selected execution strategy is *SqlAzureExecutionStrategy* with default maximum number of retries and delay.

5.2.3.7 Other Components

- “Highcharts” framework is used for drawing high-quality, interactive charts to the web pages.
- Math.Net is used for matrix operations. It is an open source initiative to build and maintain toolkits covering fundamental mathematics.

5.2.4 Visual Aid and Help System

Although it is a part of the user interface, a separate section is dedicated to “Visual aid and help system” of the application, because it is a major component of UI that is designed to make the overall system usable by people without technical knowledge.

Walk-down surveys completely rely on identification of visible structural conditions that may cause problems (such as short columns) and surface manifestation of non-visible properties (such as apparent material quality). Identifying and classifying these features from a text list require theoretical knowledge and prior experience, which is not an issue for professional site teams. For untrained residents, sample visual aids and simplified explanations are supplied so that they are able to conduct walk-down surveys as well. In order to keep the application interface simple and efficient, these help sections are connected via hyperlinks so that they can be opened on demand, instead of occupying a space in the screen permanently (Figure 5.2). In the hyperlink, ‘*shortColumn*’ denotes the help HTML file name and *target* query string points the value to be updated when a user clicks on an image in the help screen.

Help windows are opened as modals; they are streamlined and flexible dialog prompts with the minimum required functionality and smart defaults. In other words, basically, a modal is a dialog box/pop-up window that is displayed on top of the current page (Figure 5.3). They darken the background, focusing user’s attention completely to the new content displayed on the screen.

Soft Story
 Exist
 Help me on this question

Short Column
 Exist
[Help me on this question](https://localhost:44300/Help/Help/shortColumn?target=RBTV)

Vertical Irregularity
 Exist
 Help me on this question

Figure 5.2: Help Hyperlink for 'Soft Story' Question

Risk Analysis System Seismic Risk Analysis Tools Contact Hello trialuser1! Log out

Soft Story

Exist
Help me on this question

Heavy Overhang

Exist
Help me on this question

Soft Story

Exist
Help me on this question

Short Column

Exist
Help me on this question

Vertical Irregularity

Exist
Help me on this question

Plan Irregularity

Exist
Help me on this question

Apparent Quality


Please select the image that represents

Soft Story

A soft story usually exists in a building when the ground story has less stiffness and strength compared to the upper stories. This situation mostly arises in buildings located along the side of a main street. The ground stories, which have level access from the street, are employed as a street side store or a commercial space whereas residences occupy the upper stories. These upper stories benefit from the additional stiffness and strength provided by many partition walls, but the commercial space at the bottom is mostly left open between the frame members, for customer circulation. Besides, the ground stories may have taller clearances and a different axis system causing irregularity. The compound effect of all these negative features from the earthquake engineering perspective is identified as a soft story. Many buildings with soft stories were observed to collapse due to a pancaked soft story in past earthquakes all over the world.

You can see examples of soft stories below. If an image resembles your structure, please select it (only 1 image):

Samples



[Enlarge Image](#)

Figure 5.3: Modal Help Page for 'Soft Story' Question

One problem here is that modal windows are static, i.e. should be defined within the body of their parent page, and can only be initiated by button controls. However, considering there are almost 50 questions per analysis, and a lot of help images per question, embedding all these into a single page would have resulted in an HTML file of unmanageable size. To overcome this problem, first of all, modal-container Bootstrap attributes are attached to links with ‘.modal-link’ class. Thus, when a link with these attributes is clicked, Bootstrap will display the href content in a modal dialog, eliminating the need to include all help pages in the parent file. Another important user experience issue encountered in this phase is about help window loading times. Modal dialogs are designed to present simple text and few choices to the user; however, in this particular case, one help window can have 9-10 images. This large content causes loading times to deflate, and modal windows show no indication of their opening process, leaving the user with the impression that nothing is happening in the background (even though images are being downloaded). To inform the user of the loading process, help pages are loaded into modal dialogs at runtime with asynchronous AJAX requests. In addition, using JQuery’s hooking ability into AJAX events, an animated loading GIF image is shown to the user, so that they will realize the process is continuing in the background.

For modularity, scalability and manageability purposes, target query strings are not implemented as *magic strings*, but enumerations. Moreover, each and every form control (check boxes, radio buttons) are given a **data-checkId** attribute, which is connected to the images on modal help views (Code 5.1). By this way, when the user clicks any ‘soft story’ example image on the help page, all soft story controls in the main analysis window are checked. These automated checking works are performed by JavaScript routines hooked into different events of form controls.

```
1 <div class="form-group">
2 <label for="
   ↳ Structure_YalimTurerModel_VerticalDiscontinuity"
   ↳ >Vertical Irregularity</label>
3 <br>
4 <label class="checkbox-inline">
5 <input checked="checked" data-checkid="
```

```

↪ VerticalIrregularity" id="
↪ YALIMTURER_VERTICALDISCONTINUITY" name="
↪ Structure.YalimTurerModel.VerticalDiscontinuity"
↪ onclick="CheckSimilar(this)" type="checkbox"
↪ value="true"><input name="Structure.
↪ YalimTurerModel.VerticalDiscontinuity" type="
↪ hidden" value="false"> Exist
6 </label>
7 <a class="help-block modal-link" href="/en/Help/Help/
↪ verticalDiscontinuity?target=YALIMTURER">Help me
↪ on this question</a>
8 </div>

```

Code 5.1: data-checkId Attribute for Modal Help Windows

5.2.5 Localization of User Interface

With the aim of targeting international audience in the future, the whole system is prepared with globalization approaches in mind. Globalization is the combined process of internationalization (i18n), which is making your application able to support a range of languages and locales, and localization (L10n), which is making your application support a specific language/locale. There are different approaches for implementing globalization, such as using distinct pages for every language, using resource files instead of static values...etc.

In this application, resource file technique is implemented, assuming it is the best approach for multi-language web applications. In this method, every translation of strings to be used in the interface are written into different resource files which are in XML format. The first extension of these files denotes the language it includes (for example; 'strings.en.resx' contains English whereas 'strings.tr.resx' have Turkish translations). The user's browser will report their language preferences in the Accept-Languages HTTP header as a weighed list, and if configured, ASP.NET has the ability to use the appropriate resource file according to this list.

All the strings in the user interface should be referenced to items in these resource files. Fortunately, they have converted to enumerations automatically, and one can call them using the auto-complete feature within page syntax (5.4).

```
@using shared.Localization
@using shared
@model HTMLID
<div class="modal-body">
  <input type="hidden" id="sender" value="@Model" />
  <h2>@Localization.FrontPlanWidth</h2>
  <div class="panel panel-default">
    <div class="panel-body">
      <p class="text-justify">
        @Localization.FrontPlanWidthHelpBodyText
      </p>
      <div class="container-fluid">
        <div class="row">
          <div class="col-xs-12 text-center">
            
            <a href="~/Images/Help/frontTotalWidth-1.png" target="_blank">@Localization.EnlargeImage</a>
          </div>
        </div>
      </div>
    </div>
  </div>
  <button type="button" class="btn btn-warning btn-block"
    data-dismiss="modal">
    @Localization.Close
  </button>
</div>
```

Figure 5.4: Localization Syntax in Page

5.3 Database Layer

The system should have a database component to store registered user information, and structures analyzed by these users. In order to achieve modularity and independence of these two types of data, two different databases are used in the web application. The type of database used is SQL, and a single server (MSSQL) is utilized to host both of the databases. As stated in Section 5.2.3.6, Entity Framework object-relational mapping tool is used, and since Code-First approach is followed, all databases and their relations are created automatically by EF. Authentication and authorization framework Identity also heavily relies on EF, and user database is also deployed by it.

5.4 Analysis and Reporting Engine

This engine consists of methods for individual analysis types, auxiliary functions that compute parameters required in different analyses (such as slab area, element section

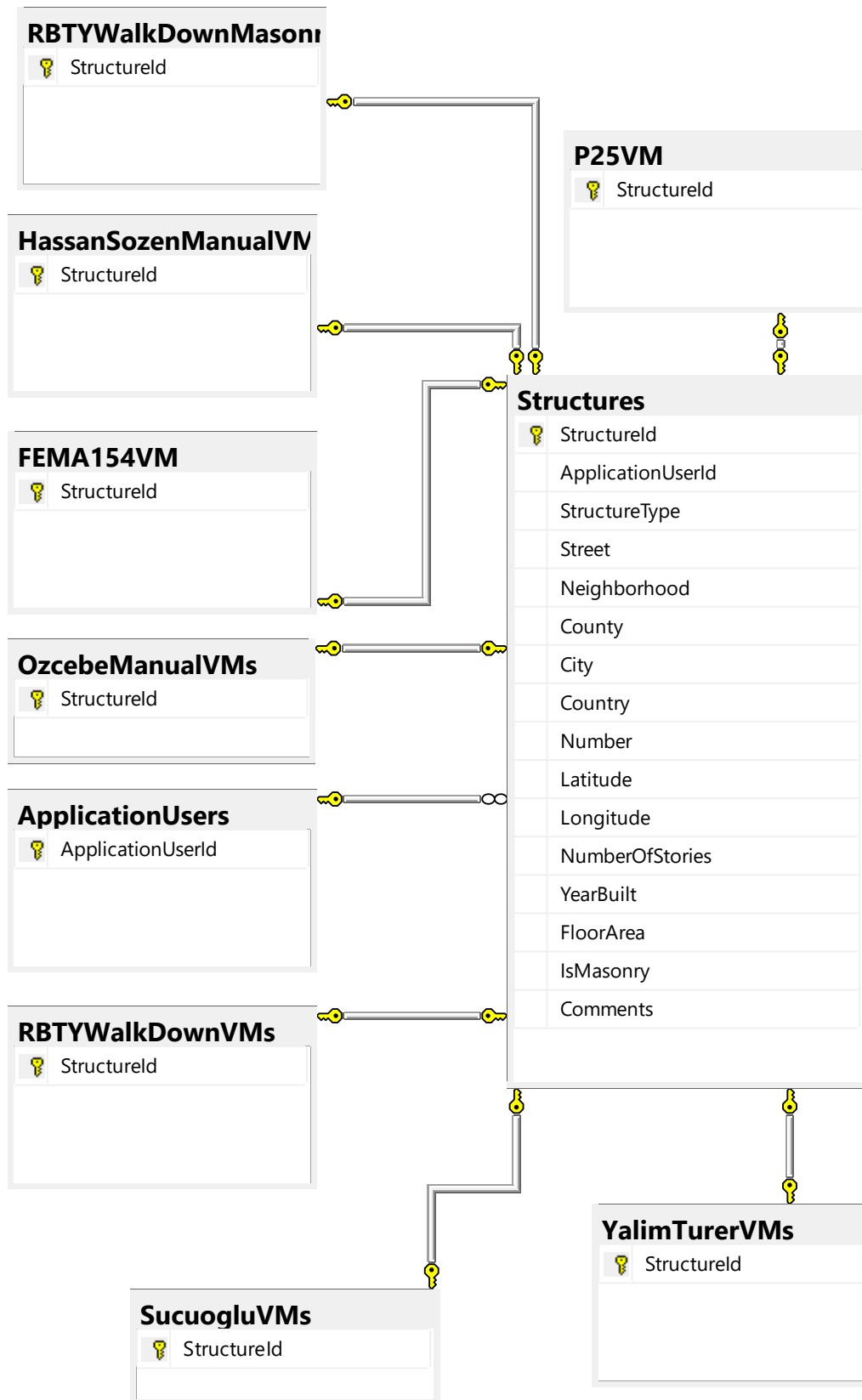


Figure 5.5: Database ER Diagram for Application Data

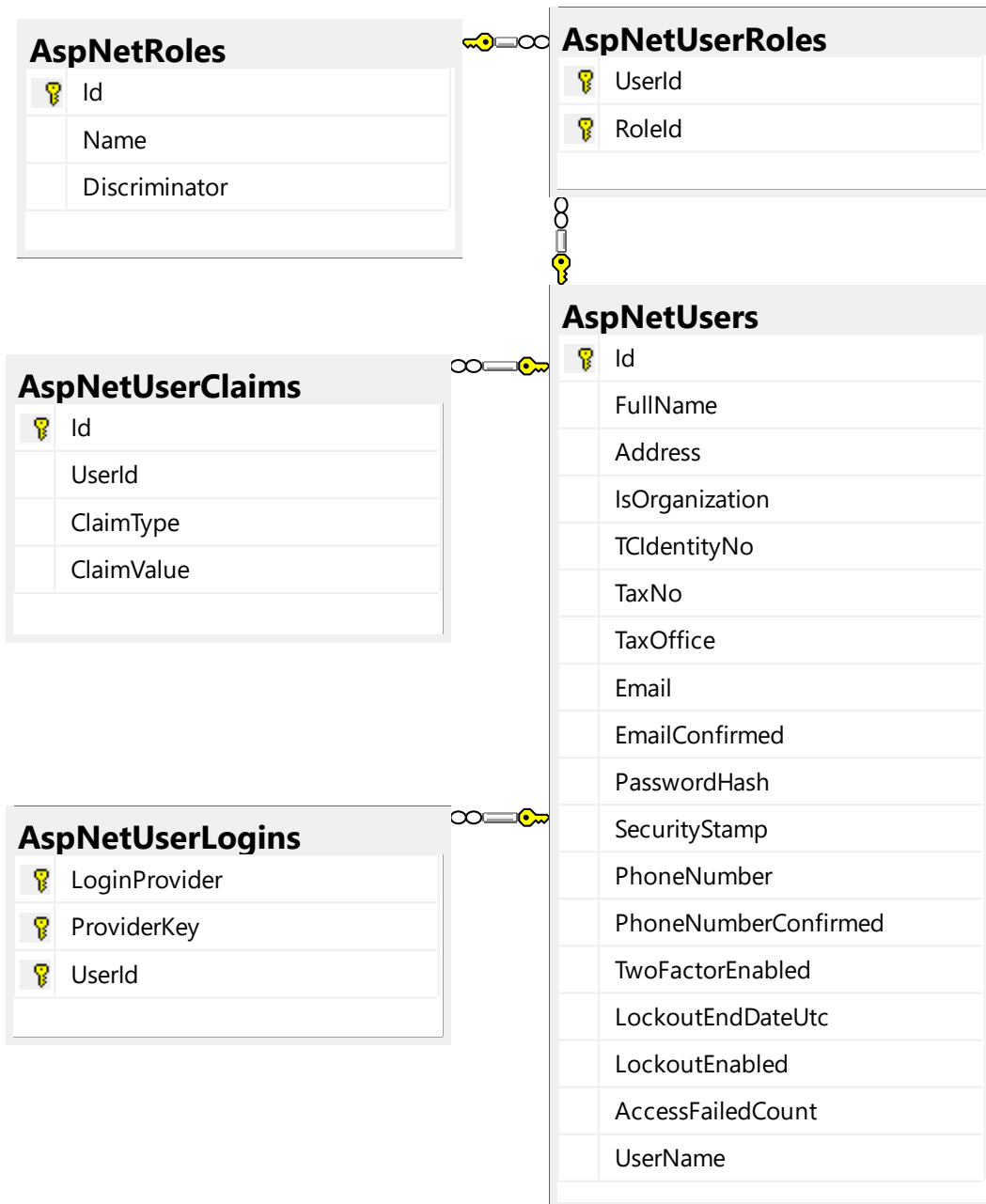


Figure 5.6: Database ER Diagram for Users

moment capacity...etc.), subroutines for managing file and folder (IO) operations and reporting methods. The functions (formally named as methods in .NET) in this class are abstracted away from the analysis code due to increased manageability and extensibility.

A set of operations is extracted under a method name in this class if:

- It is called multiple times in different places. By creating a new function, all these operations are moved to a single location, making debugging and updating much more efficient. Moreover, it highly increased reusability.
- It is too long or complex to leave in its current location. Some computations (such as area or section moment capacity calculations) are quite long, and if not abstracted away, they sophisticate the method they reside unnecessarily. To prevent this, tedious calculations are extracted under their own functions.
- It does a job completely unrelated with its parent method. For example, saving user images to a folder, and then converting these images to base64 strings is a necessary task during report creation. However, these jobs are just technicalities of the process, therefore they are relocated under a different function.

The language of which engine is written is C#, and several additional third-party libraries are used for different jobs such as matrix operations.

5.4.1 Calculation Methods

The methods in this class are for computing a value based on input parameters. These jobs include calculating peak ground acceleration from coordinates, finding moment capacity from section properties, creating and condensing stiffness matrices, computing element end forces from its deformations...etc. (Figure 5.7).

Since there are a large number of methods defined, only two of them are exemplified here for a demonstration and giving insight on the inner workings.

- 🌿 CalculateElementLength(ShearWall shearWall):double
- 🌿 CalculateElementLength(InfillWall infillWall):double
- 🌿 CalculateElementLength(Beam beam):double
- 🌿 CalculateFEMA154EarthquakeZone(double latitude, double longitude):FEMA154Seismicity
- 🌿 CalculateHassanSozenRegion(double wallIndex, double ColumnIndex):HassanSozenRegion
- 🌿 CalculateLocalStiffnessMatrix(Column column, double columnLength, Direction direction):Matrix<double>
- 🌿 CalculateLocationLineNumber(double latitude, double longitude):int
- 🌿 CalculateMomentOfInertia(object member, Direction direction):double
- 🌿 CalculateNextGuess(double y1, double of1, double y2, double of2):double
- 🌿 CalculateOF(Guess guess, Direction direction):double
- 🌿 CalculatePGAFromCoordinates(double latitude, double longitude):double
- 🌿 CalculatePointSide(Point P, List<Point> CCWPolygonNodes):List<double>
- 🌿 CalculateSectionProperties(MainVM mainViewModel, Column column, Direction direction):SectionResult

Figure 5.7: An Overview of Several Calculation Methods

5.4.1.1 Sample Method 1: Slab Area and Centroid Calculations

Green's theorem gives the relation between a line integral of a simple closed curve C and a double integral over the plane region D bounded by C , so can be used for corner coordinates of a slab area bounded by lines connecting the corners (5.1).

$$\oint_C (Ldx + Mdy) = \iint_D \left(\frac{\partial M}{\partial X} - \frac{\partial L}{\partial Y} \right) dx dy \quad (5.1)$$

If we choose the direction such that the region D is on the left when traveling around ∂D , and specify the closed curves parametrically as $(x(t), y(t))$ for $t \in [t_0, t_1]$, (5.1) greatly simplifies to:

$$A = \frac{1}{2} \int_{t_0}^{t_1} (xy' - yx') dt \quad (5.2)$$

As slabs will have discrete values instead of continuous functions, numerical implementations of (5.2) should be used (5.3).

$$A = \frac{1}{2} \cdot \sum_{i=0}^{i=n} (x_i \cdot y_{i+1} - x_{i+1} \cdot y_i) \quad (5.3)$$

In Equation (5.3), counter-clockwise arrangement of points result in positive values whereas clockwise processing will yield negative. In order to compensate this, the absolute value of A is used to ensure positive area results.

Green's theorem could further be extended to moment of areas about x and y axes

using $P_x = -y^2/2$, $Q_x = 0$, $P_y = 0$, and $Q_y = x^2/2$:

$$\begin{aligned} M_x &= \iint y dx dy = -\frac{1}{2} \oint y^2 dx = -\frac{1}{2} \int_{t_0}^{t_1} y^2 x' dt \\ M_y &= \iint x dx dy = -\frac{1}{2} \oint x^2 dy = -\frac{1}{2} \int_{t_0}^{t_1} x^2 y' dt \\ \bar{O} &= (\bar{x}, \bar{y}) = (M_y/A, M_x/A) \end{aligned} \quad (5.4)$$

where \bar{O} is centroid point. Similar to area calculations, having discrete station points instead of continuous boundary functions, numerical approaches are implemented:

$$\bar{x} = \frac{1}{6 \cdot A} \cdot \sum_{i=0}^{i=n} ((x_i + x_{i+1}) \cdot (x_i \cdot y_{i+1} - x_{i+1} \cdot y_i)) \quad (5.5)$$

$$\bar{y} = \frac{1}{6 \cdot A} \cdot \sum_{i=0}^{i=n} ((y_i + y_{i+1}) \cdot (x_i \cdot y_{i+1} - x_{i+1} \cdot y_i)) \quad (5.6)$$

The implementation example is given in Code 5.2.

```

1 private double CalculateSlabArea(Slab slab)
2 {
3     double area = 0;
4     Point currentPoint, nextPoint;
5     for (int i = 0; i < slab.CornerNodesPhysical.Count -
        ↪ 1; i++)
6     {
7         currentPoint = slab.CornerNodesPhysical[i];
8         nextPoint = slab.CornerNodesPhysical[i + 1];
9         area = area + (currentPoint.X * nextPoint.Y) - (
        ↪ nextPoint.X * currentPoint.Y);
10    }
11    area = area / 2;
12    return Math.Abs(area);
13 }
14 private Point CalculateMassCenter(Slab slab)
15 {
16     double centroidX, centroidY;
17     centroidX = centroidY = 0;

```



```

18 Point currentPoint , nextPoint ;
19 for ( int i = 0 ; i < slab . CornerNodesPhysical . Count -
    ↪ 1 ; i ++ )
20 {
21     currentPoint = slab . CornerNodesPhysical [ i ] ;
22     nextPoint = slab . CornerNodesPhysical [ i + 1 ] ;
23     centroidX = centroidX + ( currentPoint . X +
    ↪ nextPoint . X ) * ( currentPoint . X * nextPoint . Y
    ↪ - nextPoint . X * currentPoint . Y ) ;
24     centroidY = centroidY + ( currentPoint . Y +
    ↪ nextPoint . Y ) * ( currentPoint . X * nextPoint . Y
    ↪ - nextPoint . X * currentPoint . Y ) ;
25 }
26 centroidX = centroidX / ( 6 * slab . Area ) ;
27 centroidY = centroidY / ( 6 * slab . Area ) ;
28 return new Point ( Math . Abs ( centroidX ) , Math . Abs (
    ↪ centroidY ) ) ;
29 }

```

Code 5.2: Sample Slab Calculations in C#

5.4.1.2 Sample Method 2: Walk-Down Method Calculations

All the computations in walk-down methods are simply addition or subtraction of factors determined by conditions to the base score that depends on several items (such as seismicity, structure type . . . etc.). However, implementing this approach by standard “if-else” or “switch” decision clauses will result in a cumbersome code, both difficult to track and debug since there are a lot of conditions to check, some of which are even intertwined (i.e. penalty score is determined by a combination of several factors for some damage indices, such as seismic region, soil type, and number of stories). Therefore an alternate approach is preferred; using base score and modifier matrices all the work is reduced to row operations that can be performed in a single “for” loop (Code 5.3).

```

1 public static Matrix<double> BaseScores ()
2 {
3     double [,] x = {
4         {100, 130, 150},
5         {90, 120, 140},
6         {75, 100, 120},
7         {65, 85, 100},
8         {60, 80 ,90}
9     };
10    return DenseMatrix. OfArray(x);
11 }
12 public static double PerformSucuogluWalkDown(
13     ↪ SucuogluVM sucuogluModel)
14 {
15     double finalScore;
16     double currentScore;
17     Matrix<double> baseScoreMatrix = Constants.
18     ↪ SucuogluBaseScores ();
19     Matrix<double> gradeMatrix = Constants.
20     ↪ SucuogluVulnerabilityScores ();
21     finalScore = baseScoreMatrix [(int) sucuogluModel.
22     ↪ NumberOfStories , (int) sucuogluModel.
23     ↪ EarthquakeZone ];
24     foreach (SucuogluWalkDownParameters parameter in Enum.
25     ↪ GetValues (typeof (SucuogluWalkDownParameters)))
26     {
27         currentScore = 0;
28         switch (parameter)
29         {
30             case SucuogluWalkDownParameters. SoftStory :
31                 currentScore = Convert. ToInt16 (sucuogluModel.
32                 ↪ SoftStory) * gradeMatrix [(int)

```

```

    ↪ sucuogluModel . NumberOfStories , ( int )
    ↪ parameter ] ;
26 break ;
27 case SucuogluWalkDownParameters . HeavyOverhang :
28     currentScore = Convert . ToInt16 ( sucuogluModel .
    ↪ HeavyOverhang ) * gradeMatrix [ ( int )
    ↪ sucuogluModel . NumberOfStories , ( int )
    ↪ parameter ] ;
29 break ;
30 case SucuogluWalkDownParameters . ApparentQuality :
31     currentScore = ( int ) sucuogluModel .
    ↪ ApparentQuality * gradeMatrix [ ( int )
    ↪ sucuogluModel . NumberOfStories , ( int )
    ↪ parameter ] ;
32 break ;
33 case SucuogluWalkDownParameters . ShortColumn :
34     currentScore = Convert . ToInt16 ( sucuogluModel .
    ↪ ShortColumn ) * gradeMatrix [ ( int )
    ↪ sucuogluModel . NumberOfStories , ( int )
    ↪ parameter ] ;
35 break ;
36 case SucuogluWalkDownParameters . Pounding :
37     currentScore = Convert . ToInt16 ( sucuogluModel .
    ↪ Pounding ) * gradeMatrix [ ( int ) sucuogluModel
    ↪ . NumberOfStories , ( int ) parameter ] ;
38 break ;
39 case SucuogluWalkDownParameters . Topography :
40     currentScore = Convert . ToInt16 ( sucuogluModel .
    ↪ Topography ) * gradeMatrix [ ( int )
    ↪ sucuogluModel . NumberOfStories , ( int )
    ↪ parameter ] ;
41 break ;

```

```
42     default :
43         currentScore = 0;
44         break ;
45     }
46     finalScore = finalScore + currentScore ;
47 }
48 return finalScore ;
49 }
```

Code 5.3: Sample Sucuoglu Calculations in C#

5.4.2 File (IO) Methods

These methods include input-output operations such as opening, reading, or saving a file. Almost all of these methods are used during report creation. Although it violates abstraction concept, several file upload functions are defined under web application itself for convenience.

5.4.3 Reporting Methods

These methods are responsible for gathering the user input data and analyses results together into a predefined report format, and then present it to user as a portable document file (PDF) to download.

The report consists of a cover page and three sections:

Introduction: This part includes overall knowledge on seismicity, the importance of earthquake assessment, and seismic assessment procedures. The aim of this section is to spread earthquake awareness by including semi-technical information for the readers.

Target Structure Information and Analysis Results: This section contains the user input about the target structure and corresponding analysis results. In addition, some deduced information about the structure (such as seismic zone) is

included with visuals (overall earthquake map of Turkey and a detailed city seismic map). Each analyses result is presented under its own subsection, and these include a definition and adverse effects of every damage index parameter; for example, under “soft story”, a semi-technical definition is included as well as the risks of the presence of it in a structure. By this way, it is aimed to give insight and improve knowledge of the public about earthquake-resistant design.

Overall Assessment Results This final section summarizes analyses results in a table and gives a suggested action plan based on these results.

For the generation of the report and pdf modifications, open source MIT-licensed third party frameworks PDFSharp and MigraDoc are used. **MigraDoc** is a basic document generator; it supports almost anything that can be found in any decent word processor. It has the ability to add paragraphs, tables, charts, the arrangement of these in sections, the creation of bookmarks to create links, table of contents, indexes... etc. It will handle the layout, creating page breaks and other components as needed. **PDFsharp**, on the other hand, is a .NET library for processing a PDF file or generating it from scratch. Pages are created using drawing routines known from GDI+; almost anything that can be done with the GDI+ will work in PDFsharp. Only basic text layout is supported and page breaks are not created automatically. The general approaches are either to create PDF files using MigraDoc since it is much easier, and then use PDFsharp to add some extra features, or using PDFsharp to create the documents, and then using MigraDoc to create individual pages. In this web application, the latter technique is used since reports include a lot of images and tables.

5.4.4 Shared Components

Currently, the project is completely web application, yet it is considered that a PC software may also be added in the future for more advanced analyses and processing. Therefore, to ensure future compatibility of the system with a standalone installed application, several components are located in a separate dynamic linked library called “shared.dll”. The aim is to house every code that will be required for the future application in this dll and simply include it in the software. The items moved to the shared library are:

- **Entities:** All elements that are used to define a structure (column, beam, slab, shear wall... etc.) and all types of analyses. All engine methods function on these classes, therefore there will be no compatibility issues when the building information is created by the future software.
- **Localization libraries:** All translated strings reside in the shared dll, which makes them both reusable in multiple projects and having the same translation across platforms.
- **Constants:** All parameters whose values do not change in any condition are included in the shared library so that they are universal across all the available platforms. These parameters include base and penalty scores for walk-down analyses, limits, soil types, earthquake zones, and sample data for some analyses.
- **Enumerations:** These ‘enums’ are used to achieve consistency within the whole code by using centrally controlled values for different control variables. In order to be able to use these values in every platform, their definitions are located in the shared library. Extension methods for enumerations are also included with enum definitions.

5.5 Combining Components and Deployment

All the components explained in the previous chapters are created as separate projects within the same empty solution of Visual Studio, and then referenced to each other by their namespace, and the code map indicating the relations between libraries is given in Figure 5.8.

CHAPTER 6

CONCLUSIONS

This thesis contributed to the current state-of-the-art by proposing two new approaches for existing building evaluation methods against earthquakes and implementing a web-based tool to be used along with the first level evaluation. In the meantime, a basic smartphone application was developed for Android OS to measure ambient vibrations of a building floor and extract fundamental period if possible. Utilizing the residents of houses to enter basic information of building that they reside was planned to reach a large number of house data, eliminating costly and limited approach of using site staff to conduct building surveys. Furthermore, residents that enter their own structure information are also supplied with a short and automatically generated informative report to explain the strengths and weaknesses about their building, designed to address their questions about earthquakes and structural safety. In this way, a public education and awareness were planned and the research and development company “Yapıdestek Ltd.” was founded to commercialize this software in the future. Each relevant conclusions are further grouped under subheadings and explained in detail below.

6.1 First Level Building Evaluation Against Earthquakes

An improved walk-down method for seismic assessment of existing structures has been developed. The method was planned to be superior to existing techniques since it has utilized all the important parameters that other methods only include partially. Furthermore, additional optional parameters have been proposed such as shear wall

symmetry, fundamental period, strong beam weak column presence... etc. One of the most important advancement is the improved interaction between parameters. Although other methods include some level of interaction, the proposed technique implements a more direct influence of several parameters on others. This becomes more prominent when considering a) soil-structure interaction (in terms of fundamental periods) b) overhang and number of stories (total overhang mass) and c) ground slope and soil type (stability issues). A strategy is developed to self-scale and normalize the final score of the proposed method, even though some of the parameters are optional and may be omitted if not possible to observe. This provides a more flexible use if these values cannot be determined, while the evaluation accuracy is improved when they are available.

The proposed method is highly suitable for computerized evaluations since the number of parameters and their interaction may make it harder to perform using the conventional pen and paper only. A team can collect data including GPS coordinates with mobile devices that would instantly transfer this information to a central server, where these coordinates are also used to seek PGA and other relevant data from available databases (such as micro-zonation). It is also common to have mobile devices with built-in sub milli-g resolution accelerometers. One of the advancements of the proposed method is to obtain fundamental period of buildings by making simple measurements from the top story using smartphones' own accelerometers as an optional parameter. An Android OS application has been developed specifically for this purpose and currently available as a closed beta in Google Play app store.

Simplified analysis approaches such as equivalent static earthquake load are usually allowed for buildings with height less than 20 or 25 meters, which corresponds to about 7 stories high. Most of the first level evaluation methods are also limited to 7-8 stories, therefore the proposed technique is suggested for buildings with 7 stories or less.

The first level evaluation techniques may be considered as non-assertive and mostly used to rank building stock in a crude order based on their seismic vulnerability. Several of the existing methods do not have a present cut-off or threshold values. A statistical random building set of 1000 cases was generated to carry out Monte Carlo

simulation and compare the outcomes of all five methods including the proposed method. Different cut-off values were tried in optimization study to find the maximum overlapping between the proposed and the existing methods. The result of two distinct approaches (considering only common parameters and the whole parameter set) have yielded in the range of 80% to 85% correlation with the proposed method. The optimum threshold score for “pass” and “fail” is obtained as 48 out of 100 for the new Yucel-Turer approach. The proposed method could not be tested against an existing damage database since not all of the proposed parameters are available in the existing databases. Furthermore, testing the method using a specific earthquake damage database will cause bias as a function of a single seismic action, certain building stock, similar soil conditions... etc. A more general evaluation is required to have a multitude of different damage cases with a variety in building properties, seismic action, soil conditions, building stock, history of codes in effect, and many others.

The proposed new method is suitable for the development of a web-based tool. A website at <https://analiz.yapidestek.com.tr/> is prepared as a part of this study, which will make it possible to connect remotely and enter building information for a rapid assessment. This tool will also be an evolving system and make it possible to improve the threshold values and parameter scores as new earthquakes take place in the future. This new method will make it possible to fully utilize the new advancements in information technologies as well.

6.2 A New Capacity Calculation Method: Two and a Half Level Evaluation Against Earthquakes

A relatively more advanced assessment technique to calculate the capacity of a building was developed considering the ground floor for simplified structural analysis. In this new method, a basic structural analysis was introduced while keeping the necessary input data at a simpler level compared to full three-dimensional (3D) finite element (FE) analysis. Certain assumptions and simplifications for upper floor structural members and reinforcement percentage still yields high correlation with 3D FE analyses, with less than 20% error for complex irregular structures having torsional responses and even around 10% error for more symmetrical regular structures, in

terms of structural capacity (maximum base shear attained). Development of a simple, yet a method for capacity determination was one of the major contributions of this study.

The structural model is formed by defining a tree structure for each column, considering mid-length inflection points for all beams. The simplified tree structure's stiffness matrix is formed for translation and rotation on each floor and then condensed to translational degrees of freedom only. The calculated base shear force is divided between floors as an inverted triangle distribution and the first story deflection is linked to the ground floor column base shear, extracting an "effective" stiffness value for each column. Shear walls are converted to "central column"s using an approximated technique which combines the effect of flexural and shear behavior into a single stiffness value. Column and shear wall stiffness values are then combined into global x and y translational and z rotational degrees of freedom. Floor mass center and stiffness center are further calculated to find the torsional effect of earthquake forces, deflection demand for all columns (including converted shear walls) are calculated and fed into a nonlinear analysis to obtain the resultant capacity curve. Once this curve is obtained, it can be used in conjunction with the available performance point calculation methods such as capacity spectrum or displacement coefficients method. The conversion of most critical story displacements to roof deflections is also discussed and obtained by first mode dominant response assumption.

This analysis tool is relatively more advanced than second level evaluation techniques and simpler than the third level full 3D FE modeling; therefore it was named as two and a half capacity determination method. This robust approach is considered to be a contribution to the practice.

6.3 A Web Application for Basic Seismic Assessment of Structures

One of the major objectives of this study was to create an online seismic assessment tool which has the capabilities of basic evaluation, generation of automatic reports, and constructing a building stock database of structural performance results obtained from the analyses performed by the public. This online system is accom-

plished with the use of the contemporary web technologies and frameworks such as HTML5, JQuery, AngularJS, and ASP.NET with Identity and Entity-Framework kits. The overall system was planned to have three root modules; the user interface (UI), analysis and reporting engine, and data access layer which includes database and query parts. The user interface is decided to be a web page instead of a standalone installed software due to its superiorities and advantages, and other modules are connected to the UI. The analysis and reporting engine is coded using C# language and the database is selected as SQL.

The system is deployed to Microsoft Azure cloud services for its high reliability and dependability and can be accessed from <https://analiz.yapidestek.com.tr/>. The connection is secured using highest available SSL certification (extended validation certificate).

The user interface is generated as simple as possible with easy-to-follow instructions which include figures to help non-technical people (for example; residents of a house) to analyze their own structures. The help system is designed to have see-and-click paradigm as much as possible; users are shown several potential choices of an evaluation parameter (overhang, existing damage, short column. . . etc.) and asked to click on the picture which looks most similar to their case. After all questions have been answered, the analyses results are presented to the user on the screen as a summary, and a highly detailed and explanatory report is given in a downloadable PDF format. This document includes data on the evaluated structure (with any photos if supplied by the user), information written in a non-technical language on various seismic assessment levels and methods, and elaborate details of the analyses performed. These details include values of the evaluation parameters given by the user and their impact on the overall seismic performance of the structures. By this way, it is aimed to increase the awareness of the public on the importance of structural design and construction over earthquake hazard reduction; if a sufficient number of people realize short columns or removing structural elements are risky and seek these parameters when searching for houses, it is a tremendous leap for earthquake risk mitigation. Another major advantage of the system is its platform-independence; the web application can be used on desktop and laptop personal computers, tablets, and phones with any operating system (though small screen devices will possibly hinder user experience due to a

limited number of items that can be seen on the screen at a time).

The system can also be used by insurance companies during their risk assessments for determination of premium, municipalities to track building stocks and other private of public institutions for earthquake assessment and inventory management of structures.

As the system is used more and more, performance values obtained from the performed analyses will be collected in a database, forming an assessment map which can be used in city disaster planning and management works, urban reconstruction and modernization projects, and many more academic studies. In addition, assessment methods may be improved by the damage feedback obtained from users and site surveyors after medium or major earthquakes. Facebook ads and LinkedIn advertisements are used for publicizing the currently-active system to masses, however, their success is limited up to now.

6.4 Future Projections

One of the major future objectives for the online assessment system is making public aware of such a tool and spreading its use to people, companies, municipalities and other government institutions. It is also planned to create new add-ons for numerous other disaster evaluation needs such as blasts and fire as well as including risk assessment for different types of structures such as mines, power transmission line towers, and dams.

Another objective is to implement full integration with existing database and services (such as GIS), therefore construct a more all-in-one suite for various purposes like micro-zonation, building inventory management, and urban risk planning and mitigation.

REFERENCES

- [1] Applied Technology Council, *Seismic Evaluation and Retrofit of Concrete Buildings*. Applied Technology Council, 1996.
- [2] Applied Technology Council, *ATC-21-T: Rapid Visual Screening of Buildings for Potential Seismic Hazards Training Manual 2. Ed.* ATC-21-T: Rapid Visual Screening of Buildings for Potential Seismic Hazards Training Manual 2. Ed. Applied Technology Council, 2002.
- [3] H. Sucuoğlu, U. Yazgan, and A. Yakut, “A screening procedure for seismic risk assessment in urban building stock,” *Earthquake Spectra*, vol. 23, pp. 441–158, 2007.
- [4] R. of Turkey Ministry of Environment an Urbanisation, *Principles on Determination of Structures with Ri*, 2013.
- [5] FEMA, *Prestandard and Commentary for the Seismic Rehabilitation of Buildings*, 2000.
- [6] A. F. Hassan and M. A. Sozen, “Seismic vulnerability assessment of low-rise buildings in regions with infrequent earthquakes,” *ACI Structural Journal*, vol. 2, pp. 31–39, 1997.
- [7] M. A. Sözen and P. Güllkan, “Procedure for determining seismic vulnerability of building structures,” *ACI Structural Journal*, vol. 1, pp. 336–342, 1999.
- [8] M. E. Rodriguez and J. C. Aristizabal, “Evaluation of a seismic damage parameter,” *Earthquake Engineering and Structural Dynamics*, vol. 28, pp. 463–467, 1999.
- [9] S. T. Wasti, H. Sucuoğlu, and M. Utku, “Structural rehabilitation of damaged rc buildings after the 1 october 1995 dinar earthquake,” *Journal of Earthquake Engineering*, vol. 5, pp. 131–151, 2001.
- [10] A. Güler, “Seismic vulnerability assessment using artificial neural networks,” Master’s thesis, Middle East Technical University, 2005.
- [11] G. Ozcebe, S. Yüçemen, V. Aydoğan, and A. Yakut, “Preliminary seismic vulnerability assessment of existing reinforced concrete buildings in turkey,” in *Proceedings of the NATO Science for Peace Workshop*, 2003.

- [12] C. O. Karasu, “Mevcut betonarme binaların deprem performansının doğrusal elastik yöntem ile belirlenmesi ve p25 hızlı değerlendirme yöntemi ile karşılaştırılması,” 2007.
- [13] I. E. Bal, S. S. Tezcan, and F. G. Gülay, “Betonarme binaların göçme riskinin belirlenmesi için p25 hızlı değerlendirme yöntemi,” in *Altıncı Ulusal Deprem Mühendisliği Konferansı*, 2007.
- [14] A. Yakut, “Preliminary seismic performance assessment procedure for existing rc buildings,” *Engineering Structures*, vol. 26, pp. 1447–1461, 2004.
- [15] K. Kaatsız and H. Sucuoğlu, “Generalized force vectors for multi-mode pushover analysis of torsionally coupled systems,” *Earthquake Engineering and Structural Dynamics*, vol. 43, pp. 2015–2033, 2014.
- [16] F. S. Alici and H. Sucuoğlu, “Practical implementation of generalized force vectors for the multi-mode pushover analysis of building structures,” *Earthquake Spectra*, vol. Online, p. Online, 2014.
- [17] M. Saiidi and M. A. Sozen, “Simple nonlinear seismic analysis of r/c structures,” *Journal of the Structural Division*, vol. 107, no. 5, pp. 937–953, 1981.
- [18] H. Krawinkler and G. D. P. K. Seneviratna, “Pros and cons of a pushover analysis of seismic performance evaluation,” *Engineering Structures*, vol. 20, pp. 452–464, 1997.
- [19] P. Yang and Y. Wang, “A study on improvement of pushover analysis,” *Proceedings - 12. World Conference on Earthquake Engineering*, vol. 1940, pp. 1–8, 2000.
- [20] A. Mwafy and A. Elnashai, “Static pushover versus dynamic collapse analysis of rc buildings,” *Engineering Structures*, vol. 23, pp. 407–424, 2001.
- [21] J. M. Bracci, S. K. Kunnath, and A. M. Reinhorn, “Seismic performance and retrofit evaluation of reinforced concrete structures,” *Journal of Structural Engineering*, vol. 123, pp. 3–10, 1997.
- [22] B. Gupta and S. K. Kunnath, “Adaptive spectra based pushover procedure for seismic evaluation of structures,” *Earthquake Spectra*, vol. 16, pp. 367–392, 2000.
- [23] S. Antoniou and R. Pinho, “Advantages and limitations of adaptive and non-adaptive force-based pushover procedures,” *Journal of Earthquake Engineering*, vol. 8:4, pp. 497–522, 2004.
- [24] S. Antoniou and R. Pinho, “Development and verification of a displacement-based adaptive pushover procedure,” *Journal of Earthquake Engineering*, vol. 8:5, pp. 643–661, 2004.

- [25] F. Rofooeia, N. Attaria, A. Rasekhh, and A. Shodjaa, "Adaptive pushover analysis," *Asian Journal of Civil Engineering (Building and Housing)*, vol. 8:3, pp. 343–358, 2007.
- [26] T. F. Paret, K. K. Sasaki, D. H. Eilbeck, and S. A. Freeman, "Approximate inelastic procedures to identify failure mechanisms from higher mode effects," *11th World Conference on Earthquake Engineering*, vol. 1:966, p. 966, 1996.
- [27] A. K. Chopra and R. K. Goel, "A modal pushover analysis procedure for estimating seismic demands for buildings," *Earthquake Engineering and Structural Dynamics*, vol. 31, pp. 561–582, 2002.
- [28] C. Chintanapakdee and A. K. Chopra, "Evaluation of modal pushover analysis using generic frames," *Earthquake Engineering and Structural Dynamics*, vol. 21, pp. 417–442, 2003.
- [29] C. Chintanapakdee and A. K. Chopra, "Seismic response of vertically irregular frames: Response history and modal pushover analyses," *Journal of Structural Engineering*, vol. 130, pp. 1177–1185, 2004.
- [30] A. K. Chopra and R. K. Goel, "A modal pushover analysis procedure to estimate seismic demands for unsymmetric-plan buildings," *Earthquake Engng. Struct. Dyn.*, vol. 33, pp. 903–927, jun 2004.
- [31] R. K. Goel and A. K. Chopra, "Extension of modal pushover analysis to compute member forces," *Earthquake Spectra*, vol. 21, pp. 125–139, 2005.
- [32] E. Kalkan and S. Kunnath, "Adaptive modal combination procedure for non-linear static analysis of building structures," *Journal of Structural Engineering*, vol. 132, pp. 1721–1731, 2006.
- [33] M. Jianmeng, Z. Changhai, and X. Lili, "An improved modal pushover analysis procedure for estimating seismic demand of structures," *Earthquake Engineering and Engineering Vibration*, vol. 7, pp. 25–31, 2008.
- [34] J. C. Reyes and A. K. Chopra, "Three-dimensional modal pushover analysis of buildings subjected to two components of ground motion, including its evaluation for tall buildings," *Earthquake Engineering and Structural Dynamics*, vol. 40, pp. 789–806, 2011.
- [35] S. Jereza and A. Mebarkia, "Seismic assessment of framed buildings: A pseudo-adaptive uncoupled modal response analysis," *Journal of Earthquake Engineering*, vol. 15, pp. 1015–1035, 2011.
- [36] H. Sucuoğlu and M. S. Günay, "Generalized force vectors for multi-mode pushover analysis," *Earthquake Engineering and Structural Dynamics*, 2010.

- [37] F. S. Alıcı, K. Kaatsız, and H. Sucuoğlu, “Genel yük vektörleri ile Çok modlu itme analizi (genel itme analizi),” in *Birinci Türkiye Deprem Mühendisliği ve Sismoloji Konferansı*, 2011.
- [38] A. Rutenberg and A. Heidebrecht, “Approximate analysis of asymmetric wall-frame structures,” *Building Science*, 1975.
- [39] A. Reinhorn, A. Rutenberg, and J. Glück, “Dynamic torsional coupling in asymmetric building structures,” *Building and Environment*, 1977.
- [40] V. Kilar and P. Fajfar, “Simple push-over analysis of asymmetric building,” *Earthquake Engineering and Structural Dynamics*, 1997.
- [41] A. S. Moghadam and W. K. Tso, “Pushover analysis for asymmetrical multi-storey buildings,” in *Proceedings of the 6th U.S. National Conference on Earthquake Engineering, EERI*, 1998.
- [42] S. Wilkinson and D. Thambiratnam, “Simplified procedure for seismic analysis of asymmetric buildings,” *Computers and Structures*, vol. 79, no. 32, pp. 2833–2845, 2001.
- [43] P. Fajfar and P. Gaspersic, “The n2 method for the seismic damage analysis of rc buildings,” *Earthquake Engineering and Structural Dynamics*, vol. 25, pp. 31–46, 1996.
- [44] M. Kreslin and P. Fajfar, “The extended n2 method taking into account higher mode effects in elevation,” *Earthquake Engineering and Structural Dynamics*, vol. 40, pp. 1571–1589, 2011.
- [45] M. Kreslin and P. Fajfar, “The extended n2 method considering higher mode effects in both plan and elevation,” *Bulletin of Earthquake Engineering*, vol. 10, pp. 695–715, 2012.
- [46] P. Fajfar, D. Marusic, and I. Perus, “Torsional effects in the pushover-based seismic analysis of buildings,” *Journal of Earthquake Engineering*, vol. 9, no. 6, pp. 851–854, 2005.
- [47] A. K. Chopra, *Dynamics of Structures - Theory and Application to Earthquake Engineering*. Prentice Hall, 2001.
- [48] J. A. Mahaney, T. F. Paret, B. E. Kehoe, and S. A. Freeman, “The capacity spectrum method for evaluation structural response during the loma prieta earthquake,” in *National Earthquake Conference*, 1993.
- [49] D. LeBoeuf, M.-J. Nollet, J. Khelalfa, and L. Jolicoeur, “Development of a web-based information system for urban seismic risk management,” in *Joint International Conference on Computing and Decision Making in Civil and Building Engineering*, 2006.

- [50] B. Yalım, “Internet based seismic vulnerability assessment software development for r/c buildings,” Master’s thesis, Middle East Technical University, 2004.
- [51] HomeRisk, “Homerisk (tm) website.” <https://goo.gl/XNirYM>, last visited on September 2014.
- [52] FEMA, *FEMA310 - Handbook for the Seismic Evaluation of Buildings*. FEMA, California, 1 ed., 1998.
- [53] H. Sucuoglu and U. Yazgan, “Simple survey procedures for seismic risk assessment in urban building stocks,” in *Seismic Assessment and Rehabilitation of Existing Buildings* (S. Wasti and G. Ozcebe, eds.), vol. 29 of *NATO Science Series*, pp. 97–118, Springer Netherlands, 2003.
- [54] Turkish Standards Institute, *Specifications for Structures to be Built on Earthquake Zones*. Turkish Standards Institute, 2007.
- [55] G. Ozcebe, H. Sucuoglu, M. S. Yucemen, A. Yakut, and J. Kubin, “Seismic risk assessment of existing building stock in istanbul a pilot application in zeytinburnu district,” in *Proc. 8th US National Conference on Earthquake Engineering, San Francisco*, Citeseer, 2006.
- [56] A. Türer, U. Akyüz, T. Gür, A. İrfanoğlu, A. Matamoros, G. Özcebe, A. Sözen, and T. Wasti, “Types of structures and observed damage,” *1 May 2003 Bingöl Earthquake Engineering Report*, pp. 55–122, 2004.
- [57] B. ve İskan Bakanlığı, *Planlı Alanlar Tıp İmar Yönetmeliği*. Bayındırlık ve İskan Bakanlığı, 1985.
- [58] M. C. Yücel, “Period finder.” <https://goo.gl/51AJ2w>, last visited on January 2017.
- [59] S. of New York Department of Transportation Geotechnical Engineering Bureau, *Geotechnical Design Procedure: Liquefaction Potential of Cohesionless Soils*, 2015.
- [60] P. Wendykier, “Jtransforms.” <https://goo.gl/iA0EG>, last visited on January 2017.
- [61] A. Papoulis, *The Fourier Integral and Its Applications*. McGraw-Hill, 1962.
- [62] L. R. Rabiner and R. W. Schafer, *Digital Processing of Speech Signals*. PRENTICE HALL, 1978.
- [63] M. Pastor, M. Binda, and T. Harčarik, “Modal assurance criterion,” *Procedia Engineering*, vol. 48, pp. 543–548, 2012.
- [64] U. Ersoy, G. Ozcebe, and T. Tankut, *Reinforced Concrete*. METU, 2004.
- [65] U. Ersoy, “Betonarme kiriş ve kolonların moment kapasitelerinin saptanması,” *İMO Teknik Dergi*, pp. 1781–1797, 1998.

- [66] X. Zhao, Y.-F. Wu, A. Leung, and H. F. Lam, “Plastic hinge length in reinforced concrete flexural members,” *Procedia Engineering*, vol. 14, pp. 1266–1274, 2011.
- [67] A. L. L. Baker, *The Ultimate-load Theory Applied to the Design of Reinforced and Prestressed Concrete Frames*. London : Concrete Publications, 1956.
- [68] H. A. J. Sawyer, “Design of concrete frames for two failure stages,” in *International Symposium on the Flexural Mechanics of Reinforced Concrete*, 1964.
- [69] M. J. N. Priestley and R. Park, “Strength and ductility of concrete bridge columns under seismic loading,” *ACI Structural Journal*, vol. 84, no. 1, 1987.
- [70] T. Paulay and M. J. N. Priestley, *Seismic Design of Reinforced Concrete and Masonry Buildings*. Wiley-Blackwell, aug 2009.
- [71] S. A. Sheikh and S. S. Houry, “Confined concrete columns with stubs,” *ACI Structural Journal*, vol. 90, no. 4, 1993.
- [72] J. Coleman and E. Spacone, “Localization issues in force-based frame elements,” *Journal of Structural Engineering*, vol. 127, pp. 1257–1265, nov 2001.
- [73] T. B. Panagiotakos and M. N. Fardis, “Deformation of reinforced concrete members at yielding and ultimate,” *ACI Structural Journal*, vol. 98, no. 2, 2001.
- [74] S. J. Bae and O. Bayrak, “Plastic hinge length of reinforced concrete columns,” *ACI Structural Journal*, vol. 105, no. 3, 2008.
- [75] J. A. Snyman, *Practical Mathematical Optimization*. Springer, 2005.
- [76] R. Fletcher, *Practical Methods of Optimization*. John Wiley & Sons, 1987.
- [77] D. W. Marquardt, “An algorithm for least-squares estimation of nonlinear parameters,” *Journal of Society for Industrial and Applied Mathematics*, vol. 11, pp. 431–441, 1963.
- [78] F. Glover, “Future paths for integer programming and links to artificial intelligence,” *Computers & Operations Research*, vol. 13, pp. 533–549, 1986.
- [79] F. G. M. Laguna, *Tabu Search*. Springer, 1997.
- [80] C. Blum and A. Roli, “Metaheuristics in combinatorial optimization: Overview and conceptual comparison,” *ACM Computing Surveys*, vol. 35, pp. 268–308, 2003.
- [81] S. Kirkpatrick, J. C. D. Gelatt, and M. P. Vecchi, “Optimization by simulated annealing,” *Science*, vol. 220, no. 4598, pp. 671–680, 1983.
- [82] D. E. Goldberg and J. H. Holland, “Genetic algorithms and machine learning,” *Machine Learning*, vol. 3, no. 2, pp. 95–99, 1988.

- [83] R. Storn and K. Price, "Differential evolution - a simple and efficient heuristic for global optimization over continuous spaces," *Journal of Global Optimization*, vol. 11, pp. 341–359, 1997.
- [84] M. Dorigo, V. Maniezzo, and A. Colorni, "Ant system: optimization by a colony of cooperating agents," *IEEE Trans. Syst., Man, Cybern. B*, vol. 26, no. 1, pp. 29–41, 1996.
- [85] J. Kennedy and R. Eberhart, "Particle swarm optimization," in *Proceedings of ICNN - International Conference on Neural Networks*, Institute of Electrical & Electronics Engineers (IEEE), 1995.
- [86] O. K. Erol and I. Eksin, "A new optimization method: Big bang-big crunch," *Advances in Engineering Software*, vol. 37, pp. 106–111, feb 2006.
- [87] X.-S. Yang and S. Deb, "Engineering optimisation by cuckoo search," *International Journal of Mathematical Modelling and Numerical Optimisation*, vol. 1, no. 4, pp. 330–343, 2010.
- [88] I. Pavlyukevich, "Lévy flights, non-local search and simulated annealing," *Journal of Computational Physics*, vol. 226, pp. 1830–1844, oct 2007.
- [89] B. A. Myers, "Window interfaces - a taxonomy of window manager user interfaces," *Computer Graphics and Applications*, vol. 8, pp. 65–84, 1988.
- [90] W. O. Galitz, *The Essential Guide to User Interface Design: An Introduction to GUI Design Principles and Techniques*. John Wiley & Sons, 2007.
- [91] A. van Dam, "Post-wimp user interfaces," *Communications of the ACM*, vol. 40, pp. 63–67, 1997.
- [92] A. van Dam, "Beyond wimp," *Computer Graphics and Applications*, vol. 20, pp. 50–51, 2000.
- [93] B. D. Smet, *C# 4.0 Unleashed*. Sams Publishing, 2011.
- [94] IBM, "Ibm annual report," tech. rep., International Business Machines Corporation, 2013.

CURRICULUM VITAE

PERSONAL INFORMATION

Surname, Name: Yücel, Mustafa Can

Nationality: Turkish (TC)

Date and Place of Birth: 29.10.1983, Atkaracalar

Marital Status: Single

Phone: 0535 553 0564

Fax: None

EDUCATION

Degree	Institution	Year of Graduation
M.S.	METU Civil Engineering Department	2010
B.S.	METU Civil Engineering Department	2006
High School	Ankara Atatürk Anatolian High School	2002

PROFESSIONAL EXPERIENCE

Year	Place	Enrollment
2006-2013	METU	Research Assistant
2015-	Yapıdestek Mühendislik	R&D Engineer

PUBLICATIONS

International Conference Publications

- Time-Efficient Visual Inspection of Zonguldak-Irmak Railroad Bridges, 7th International Conference on Bridge Maintenance, Safety and Management, Yücel, M. C., Caner, A.; Türer, A., Shanghai, 2014.
- International Applications In Inspection of Railroad Bridges and Recommendations For Turkish Practice, Istanbul International Bridge Conference, Yücel, M.C., Caner, A., Istanbul, 2014.

National Conference Publications

- Kiriş tipi yapılarda hasarsız durum tespiti, IV. Ulusal Çelik Yapılar Konferansı, Yücel, M. C., Türer, A., Istanbul, 2011.

Thesis

- Structural Identification, Damage Detection by Non-Destructive Tests and Determining Axial Loads In Cables, M.Sc. Thesis, METU, 2010.

Books

- Structural Damage Detection by NDT and Finding Axial Loads in Cables, LAP Lambert Academic Publishing, ISBN-13: 978-3846507407, 2011.